

Temporal Logic Task Allocation in Heterogeneous Multi-Robot Systems

Xusheng Luo¹ and Michael M. Zavlanos¹

Journal Title
XX(X):1–47
©The Author(s) 0000
Reprints and permission:
sagepub.co.uk/journalsPermissions.nav
DOI: 10.1177/ToBeAssigned
www.sagepub.com/



Abstract

In this paper, we consider the problem of optimally allocating tasks, expressed as global Linear Temporal Logic (LTL) specifications, to teams of heterogeneous mobile robots. The robots are classified in different types that capture their different capabilities, and each task may require robots of multiple types. The specific robots assigned to each task are immaterial, as long as they are of the desired type. Given a discrete workspace, our goal is to design paths, i.e., sequences of discrete states, for the robots so that the LTL specification is satisfied. To obtain a scalable solution to this complex temporal logic task allocation problem, we propose a hierarchical approach that first allocates specific robots to tasks using the information about the tasks contained in the Nondeterministic Büchi Automaton (NBA) that captures the LTL specification, and then designs low-level executable plans for the robots that respect the high-level assignment. Specifically, we first prune and relax the NBA by removing all negative atomic propositions. This step is motivated by “lazy collision checking” methods in robotics and allows to simplify the planning problem by checking constraint satisfaction only when needed. Then, we extract sequences of subtasks from the relaxed NBA along with their temporal orders, and formulate a Mixed Integer Linear Program (MILP) to allocate these subtasks to the robots. Finally, we define generalized multi-robot path planning problems to obtain low-level executable robot plans that satisfy both the high-level task allocation and the temporal constraints captured by the negative atomic propositions in the original NBA. We provide theoretical results showing completeness and soundness of our proposed method and present numerical simulations demonstrating that our method can generate robot paths with lower cost, considerably faster than existing methods.

Keywords

Temporal logic, formal methods, multi-robot systems, task allocation, motion planning.

1 Introduction

Robot motion planning traditionally consists of generating robot trajectories between a start and a goal region, while avoiding obstacles (LaValle 2006). More recently, new planning methods have been proposed that can handle a richer class of tasks than the standard point-to-point navigation that also include temporal goals. Such tasks can be captured using formal languages, such as Linear Temporal Logic (LTL) (Baier and Katoen 2008), and include sequencing or coverage (Fainekos et al. 2005), data gathering (Guo and Zavlanos 2017), intermittent communication (Kantaros and Zavlanos 2017a), and persistent surveillance (Leahy et al. 2016), to name a few. A survey on formal specifications and synthesis techniques for robotic systems can be found in Luckcuck et al. (2019).

In this paper, we consider LTL tasks that require robots of different types to collaborate to satisfy the specification. The different robot types capture the different robot capabilities, and each task may require robots of multiple types to accomplish. The specific robots assigned to each task are immaterial, as long as they are of the desired type. An example such LTL tasks is: *At most five robots of type 1 pick up the mail by visiting houses in a given order. Next, visit a delivery site. Never leave the delivery site until one ground robot of type 2 is present to pick up the mail (a robot of type 2 can carry mail from at most 5 robots of type 1).*

Repeat this process every day. In this task, several robots are required to work cooperatively and meet simultaneously at the same place. Note that the specific robots to participate in this task are not important and are not specified by the LTL formula. Instead, it is only required that no more than five robots of type 1 and exactly one robot of type 2 collaborate to accomplish this task. Therefore, there are multiple ways that this LTL task can be satisfied, which grow combinatorially with the number of robots, robot types, and the complexity of the LTL task. We refer to this problem as the Multi-Robot Task Allocation (MRTA) problem for LTL tasks, in short, LTL-MRTA. Existing control synthesis methods under temporal logic specifications, such as the ones proposed in Smith et al. (2010); Ulusoy et al. (2013); Guo and Dimarogonas (2015); Kantaros and Zavlanos (2015a), build a large product automaton composed of the Nondeterministic Büchi Automaton (NBA) that captures the LTL specification and the discrete transition systems describing the motion of each one of the robots in the world.

¹ Department of Mechanical Engineering and Materials Science, Duke University, Durham, NC 27708, USA

Corresponding author:

Xusheng Luo, Department of Mechanical Engineering and Materials Science, Duke University, Durham, NC 27708, USA
Email: xusheng.luo@duke.edu

Then, these methods employ graph search techniques on this product graph to find the optimal plan that satisfies the LTL specification. However, as the number of robots, the size of the environment, and the complexity of the LTL task grows, the size of this product graph grows exponentially large and, therefore, graph search methods become intractable. This is particularly the case in the LTL-MRTA problem considered here, where the multiple possible assignments of robots to tasks, increase the complexity of the LTL specification dramatically.

To mitigate the computational complexity of the LTL-MRTA problem, we propose a novel hierarchical approach that first allocates specific robots to tasks using the information about tasks provided by the Nondeterministic Büchi Automaton (NBA) that captures the LTL specification, and then designs low-level executable plans for the robots that respect the high-level assignment. Specifically, we first prune and relax the NBA by removing all negative atomic propositions. This step is motivated by "lazy collision checking" methods in robotics (Sánchez and Latombe 2003; Hauser 2015) and allows to simplify the planning problem by checking constraint satisfaction only when needed. Then, we extract sequences of subtasks from the relaxed NBA along with their temporal orders, and formulate a Mixed Integer Linear Program (MILP), inspired by the vehicle routing problem, to allocate these subtasks to the robots, while respecting the temporal order between subtasks. The solution to this MILP generates a time-stamped task allocation plan for each robot, which is a sequence of essential waypoints that the robot needs to visit. Finally, given this time-stamped task allocation plan for each robot, we formulate a sequence of generalized multi-robot path planning (GMRPP) problems, one for each subtask, to obtain executable paths that also respect the negative atomic propositions that were relaxed from the original NBA. We show through extensive simulations that our method can handle LTL-MRTA problems with up to 10^{90} states in the product graph, considerably outperforming existing methods. Moreover, we provide theoretical guarantees on the completeness and soundness of our proposed framework, under mild assumptions on the structure of the NBA that were satisfied by all meaningful LTL specifications we considered in practice, no matter their complexity. While not theoretically optimal, our method is still able to improve on the cost of the returned plans, unlike existing methods in the literature that only focus on feasibility.

1.1 Related work

In existing literature on optimal control synthesis methods from LTL specifications, LTL tasks are either assigned locally to the robots in a multi-robot team, as in Guo and Dimarogonas (2015); Tumova and Dimarogonas (2016) or a global LTL specification is assigned to the team that captures the collective behavior of all robots. In the latter case, the global LTL specification can explicitly assign tasks to the individual robots, as in Loizou and Kyriakopoulos (December 2004); Smith et al. (2011); Saha et al. (2014); Kantaros and Zavlanos (2015b, 2017b, 2018a,b,c, 2020); Luo and Zavlanos (2019); Luo et al. (2019), or it may not explicitly assign tasks to the robots as in Kloetzer et al. (2011); Shoukry et al. (2017); Moarref and Kress-Gazit

(2017); Lacerda and Lima (2019), and our current work in this paper.

Global temporal logic specifications that do not explicitly allocate tasks to robots typically need to be decomposed in order to obtain the required allocation. For example, Tumova and Dimarogonas (2015); Kantaros and Zavlanos (2016) decompose a global specification directly into local specifications and assign them to individual robots. Similarly, Camacho et al. (2017); Luo and Zavlanos (2019); Camacho et al. (2019); Schillinger et al. (2019) decompose a global specification into multiple subtasks by exploiting the structure of the finite automata. Particularly, Camacho et al. (2017) convert temporal planning problems to standard planning problems by defining actions based on transitions in the NBA, while Luo and Zavlanos (2019) define subtasks associated with transitions in the NBA and synthesize plans for these subtasks which they store in a library so that they can be reused to efficiently synthesize plans for new LTL formulas. Schillinger et al. (2019) also define subtasks associated with transitions in the automaton, but use reinforcement learning to learn plans that execute these subtasks under uncertainty. Camacho et al. (2019) also use reinforcement learning but with the purpose of converting formal languages to reward machines that capture the structure of the task. Similar to these works, here too we define subtasks associated with transitions in the NBA. However, we do not assume that these subtasks are preassigned to the robots.

Temporal logic control synthesis without an explicit assignment of robots to tasks has been considered in Karaman and Frazzoli (2011) that combine the vehicle routing problem with metric temporal logic specifications and leverage MILP to solve this problem for heterogeneous robots. However, this approach can only handle finite horizon tasks and does not design the low-level executable paths as we do here. An alternative approach is proposed in Chen et al. (2011); Leahy et al. (2015) that decomposes a global automaton into individual automata that are assigned to the heterogeneous robots and then builds a synchronous product of these automata to synthesize parallel plans. However, the size of the synchronous product automaton grows exponentially large with the number of robots. Also, the requirement that parallel plans exist does not allow application of this method to tasks that lack such parallel executions. Furthermore, this method also focuses only on finite robot trajectories. In relevant literature, teams of homogeneous robots have also been modeled using Petri Nets as in Lacerda and Lima (2019); Kloetzer and Mahulea (2020). Specifically, Lacerda and Lima (2019) propose a job shop problem under safe temporal logic specifications, but do not consider the "eventually" operator so that liveness in terms of good future outcomes can not be guaranteed. Additionally, this approach only focuses on robot coordination at the task level without considering execution. To the contrary, Kloetzer and Mahulea (2020) select multiple shortest accepting runs in the NBA and for each accepting run, determine whether an executable plan exists. Finally, Schillinger et al. (2018a,b); Faruq et al. (2018); Banks et al. (2020) automatically decompose the automaton representation of the LTL formula into independent subtasks that can be fulfilled by different robots.

However, they only consider LTL formulas that can be satisfied by finite robot trajectories, limiting the applicability of the proposed method to tasks such as recurrent sequencing and persistent monitoring. Also, subtasks subject to precedence relations can only be executed by a single robot.

Common in the above approaches is that they do not consider cooperative tasks where robots of the same or different types need to meet at a common location to complete a task. Such tasks require strong synchronization between robots. In our recent work (Kantaros and Zavlanos 2018b, 2020), we have proposed a sampling-based planning method named STyLuS* that incrementally builds trees to approximate the product of the NBA and the model of the team. Using the powerful biased sampling method proposed in Kantaros and Zavlanos (2020), STyLuS* can synthesize plans for product automata with up to 10^{800} states without considering collision avoidance. However, STyLuS* requires global LTL specifications that explicitly assign tasks to robots. Although a subset of specifications we consider here can be converted into explicit LTL formulas by enumerating all possible task assignments and connecting them with “OR” operators, this would result in exponentially long LTL formulas. Furthermore, the biased sampling strategy in STyLuS* needs a fixed assignment of robots to tasks and biases search towards finding a plan for this fixed assignment. If the assignment is not given, biased STyLuS* will need to be run combinatorially many times, one for each possible assignment. With unbiased sampling, Kantaros and Zavlanos (2018b) show that STyLuS* can only solve problems with product automata that have 10^{10} states. Instead, our proposed method can synthesize plans for problems with 10^{90} states while considering collision avoidance. On the other hand, model-checkers like NuSMV (Cimatti et al. 2002), focus on finding feasible paths and are incapable of optimizing cost. As stated in Kantaros and Zavlanos (2020), NuSMV can only handle problems with 10^{30} states, and can not easily process exponentially long LTL formulas generated by explicitly expressing task assignments.

Among other methods that focus on cooperative tasks, Moarref and Kress-Gazit (2017) focus on specifications capturing behaviors of homogeneous robotic swarms at the swarm and individual levels, but they can only impose universal or existential constraints, that is, all robots or some robots visit a certain region. As a result, these specifications are incapable of imposing restrictions on the number of robots that should be present at one place at the same time. This limitation is addressed in Sahin et al. (2017a,b, 2019a) that relies on counting linear temporal logic (cLTL+/cLTL) to capture constraints on the number of robots that must be present in different regions. Specifically, the authors formulate a Integer Linear Program (ILP) inspired by Bounded Model Checking techniques (Biere et al. 2006), but can only guarantee feasibility of the resulting paths. Instead our method also optimizes cost. A sequential planning approach is proposed in Jones et al. (2019) that augments the LTL specification by introducing time and, unlike our proposed approach, plans low-level plans for the robots, one at a time, while treating the other robots as obstacles. Common in the methods in Sahin et al. (2017a,b,

2019a); Jones et al. (2019) is that the size of the workspace has a significant effect on the computation time. To mitigate the complexity due to the size of the workspace, Sahin et al. (2019b) propose a hierarchical framework that abstracts the workspace by aggregating states with the same observations. As we show in Section 7, our proposed method scales better than the method in Sahin et al. (2019b), and provides lower cost solutions with less runtime. Also, unlike our method, the completeness of solutions is not guaranteed in Sahin et al. (2019b).

Related is also work on multi-robot task allocation problems, regardless of LTL specifications (Korsah et al. 2013; Nunes et al. 2017; Gini 2017). Such problems have been typically solved using market-based methods as in Zavlanos and Pappas (2007); Zavlanos et al. (2008); Zavlanos and Pappas (2008); Michael et al. (2008), or optimization-based methods as in Gombolay et al. (2013); Jones et al. (2011). In this paper, we employ an optimization-based method to solve the assignment problem as we formulate a MILP for this purpose. Nevertheless, unlike this literature where tasks are typically predefined, here tasks are not predefined, but they are extracted from the NBA.

The contributions of this paper can be summarized as follows: We propose a new hierarchical approach to the LTL-MRTA problem that first assigns robots to tasks and then plans robot paths that satisfy the high level assignment. Under mild assumptions on the NBA that were satisfied by all meaningful LTL formulas we considered in practice (no matter their complexity), we showed that our method is complete and sound. Moreover, while not theoretically optimal, our method still incorporates optimization steps to improve on the cost of the returned plans. To the best of our knowledge, this is the first LTL-MRTA method that is both complete and includes operations to optimize the synthesized plans. The unique aspect of our approach is a clever pruning and relaxation of the NBA that removes all negative atomic propositions, and is motivated by “lazy collision checking” methods in robotics. This step significantly simplifies the planning problem by allowing to check constraint satisfaction only when needed and, as a result, contributes to significantly increasing scalability of our method. To the best of our knowledge, this is the first time that “lazy collision checking” methods that are common in point-to-point navigation are used for high-level robot planning. Compared to existing methods, our approach returns lower cost plans in significantly less time.

The rest of the paper is organized as follows. In Sections 2 and 3 we present preliminaries and define the problem under consideration, respectively. We describe the high-level task assignment component of our method in Sections 4 and 5. Specifically, in Section 4 we prune and relax the NBA, identify subtasks from the NBA and infer temporal orders between them. Then, in Section 5 we formulate a MILP to obtain the high-level plans. In Section 6, we examine the completeness and soundness of these plans, while in Section 7 we present simulation results. Finally, Section 8 concludes the paper. For completeness, the low-level component of our method to obtain executable paths, which is based on existing multi-robot path planning techniques, is presented in Appendix B.

2 Preliminaries

2.1 Linear temporal logic

Linear Temporal Logic (LTL) is composed of a set of atomic propositions \mathcal{AP} , the boolean operators, conjunction \wedge and negation \neg , and temporal operators, next \bigcirc and until \mathcal{U} (Baier and Katoen 2008). LTL formulas over \mathcal{AP} follow the grammar

$$\phi := \top \mid \pi \mid \phi_1 \wedge \phi_2 \mid \neg\phi \mid \bigcirc \phi \mid \phi_1 \mathcal{U} \phi_2,$$

where \top is unconditionally true. Other temporal operators can be derived from \mathcal{U} . For instance, $\diamond\phi$ means ϕ will be eventually satisfied sometime in the future and $\square\phi$ means ϕ is always satisfied from now on.

An infinite word w over the alphabet $2^{\mathcal{AP}}$, the power set of the set of atomic propositions, is defined as an infinite sequence $w = \sigma_0\sigma_1\dots \in (2^{\mathcal{AP}})^\omega$, where ω denotes an infinite repetition and $\sigma_k \in 2^{\mathcal{AP}}$, $\forall k \in \mathbb{N}$. The language $\text{Words}(\phi) = \{w | w \models \phi\}$ is defined as the set of words that satisfy the LTL formula ϕ , where $\models \subseteq (2^{\mathcal{AP}})^\omega \times \phi$ is the satisfaction relation. An LTL ϕ can be translated into a Nondeterministic Büchi Automaton (NBA) defined as follows (Vardi and Wolper 1986):

Definition 2.1. (NBA). A Nondeterministic Büchi Automaton B is a tuple $B = (\mathcal{Q}_B, \mathcal{Q}_B^0, \Sigma, \rightarrow_B, \mathcal{Q}_B^F)$, where \mathcal{Q}_B is the set of states; $\mathcal{Q}_B^0 \subseteq \mathcal{Q}_B$ is a set of initial states; $\Sigma = 2^{\mathcal{AP}}$ is an alphabet; $\rightarrow_B \subseteq \mathcal{Q}_B \times \Sigma \times \mathcal{Q}_B$ is the transition relation; and $\mathcal{Q}_B^F \subseteq \mathcal{Q}_B$ is a set of accepting states.

An infinite run ρ_B of B over an infinite word $w = \sigma_0\sigma_1\sigma_2\dots$, $\sigma_k \in \Sigma$, $\forall k \in \mathbb{N}$, is a sequence $\rho_B = q_B^0q_B^1q_B^2\dots$ such that $q_B^0 \in \mathcal{Q}_B^0$ and $(q_B^k, \sigma_k, q_B^{k+1}) \in \rightarrow_B$, $\forall k \in \mathbb{N}$. An infinite run ρ_B is called accepting if $\text{Inf}(\rho_B) \cap \mathcal{Q}_B^F \neq \emptyset$, where $\text{Inf}(\rho_B)$ represents the set of states that appear in ρ_B infinitely often. If an LTL formula is satisfiable, then there exists an accepting run that can be written in the prefix-suffix structure such that the prefix part, connecting an initial state to an accepting state, is traversed only once and the suffix part, a cycle around the accepting state, is traversed infinitely often. The words σ that induce an accepting run of B constitute the accepted language of B , denoted by \mathcal{L}_B . Baier and Katoen (2008) proved that the accepted language of B is equivalent to the words of ϕ , i.e., $\mathcal{L}_B = \text{Words}(\phi)$.

2.2 Partially ordered set

A finite partially ordered set or poset $P = (X, \leq_P)$ is a pair consisting of a finite base set X and a binary relation $\leq_P \subseteq X \times X$ that is reflexive, antisymmetric, and transitive. Let $x, y \in X$ be two distinct elements. We write $x <_P y$ if $(x, y) \in \leq_P$, and $x \parallel_P y$ if x and y are incomparable. Moreover, we say x is covered by y or y covers x , denoted by $x \prec_P y$, if $x <_P y$ and there is no distinct $z \in X$ such that $x <_P z <_P y$. An antichain is a subset of a poset in which any two distinct elements are incomparable. The width of a poset is the cardinality of a maximal antichain. Similarly, the height of a poset is defined as the cardinality of a chain. Finally, a chain is a subset of a poset in which any two distinct elements are comparable. The height of a poset is the cardinality of a maximal chain.

A linear order $L_X = (X, <_L)$ is a poset such that $x <_L y$, $x = y$ or $y <_L x$ holds for any pair of $x, y \in X$. A linear extension $L_P = (X, <_L)$ of a poset P is a linear order such that $x <_L y$ if $x <_P y$, i.e., a linear order that preserves the partial order. We define \mathcal{L}_P as the set of all linear extensions of a poset P . Note that a poset and its linear extensions share the same base set X_P . Given a collection of linear orders Ξ , the poset cover problem focuses on reconstructing a single poset P or a set of posets $P = \{P_1, \dots, P_k\}$ such that $L_P = \Xi$ or $\cup_{i=1}^k L_{P_i} = \Xi$. As shown in Heath and Nema (2013), the poset cover problem is NP-complete. Moreover, the partial cover problem focuses on finding a single poset P such that \mathcal{L}_P contains the maximum number of linear orders in Ξ , i.e., $\mathcal{L}_P \subseteq \Xi$ and $\#P' \text{ s.t. } \mathcal{L}_{P'} \subseteq \Xi \text{ and } |\mathcal{L}_{P'}| > |\mathcal{L}_P|$. Heath and Nema (2013) showed that the partial cover problem can be solved in polynomial time.

3 Problem Definition

3.1 Transition system

Consider a discrete workspace containing $l \in \mathbb{N}^+$ labeled regions of interest, so that each such region can span multiple cells in the workspace, and denote by $\mathcal{L} = \{\ell_k\}_{k \in [l]}$ the set of these regions, where $[l]$ is the shorthand notation for $\{1, \dots, l\}$. We call free cells in the workspace that do not belong to any region *region-free*, and paths connecting two different regions that only pass through region-free cells *label-free*. We also assume that the workspace contains obstacles that can span multiple cells and do not overlap with the regions of interest. We represent the workspace by a graph $E = (S, \rightarrow_E)$ where S is the finite set of vertices corresponding to free cells and $\rightarrow_E \subseteq S \times S$ captures the adjacency relation.

Given the workspace E , we consider a team of n heterogeneous robots. We assume that these robots are of m different types and every robot belongs to exactly one type. Let \mathcal{K}_j , $j \in [m]$, denote the set that collects all robots of type j , so that $\sum_{j \in [m]} |\mathcal{K}_j| = n$ and $\mathcal{K}_j \cap \mathcal{K}_{j'} = \emptyset$ if $j \neq j'$, where $|\cdot|$ is the cardinality of a set. We collect all n robots in the set \mathcal{R} , i.e., $\mathcal{R} = \{\mathcal{K}_j\}_{j \in [m]}$. Finally, we use $[r, j]$ to represent robot r of type j , where $r \in \mathcal{K}_j$, $j \in [m]$. To model the motion of robot $[r, j]$ in the workspace, we define a transition system (TS) for this robot as follows.

Definition 3.1. (TS). A transition system for robot $[r, j]$ is a tuple $\text{TS}_{r,j} = \{S, s_{r,j}^0, \rightarrow_{r,j}, \Pi_{r,j}, L_{r,j}\}$ where: (a) S is the set of possible locations that robot $[r, j]$ can be at and $s_{r,j}^t \in S$ is the robot's location at time t ; (b) $s_{r,j}^0$ is the initial location; (c) $\rightarrow_{r,j} \subseteq \rightarrow_E \cup_{s \in S} \{(s, s)\}$ is the transition relation that allows the robot to remain idle or move between adjacent cells; (d) $\Pi_{r,j} = \cup_{k \in [l]} \{p_{r,j}^k\} \cup \{\epsilon\}$ where the atomic proposition $p_{r,j}^k$ is true if robot $[r, j]$ is at region ℓ_k and ϵ denotes the empty label; and (e) $L_{r,j} : S \rightarrow \Pi_{r,j}$ is the labeling function that returns the atomic proposition satisfied at location $s_{r,j}^t$.

Given the transition systems of all robots $[r, j]$ we can define the product transition system (PTS), which captures all possible combinations of robot behaviors.

Definition 3.2. (PTS). Given n transition systems $\text{TS}_{r,j} = \{S, s_{r,j}^0, \rightarrow_{r,j}, \Pi_{r,j}, L_{r,j}\}$, the product transition system is a

tuple $\text{PTS} = (S^n, s^0, \rightarrow, \Pi, L)$ where (a) $S^n = S \times \dots \times S$ is the finite set of collective robot locations, and $s^t \in S^n$ collects all robot locations at time t ; (b) s^0 is the initial locations of the robots; (c) $\rightarrow \subseteq S^n \times S^n$ is the transition relation so that $(s^t, s^{t+1}) \in \rightarrow$ if $s_{r,j}^t \rightarrow_{r,j} s_{r,j}^{t+1}$ for all $r \in \mathcal{K}_j, \forall j \in [m]$; (d) $\Pi = \cup_{i \in [\lvert \mathcal{K}_j \rvert], j \in [m], k \in [l]} \{\pi_{i,j}^k\} \cup \{\epsilon\}$, where the atomic proposition $\pi_{i,j}^k$ is true if there exist i robots of type j , denoted by $\langle i, j \rangle$, at region ℓ_k at the same time, i.e., $\pi_{i,j}^k \Leftrightarrow |\{r \in \mathcal{K}_j : L_{r,j}(s_{r,j}^t) = p_{r,j}^k\}| \geq i$; (e) and $L : S^n \rightarrow 2^\Pi$ is the labeling function that returns the set of atomic propositions satisfied by all robots at time t .

3.2 Task specification

In this paper, we consider MRTA problems where the tasks are globally described by LTL formulas. Furthermore, we consider tasks in which the same fleet of robots of a certain type may need to visit different regions in sequence, e.g., to deliver objects between different regions. To capture such tasks, we define *induced atomic propositions* over the set Π defined in Definition 3.2 as follows.

Definition 3.3. (Induced atomic propositions). *For each basic atomic proposition $\pi_{i,j}^k \in \Pi$, we define an infinite set of induced atomic propositions $\{\pi_{i,j}^{k,\chi}\}_{\chi \in \mathbb{N}}$, where χ is a connector that binds the truth of atomic propositions with identical i, j and χ . Specifically, when $\chi = 0$, $\pi_{i,j}^{k,\chi}$ is equivalent to $\pi_{i,j}^k$ whose truth is state-dependent. When $\chi \neq 0$, the truth of $\pi_{i,j}^{k,\chi}$ is state-and-path-dependent, meaning that it additionally depends on other induced atomic propositions that share the same i, j and χ . That is, both $\pi_{i,j}^{k,\chi}$ and $\pi_{i,j}^{k',\chi}$ with $\chi \neq 0$ are true if the same i robots of type j visit regions ℓ_k and $\ell_{k'}$. Furthermore, the negative atomic proposition $\neg\pi_{i,j}^{k,\chi}$ is equivalent to its basic counterpart $\neg\pi_{i,j}^k$, i.e., less than $\langle i, j \rangle$ robots are at region ℓ_k .*

Let \mathcal{AP} collect all basic and induced atomic propositions and denote by $\Sigma = 2^{\mathcal{AP}}$, its power set. In what follows, we omit the superscript χ when $\chi = 0$. We denote by LTL^χ , the set of formulas defined over the set of basic and induced atomic propositions and by LTL^0 , the set of formulas defined only over basic atomic propositions, respectively. Clearly, $\text{LTL}^\chi \supset \text{LTL}^0$, which means that LTL^χ is able to capture a broader class of tasks. While there exists literature on optimal control synthesis over LTL^0 (Sahin et al. 2017a,b, 2019a), to the best of our knowledge there is no work on optimal control synthesis over LTL^χ formulas. Next, we introduce the notion of *valid* temporal logic tasks.

Definition 3.4. (Valid temporal logic task). *A temporal logic task specified by a LTL^χ formula defined over \mathcal{AP} is valid if atomic propositions with the same nonzero connector χ involve the same number of robots of the same type.*

Example 1. (Valid temporal logic tasks). *Consider a mail delivery task amidst the COVID-19 pandemic (shown in Fig. 1) where three robots of type 1 (indicated by \star) and two robots of type 2 (indicated by \bullet) are located at region ℓ_1 , ℓ_2 is an office building where robots visit to pick up the mail, ℓ_3 and ℓ_5 are two delivery sites, and ℓ_4 is a control room from where other robots are driven to the orange area between ℓ_3 and ℓ_4 to get disinfected and then drop off the*

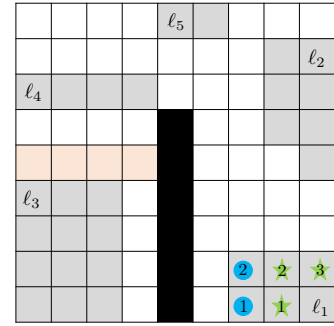


Figure 1. Illustration of the workspace and robot initial locations for the delivery tasks; see Example 1.

mail at the delivery site ℓ_3 . We consider two delivery tasks: (i) Two robots of type 1 visit building ℓ_2 to collaboratively pick up the mail and deliver it to the delivery site ℓ_3 , and one robot of type 2 must visit the control room ℓ_4 to disinfect robots of type 1 before they get to the delivery site ℓ_3 . (ii) One robot of type 1 travels between building ℓ_2 and the delivery site ℓ_3 back and forth to transport equipment, assuming that the disinfection area operates automatically after task (i). These tasks are more complex than typical task allocation problems due to the temporal operators like “before” and “back and forth”. Observe that in Fig. 1, the atomic propositions in Σ satisfied by initial robot locations are $\pi_{3,1}^1$ and $\pi_{2,2}^1$. Moreover, tasks (i) and (ii) can be captured by the valid formulas $\phi_1 = \diamond ((\pi_{2,1}^{2,1} \wedge \neg\pi_{2,1}^3) \wedge \diamond\pi_{2,1}^{3,1}) \wedge \diamond\pi_{1,2}^4 \wedge \neg\pi_{2,1}^3 \cup \pi_{1,2}^4$ and $\phi_2 = \square\diamond (\pi_{1,1}^{2,1} \wedge \diamond\pi_{1,1}^{3,1})$, respectively. Note that when binding the truth of atomic propositions, the value of χ is immaterial as long as it is the same non-zero number. Therefore, ϕ_2 can also be written as $\square\diamond (\pi_{1,1}^{2,2} \wedge \diamond\pi_{1,1}^{3,2})$. However, formulas $\diamond (\pi_{1,1}^{2,1} \wedge \diamond\pi_{2,1}^{3,1})$ and $\diamond (\pi_{2,2}^{2,1} \wedge \diamond\pi_{2,1}^{3,1})$ are two invalid formulas as they connect different numbers of robots i and robot types j , respectively.

A path of length h is defined as $\tau = s^0 \dots s^h$ and it captures the collective behavior of the team such that $s^{t-1} \rightarrow s^t, \forall t \in [h]$. Given a valid LTL^χ formula ϕ , a path τ that satisfies ϕ can be written in a prefix-suffix structure $\tau = \tau^{\text{pre}}[\tau^{\text{suf}}]^\omega$, where the prefix part $\tau^{\text{pre}} = s^0 \dots s^{h_1}$ is executed once followed by the indefinite execution of the suffix part $\tau^{\text{suf}} = s^{h_1} \dots s^{h_1+h_2} s^{h_1+h_2+1}$, where $s^{h_1+h_2+1} = s^{h_1}$ (Baier and Katoen 2008). We say that a path τ satisfies ϕ if (a) the trace, defined as $\text{trace}(\tau) := L(s^0) \dots L(s^{h_1})[L(s^{h_1}) \dots L(s^{h_1+h_2+1})]^\omega$, belongs to $\text{Words}(\phi^0)$, where ϕ^0 is obtained by replacing all induced atomic propositions in ϕ by their counterparts with the zero connector and (b) it is the same $\langle i, j \rangle$ that satisfy the induced atomic propositions $\pi_{i,j}^{k,\chi}$ in ϕ sharing the same nonzero connector χ . In other words, condition (a) restricts the label of the path, while condition (b) restricts the robots that participate in the satisfaction of induced atomic propositions. If $\phi \in \text{LTL}^0$, the satisfaction conditions only include (a).

3.3 Problem definition

Given a path $\tau_{r,j} = s_{r,j}^0, s_{r,j}^1, \dots, s_{r,j}^h$ of length h for robot $[r, j]$, we define the cost of $\tau_{r,j}$ as $J(\tau_{r,j}) = \sum_{t=0}^{h-1} d(s_{r,j}^t, s_{r,j}^{t+1})$, where $d : S \times S \rightarrow \mathbb{R}^+ \cup \{0\}$ is a cost function that maps a pair of free cells to a non-negative value like travel distance. The cost of path τ that combines all robot paths $\tau_{r,j}$ of length h is given by

$$J(\tau) = \sum_{r \in \mathcal{K}_j, j \in [m]} J(\tau_{r,j}). \quad (1)$$

For plans written in prefix-suffix form, we get

$$J(\tau) = \beta J(\tau^{\text{pre}}) + (1 - \beta) J(\tau^{\text{suf}}), \quad (2)$$

where $\beta \in [0, 1]$ is a user-specified parameter. Then, the problem addressed in this paper can be formulated as follows.

Problem 1. Consider a discrete workspace with labeled regions and obstacles, a team of n robots of m types, and a valid formula $\phi \in LTL^\chi$. Plan a path for each robot such that the specification ϕ is satisfied and the cost in (2) is minimized.

We refer to Problem 1 as the Multi-Robot Task Allocation problem under LTL specifications or LTL-MRTA. This is a single-task robot and multi-robot task (ST-MR) problem, where a robot is capable of one task and a task may require multiple robots. Since the ST-MR problem is NP-hard (Korsah et al. 2013; Nunes et al. 2017), so is the LTL-MRTA problem. Consequently, existing approaches to this problem become intractable for large-scale applications (Sahin et al. 2017a,b). In this work, we propose a new hierarchical framework to solve LTL-MRTA problems efficiently.

3.4 Assumptions

In this section, we discuss assumptions on the workspace and the NBA translated from the LTL specifications that are necessary to ensure completeness of our proposed hierarchical framework. As we discuss later in Section 7, these assumptions are mild and were satisfied by all tasks we tested our method on, regardless of their complexity.

3.4.1 Workspace: The following assumption ensures that regions in the workspace are well-defined and mutually exclusive.

Assumption 3.5. (Workspace). *Regions are disjoint, and each region spans consecutive cells. There exists a label-free path between any two regions, between any two label-free cells, and between any label-free cells and any regions.*

If regions are partially overlapping or span multiple clusters of cells, we can define additional atomic propositions to satisfy Assumption 3.5. Assumption 3.5 implies that there are no “holes” inside regions that generate different labels, label-free cells are connected, and each region is adjacent to a label-free cell.

3.4.2 Nondeterministic Büchi Automaton (NBA): Given a team of n robots and an LTL^χ formula ϕ , we can find a path τ that satisfies ϕ by operating on the corresponding NBA $\mathcal{A}_\phi = (\mathcal{V}, \mathcal{E})$, which can be constructed using existing tools, such as LTL2BA developed by Gastin and Oddoux (2001); see also Fig. 2 for the NBA of tasks (i) and (ii). Note that the NBA in Definition 2.1 is essentially a graph. Thus, in the remainder of this paper, we refer to the NBA by the graph \mathcal{A}_ϕ for notational convenience. Before we discuss our assumptions on the structure of the NBA \mathcal{A}_ϕ , we describe a list of pre-processing steps to obtain an “equivalent” NBA that does not lose any feasible paths that satisfy the specification ϕ . The goal is to remove infeasible and redundant transitions and the NBA and, therefore, reduce its size.

Specifically, let the propositional formula $\gamma \in \Sigma$ associated with every transition $v_1 \xrightarrow{\gamma} v_2$ in the NBA \mathcal{A}_ϕ be in *disjunctive normal form* (DNF), i.e., $\gamma = \bigvee_{p \in \mathcal{P}} \bigwedge_{q \in \mathcal{Q}_p} (\neg)\pi_{i,j}^{k,\chi}$, where the negation operator can only precede the atomic propositions and \mathcal{P} and \mathcal{Q}_p are proper index sets. Note that any propositional formula has an equivalent formula in DNF (Baier and Katoen 2008). We call $\mathcal{C}_p^\gamma = \bigwedge_{q \in \mathcal{Q}_p} (\neg)\pi_{i,j}^{k,\chi}$ the p -th clause of γ that includes a set \mathcal{Q}_p of positive and negative literals and each positive literal is an atomic proposition $\pi_{i,j}^{k,\chi} \in \mathcal{AP}$. Let $\text{cls}(\gamma)$ denote the set of clauses \mathcal{C}_p^γ in γ . And let $\text{lits}^+(\mathcal{C}_p^\gamma)$ and $\text{lits}^-(\mathcal{C}_p^\gamma)$ be the *positive subformula* and *negative subformula*, consisting of all positive literals and all negative literals in the clause \mathcal{C}_p^γ . Those subformulas are \top (constant true) if the corresponding literals do not exist. In what follows, we do not consider self-loops when we refer to edges in \mathcal{A}_ϕ , since self-loops can be captured by vertices. We call the propositional formula γ a *vertex label* if $v_1 = v_2$, otherwise, an *edge label*. With a slight abuse of notation, let $\gamma : \mathcal{V} \rightarrow \Sigma$ and $\gamma : \mathcal{V} \times \mathcal{V} \rightarrow \Sigma$ be the functions that map a vertex and edge in the NBA to its vertex label and edge label, respectively. Given an edge (v_1, v_2) , we call labels $\gamma(v_1)$ and $\gamma(v_2)$ the *starting* and *end* vertex labels, respectively. Next, we pre-process the NBA \mathcal{A}_ϕ by removing infeasible clauses and merging redundant literals. In particular, given a vertex or edge label γ in \mathcal{A}_ϕ we perform the following operations:

(1) *Absorption in $\text{lits}^+(\mathcal{C}_p^\gamma)$:* For each clause $\mathcal{C}_p^\gamma \in \text{cls}(\gamma)$, we delete the positive literal $\pi_{i,j}^k \in \text{lits}^+(\mathcal{C}_p^\gamma)$, replacing it with \top , if another $\pi_{i',j}^{k,\chi'} \in \text{lits}^+(\mathcal{C}_p^\gamma)$ exists such that $i \leq i'$. This is because if $\langle i', j \rangle$ are at region ℓ_k , i.e., $\pi_{i',j}^{k,\chi'}$ is true, so is $\pi_{i,j}^k$. Similarly, we replace $\pi_{i,j}^k$ by $\pi_{i-i',j}^k$ if $i > i'$, since $i - i'$ additional robots are needed to make $\pi_{i,j}^k$ true if $\pi_{i',j}^{k,\chi'}$ is true.

(2) *Absorption in $\text{lits}^-(\mathcal{C}_p^\gamma)$:* We delete the negative literal $\neg\pi_{i,j}^k \in \text{lits}^-(\mathcal{C}_p^\gamma)$, if another $\neg\pi_{i',j}^{k,\chi} \in \text{lits}^-(\mathcal{C}_p^\gamma)$ exists such that $i' < i$. This is because if $\neg\pi_{i',j}^{k,\chi}$ is true, so is $\neg\pi_{i,j}^k$.

(3) *Mutual exclusion in $\text{lits}^+(\mathcal{C}_p^\gamma)$:* We delete the clause $\mathcal{C}_p^\gamma \in \text{cls}(\gamma)$, replacing it with constant false \perp , if there exist two positive literals $\pi_{i,j}^{k,\chi}, \pi_{i,j}^{k',\chi} \in \text{lits}^+(\mathcal{C}_p^\gamma)$ such that $k \neq k'$ and $\chi \neq 0$. The reason is that the same i robots of type j cannot be at different regions at the same time.

(4) *Mutual exclusion in $\text{lits}^+(\mathcal{C}_p^\gamma)$ and $\text{lits}^-(\mathcal{C}_p^\gamma)$:* We delete the clause $\mathcal{C}_p^\gamma \in \text{cls}(\gamma)$ if there exist a positive literal $\pi_{i,j}^{k,\chi} \in \text{lits}^+(\mathcal{C}_p^\gamma)$ and a negative literal $\neg\pi_{i',j}^k \in \text{lits}^-(\mathcal{C}_p^\gamma)$

such that $i' \leq i$. This is because these literals are mutually exclusive.

(5) *Violation of team size*: For each clause $C_p^\gamma \in \text{cls}(\gamma)$, let $\text{lits}^+(j')$ denote literals in $\text{lits}^+(C_p^\gamma)$ that involve robots of type j' , i.e., $\text{lits}^+(j') = \{\pi_{i,j}^{k,\chi} \in \text{lits}^+(C_p^\gamma) | j = j'\}$. We delete the clause C_p^γ if the total required number of robots of type j exceeds the size $|\mathcal{K}_j|$, i.e., if there exists $j \in [m]$ such that $\sum_{\pi_{i,j}^{k,\chi} \in \text{lits}^+(j)} i > |\mathcal{K}_j|$.

Note that these pre-processing steps merely remove infeasible clauses and merge redundant literals in the NBA \mathcal{A}_ϕ , and they do not compromise any accepting words in $\mathcal{L}(\mathcal{A}_\phi)$ that can be generated by a feasible path. Therefore, with a slight abuse of notation, we continue to use \mathcal{A}_ϕ to refer to the NBA associated with formula ϕ that is obtained after these pre-processing steps.

Consider now an edge $e = (v_1, v_2)$ and its starting vertex v_1 in the NBA \mathcal{A}_ϕ and assume that the current state of \mathcal{A}_ϕ is vertex v_1 . For the NBA to transition to vertex v_2 , certain robots need to simultaneously reach certain regions or avoid certain regions in order to make $\gamma(v_1, v_2)$ true, while maintaining $\gamma(v_1)$ true en route. We assume that the transition to v_2 occurs immediately once $\gamma(v_1, v_2)$ becomes true. Therefore, we can define by a *subtask* the set of actions that need to be taken by a group of robots in order to activate a transition in the NBA. Formally, we have the following definition.

Definition 3.6. (Subtask). *Given an edge (v_1, v_2) in the NBA \mathcal{A}_ϕ , a subtask is defined by the associated edge label $\gamma(v_1, v_2)$ and starting vertex label $\gamma(v_1)$.*

Subtasks can be viewed as generalized reach-avoid tasks where specific types of robots should visit or avoid certain regions (the “reach” part of the tasks) while satisfying the starting vertex labels along the way (the “avoid” part of the tasks, which here is defined in a more general way compared to the conventional definition that requires robots to stay away from given regions in space).

Note that every accepting run defined in Section 2.1 consists of a sequence of subtasks, as they are defined in Definition 3.6. However, not all sequences of subtasks associated with an accepting run make progress towards accomplishing the task. In what follows, we restrict the accepting runs in an NBA to those that make progress towards accomplishing the task. But first, we provide some intuition using the following example.

Example 1. continued (Subtask progress in the pre-processed NBA \mathcal{A}_ϕ) The pre-processed NBAs corresponding to tasks (i) and (ii) are shown in Fig. 2 where the vertex labels are placed in square brackets next to each vertex. After pre-processing, the NBA \mathcal{A}_ϕ for task (i) does not change whereas some labels in the NBA \mathcal{A}_ϕ for task (ii) become \perp due to step (3). These labels are highlighted in orange.

In Fig. 2(a), v_{init} is the initial vertex and v_6 is the accepting vertex. Observe that all vertices have self-loops except for the initial vertex v_{init} . In each accepting run, e.g., $v_{\text{init}}, v_1, v_2, v_3, v_6, v_6^\omega$, the satisfaction of an edge label leads to the satisfaction of its end vertex label, assuming this end vertex label is not \perp . For instance, label $\pi_{2,1}^{2,1} \wedge \neg\pi_{2,1}^3$ of edge (v_1, v_2) implies label $\neg\pi_{2,1}^3$ of vertex v_2 , and label $\neg\pi_{2,1}^3$ of edge (v_{init}, v_1) implies label $\neg\pi_{2,1}^3$ of its end vertex

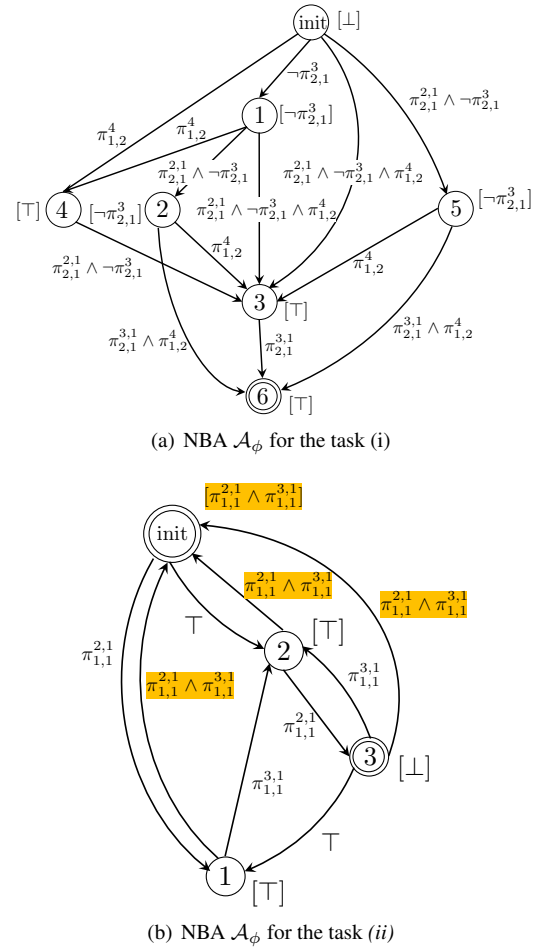


Figure 2. NBA \mathcal{A}_ϕ for tasks (i) and (ii).

v_1 . Intuitively, the completion of a subtask indicated by the satisfaction of its edge label, automatically activates the subtasks that immediately follow it indicated by the satisfaction of their starting vertex labels. This is because once the edge is enabled, its end vertex label should be satisfied at the next time instant; otherwise, progress in the NBA \mathcal{A}_ϕ will get stuck. The same observation also applies to the NBA in Fig. 2(b) where the vertex v_{init} is both an initial and accepting vertex and v_3 is another accepting vertex. The accepting run $v_{\text{init}}, v_2, v_3, (v_1, v_2, v_3)^\omega$ includes one pair of initial and accepting vertices, v_{init} and v_3 , and the accepting run $v_{\text{init}}, v_2, v_1, v_{\text{init}}^\omega$ (although infeasible) includes one pair of initial and accepting vertices, v_{init} and v_{init} . Note that we view the two v_{init} vertices differently, one as the initial vertex and the other as the accepting vertex. Furthermore, label $\pi_{1,1}^{3,1}$ of edge (v_1, v_2) implies label T of its end vertex v_2 ; the same holds for the edge (v_2, v_{init}) and its end vertex v_{init} (although infeasible). It is noteworthy that even though the accepting vertex v_3 does not have a self-loop, the satisfaction of the label $\pi_{1,1}^{2,1}$ of its incoming edge (v_2, v_3) leads to the satisfaction of the label T of its outgoing edge (v_3, v_1) . If the satisfaction of the incoming edge label does not imply satisfaction of the outgoing edge label, then progress in the NBA will get stuck at v_3 since the label $\pi_{1,1}^{2,1} \wedge \pi_{1,1}^{3,1}$ of edge (v_3, v_{init}) is infeasible and the transition between regions ℓ_2 and ℓ_3 requires more than one time steps; see Fig. 1, which makes the label $\pi_{1,1}^{3,1}$ of edge (v_3, v_2) unsatisfiable at the next time instant.

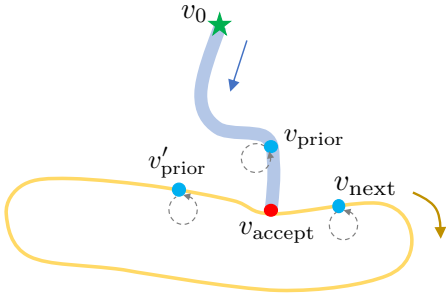


Figure 3. Graphical depiction of the accepting run in the prefix-suffix structure when v_{accept} does not have a self-loop, which resembles a lasso. The shaded blue line and the orange loop represent the prefix and suffix part, respectively. The arrow indicates the progression direction and the gray circles indicate the self-loops.

Motivated by the observations in Example 1, we introduce the notions of *implication* and *strong implication* between two propositional formulas. Then, we define a *restricted accepting run* in the NBA \mathcal{A}_ϕ in a prefix-suffix structure. The completeness of our method relies on the assumption that the set of restricted accepting runs in the NBA \mathcal{A}_ϕ is nonempty.

Definition 3.7. (Implication and strong implication). *Given two propositional formulas γ and γ' over \mathcal{AP} , we say that formula γ implies γ' , denoted by $\gamma \Rightarrow \gamma'$, if for each clause $C_p^\gamma \in \text{cls}(\gamma)$, there exists a clause $C_{p'}^{\gamma'} \in \text{cls}(\gamma')$ such that $C_{p'}^{\gamma'}$ is a subformula of C_p^γ , i.e., all literals in $C_{p'}^{\gamma'}$ also appear in C_p^γ . By default, \top is a subformula of any clause. In addition, formula γ strongly implies γ' , denoted by $\gamma \Rightarrow_s \gamma'$, if $\gamma \Rightarrow \gamma'$, and for each clause $C_{p'}^{\gamma'} \in \text{cls}(\gamma')$, there exists a clause $C_p^\gamma \in \text{cls}(\gamma)$ such that $C_{p'}^{\gamma'}$ is a subformula of C_p^γ .*

Intuitively, if $\gamma \Rightarrow \gamma'$ or $\gamma \Rightarrow_s \gamma'$, robot locations that satisfy γ also satisfy γ' .

Definition 3.8. (Restricted accepting run). *Given the NBA \mathcal{A}_ϕ (after pre-processing) corresponding to an LTL^χ formula, we call any accepting run in a prefix-suffix structure $\rho = \rho^{\text{pre}}[\rho^{\text{suf}}]^\omega = v_0, \dots, v_{\text{prior}}, v_{\text{accept}}[v_{\text{next}}, \dots, v'_{\text{prior}}, v_{\text{accept}}]^\omega$ (see Fig. 3), a restricted accepting run, if it satisfies the following conditions:*

- (a) *If a vertex is both an initial vertex v_0 and an accepting vertex v_{accept} , we treat it as two different vertices, namely an initial vertex and an accepting vertex. The accepting vertex v_{accept} appears only once at the end in both the prefix and suffix parts. In the prefix part $v_0, \dots, v_{\text{prior}}, v_{\text{accept}}$, if a vertex appears multiple times, all repetitive occurrences are consecutive. The same holds for the suffix part $v_{\text{next}}, \dots, v'_{\text{prior}}, v_{\text{accept}}$;*
- (b) *There only exist one initial vertex v_0 and one accepting vertex v_{accept} in the accepting run (they can appear multiple times in a row). Different accepting runs can have different pairs of initial and accepting vertices;*
- (c) *In the prefix part, only initial and accepting vertices, v_0 and v_{accept} , are allowed not to have self-loops, i.e., their vertex labels can be \perp . In the suffix part, only the accepting vertex v_{accept} is allowed not to have a self-loop;*

(d) *For any two consecutive vertices v_1, v_2 in the accepting run ρ , if $v_1 \neq v_2$, $v_2 \neq v_{\text{accept}}$ and v_2 has a self-loop, then the edge label $\gamma(v_1, v_2)$ strongly implies the end vertex label $\gamma(v_2)$, i.e., $\gamma(v_1, v_2) \Rightarrow_s \gamma(v_2)$;*

(e) *In the suffix part ρ^{suf} , if $v_{\text{accept}} = v_{\text{next}}$ (this happens when v_{accept} has a self-loop), then ρ^{suf} only contains the vertex v_{accept} . Meanwhile, the label of the edge $(v_{\text{prior}}, v_{\text{accept}})$ implies the label of the vertex v_{accept} , i.e., $\gamma(v_{\text{prior}}, v_{\text{accept}}) \Rightarrow \gamma(v_{\text{accept}})$;*

(f) *In the suffix part, if $v_{\text{accept}} \neq v_{\text{next}}$ (this can happen when v_{accept} does not have a self-loop), then the label of the edge $(v_{\text{prior}}, v_{\text{accept}})$ implies the label of the edge $(v_{\text{accept}}, v_{\text{next}})$, i.e., $\gamma(v_{\text{prior}}, v_{\text{accept}}) \Rightarrow \gamma(v_{\text{accept}}, v_{\text{next}})$. Also, the label $\gamma(v_{\text{prior}}, v_{\text{accept}})$ implies the label of the edge $(v'_{\text{prior}}, v_{\text{accept}})$, i.e., $\gamma(v_{\text{prior}}, v_{\text{accept}}) \Rightarrow \gamma(v'_{\text{prior}}, v_{\text{accept}})$. Note that v_{prior} and v'_{prior} can be different.*

In what follows, we discuss the conditions in Definition 3.8 in more detail. Specifically, conditions (a) and (b) require that a restricted accepting run is “simple”. Specifically, condition (a) states that vertices v_0 and v_{accept} can be treated differently since they mark different progress towards accomplishing a task. The prefix and suffix parts of a restricted accepting run end once v_{accept} is reached, as in Smith et al. (2010). By aggregating consecutive identical vertices in the prefix part of a restricted accepting run into one single vertex, there are no identical vertices in the “compressed” prefix part. That is, it contains no cycles. The presence of a cycle is redundant since it implies negative progress towards accomplishing the task. The same applies to the suffix part. On the other hand, condition (b) states that a restricted accepting run is basically an accepting run defined in Section 2.1 that is further defined over a pair of initial and accepting vertices. In Section 4, we extract smaller sub-NBAs from the NBA \mathcal{A}_ϕ for each pair of initial and accepting vertices, which helps reduce complexity of the problem.

Conditions (c)-(f) require that the completion of a subtask in a restricted accepting run automatically activates the subtasks that immediately follow it; see Example 1. This ensures that robots are given adequate time to undertake subsequent subtasks after completing the current subtask. Accepting runs that do not satisfy conditions (c)-(d) are disregarded. In fact, in Section 4.1 we prune vertices and edges in the NBA that violate these conditions, further reducing the size of the NBA. Finally, the implication $\gamma(v_{\text{prior}}, v_{\text{accept}}) \Rightarrow \gamma(v_{\text{accept}}, v_{\text{next}})$ in condition (f) requires that the robot locations enabling the last edge in the prefix part of a restricted accepting run also enable the first edge in the suffix part. As a result, we can find the prefix and suffix parts of a restricted accepting run separately. Otherwise, the progress in the NBA \mathcal{A}_ϕ may get stuck since these two edge labels need to be satisfied at two consecutive time instants, similar to conditions (d) and (e). Also, as the suffix part of a restricted accepting run is a loop, robots need to return to their initial locations in the suffix part after executing the suffix part once. The relation $\gamma(v_{\text{prior}}, v_{\text{accept}}) \Rightarrow \gamma(v'_{\text{prior}}, v_{\text{accept}})$ requires that the initial locations in the suffix part of a restricted accepting run enable the edge $(v'_{\text{prior}}, v_{\text{accept}})$, which ensures that the robots can travel back to the initial locations in the suffix part and, as a result, activate the transition in \mathcal{A}_ϕ back to the vertex v_{accept} .

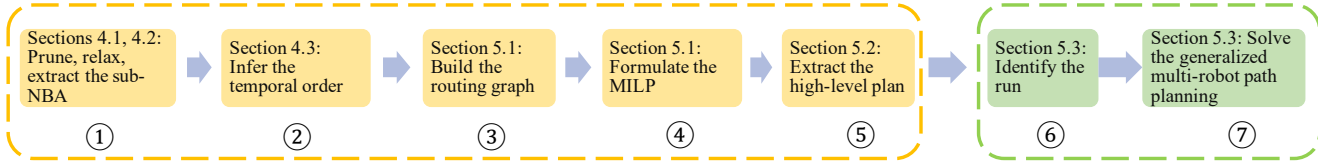


Figure 4. Schematic overview of the proposed method. The first five boxes correspond to the relaxation stage and the last two constitute the correction stage.

that allows to repeat the suffix part ρ^{suf} . Finally, we make the following assumption on the structure of the NBA \mathcal{A}_ϕ .

Assumption 3.9. (Existence of restricted accepting runs). *The set of restricted accepting runs in the NBA \mathcal{A}_ϕ is non-empty.*

We note that the existence of restricted accepting runs in the NBA \mathcal{A}_ϕ is not a restrictive assumption. For example, the sets of restricted accepting runs in the NBA \mathcal{A}_ϕ for tasks (i) and (ii) in Example 1 satisfy Assumption 3.9. Similarly, common robotic tasks like sequencing and coverage have NBAs that contain restricted accepting runs. In fact, all LTL tasks we considered in our numerical simulations in Section 7 have NBAs that contain restricted accepting runs, regardless of their complexity.

3.4.3 Robot paths: The definition of restricted accepting runs is based entirely on the structure of the NBA and logical implication relations. However, Definition 3.8 does not describe how to characterize robot paths that induce restricted accepting runs. In what follows, we discuss conditions under which robot paths satisfy restricted accepting runs. We call such paths *satisfying paths* and we assume that such satisfying paths exist.

Definition 3.10. (Satisfying paths of restricted accepting runs). *Given a team of n robots and a valid specification $\phi \in LTL^\chi$, a robot path τ is a satisfying path that induces a restricted accepting run, if the following conditions hold:*

- (a) *If a vertex label is satisfied by the path τ , it is always satisfied by the same clause that is always satisfied by the same fleet of robots;*
- (b) *If a clause in an edge label is satisfied by the path τ , then a clause in the end vertex label is also satisfied. Moreover, the fleet of robots satisfying the positive subformula of the clause in the end vertex label is the same as the fleet of robots satisfying the positive subformula of the clause in the corresponding edge label;*
- (c) *Robot locations enabling the edges $(v_{\text{accept}}, v_{\text{next}})$ and $(v'_{\text{prior}}, v_{\text{accept}})$ in the suffix part of a restricted accepting run are identical to robot locations enabling the edge $(v_{\text{prior}}, v_{\text{accept}})$ in the prefix part.*

Definition 3.10 is closely related to the definition of a restricted accepting run. Specifically, condition (a) in Definition 3.10 requires that once a fleet of robots satisfies a vertex label in a restricted accepting run, then these robots remain idle during the next time instant so that the same clause in this vertex label is still satisfied. This satisfies condition (a) in Definition 3.8. Furthermore, condition (b) in Definition 3.10 requires that once a fleet of robots satisfies

an edge label in a restricted accepting run, then these robots remain idle during the next time instant so that the clause in the end vertex label that is implied by the clause that is satisfied in the edge label is also satisfied. This satisfies condition (d) in Definition 3.8.

Finally, condition (c) in Definition 3.10 requires that the robot locations enabling the edge $(v_{\text{prior}}, v_{\text{accept}})$ in the prefix part of a restricted accepting run coincide with the initial locations of the robots that enable the edge $(v'_{\text{prior}}, v_{\text{accept}})$ in the suffix part of the restricted accepting run, as per condition (f) in Definition 3.8. Therefore, condition (c) in Definition 3.10 requires that the robots travel along a loop so that the suffix part of the restricted accepting run is executed indefinitely. In what follows, we make the following assumption.

Assumption 3.11. (Existence of satisfying paths). *There exist robot paths that satisfy the restricted accepting runs in the NBA \mathcal{A}_ϕ .*

3.5 Outline of the proposed method

A schematic diagram of our proposed method is shown in Fig. 4, which consists of a relaxation and a correction stage. Specifically, during the relaxation stage, we ignore the negative literals in the NBA \mathcal{A}_ϕ and formulate a MILP to allocate subtasks to robots and determine time-stamped robot waypoints that satisfy the task ϕ ; see the first five blocks inside the orange box in Fig. 4. To this end, we first prune the NBA \mathcal{A}_ϕ by deleting infeasible transitions and then relax it by removing negative subformulas so that transitions in the relaxed NBA are solely satisfied by robots that meet at certain regions; see Section 4.1. The idea to temporarily remove negative literals from the NBA is motivated by “lazy collision checking” methods in robotics and allows to simplify the planning problem as the constraints are not considered during planning and are only checked during execution, when needed. Then, since by condition (b) in Definition 3.8, restricted accepting runs contain only one initial vertex and one accepting vertex, for every pair of initial and accepting vertices in the relaxed NBA, we extract a sub-NBA of smaller size; see Section 4.2. The sub-NBAs are used to extract subtasks and temporal orders between them captured by a set of posets (see Section 4.3), and construct routing graphs, one for each poset, that capture the regions that the robots need to visit and the temporal order of the visits so that the subtasks extracted from the sub-NBAs are satisfied; see Section 5.1. Finally, given the routing graph corresponding to each poset we formulate a MILP inspired by the vehicle routing problem (see Section 5.1) to obtain a high-level task allocation plan along with time-stamped waypoints that the robots need to visit to satisfy

the task specification (see Section 5.2). The second part of our approach consists of the correction stage that is illustrated in the last two blocks inside the green box in Fig. 4. During the correction stage, we introduce the negative literals back into the NBA and formulate a collection of generalized multi-robot path planning problems, one for each poset, to design low-level executable robot paths that satisfy the original specification (see Section 5.3). Under the mild assumptions discussed in Section 3.4, completeness of our proposed method is shown in Theorem 6.1 in Section 6.

Remark 3.12. We note that Assumption 3.11 on the existence of satisfying paths is only a sufficient condition that needs to be satisfied to show completeness of our proposed method, as shown in the theoretical analysis of Section 6. The robot path returned by our method may not be a satisfying path, although it still satisfies the specification ϕ .

4 Extraction of Subtasks from the NBA and Inferring their Temporal Order

In this section, we first prune and relax the NBA \mathcal{A}_ϕ by removing infeasible transitions and negative literals. As discussed before, this step is motivated by "lazy collision checking" methods in robotics and allows to simplify the planning problem by checking constraint satisfaction during the execution of the plans rather than their synthesis. Then, we extract sub-NBAs from the relaxed NBA and use these sub-NBAs to obtain sequences of subtasks and a temporal order between them that need to be satisfied so that the global specification is satisfied. These steps correspond to blocks ① and ② in Fig. 4.

4.1 Pruning and relaxation of the NBA

To prune infeasible transitions from the NBA \mathcal{A}_ϕ , we first delete all edges labeled with \perp , as they cannot be enabled. We also delete vertices and edges in \mathcal{A}_ϕ that do not belong to restricted accepting runs, as defined in Definition 3.8. Specifically, we delete all vertices without self-loops except for the initial and accepting vertices, as per condition (c) in Definition 3.8. Furthermore, for every vertex other than the accepting vertex, we delete all its incoming edges with edge labels that do not strongly imply its vertex label, as per condition (d) in Definition 3.8. Finally, we delete every vertex, except for the initial vertex, that cannot be reached by other vertices. We note that these pruning steps do not compromise any feasible solution to Problem 1 that induces a restricted accepting run in \mathcal{A}_ϕ , as shown in Lemma C.2 in Appendix C.

We denote by \mathcal{A}_ϕ^- the resulting pruned NBA. Given the pruned NBA \mathcal{A}_ϕ^- , we further relax it by replacing each negative literal in vertex or edge labels with \top . Let $\mathcal{A}_{\text{relax}}$ denote the relaxed NBA. Note that, when the specification ϕ does not involve negative atomic propositions, we have $\mathcal{A}_{\text{relax}} = \mathcal{A}_\phi^-$. Furthermore, Lemma C.3 in Appendix C states that the language accepted by \mathcal{A}_ϕ^- is included in the language accepted by $\mathcal{A}_{\text{relax}}$, so this relaxation step does not remove feasible solutions to Problem 1. In other words, $\mathcal{A}_{\text{relax}}$ is an over-approximation of \mathcal{A}_ϕ^- . However, a solution to Problem 1 based on $\mathcal{A}_{\text{relax}}$ may not satisfy the specification ϕ . Therefore, the correction stage, shown in Fig. 4 and

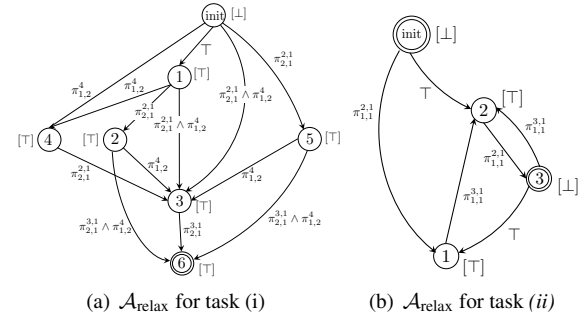


Figure 5. The relaxed NBA $\mathcal{A}_{\text{relax}}$ for tasks (i) and (ii).

described in detail in Appendix B, is necessary in order to introduce the negative literals back in the NBA and modify the solution obtained from $\mathcal{A}_{\text{relax}}$ in order to satisfy ϕ . Note that \mathcal{A}_ϕ^- and $\mathcal{A}_{\text{relax}}$ are sub-NBAs of \mathcal{A}_ϕ in terms of vertices and edges. Thus, labels and runs in \mathcal{A}_ϕ^- and $\mathcal{A}_{\text{relax}}$ can be mapped to labels and runs in \mathcal{A}_ϕ . For instance, for an edge label γ in $\mathcal{A}_{\text{relax}}$, we denote by γ_ϕ the corresponding label in \mathcal{A}_ϕ (including negative literals).

Example 1. continued (Pruning and relaxation of the NBA \mathcal{A}_ϕ) The pruned NBA \mathcal{A}_ϕ^- for the task (i) is the same as the original NBA in Fig. 2(a). The relaxed NBA $\mathcal{A}_{\text{relax}}$ is shown in Fig. 5(a). The pruned NBA \mathcal{A}_ϕ^- for the task (ii) is the same as the relaxed NBA $\mathcal{A}_{\text{relax}}$ which is shown in Fig. 5(b). Particularly, \mathcal{A}_ϕ^- is obtained from \mathcal{A}_ϕ in Fig. 2(b) by removing edges (v_1, v_{init}) , (v_2, v_{init}) , (v_3, v_{init}) and replacing $\gamma(v_{\text{init}})$ with \perp .

4.2 Extraction of sub-NBA $\mathcal{A}_{\text{subtask}}$ from $\mathcal{A}_{\text{relax}}$

In this section, we extract multiple sub-NBAs from the relaxed NBA $\mathcal{A}_{\text{relax}}$, one for every pair of initial and accepting vertices in $\mathcal{A}_{\text{relax}}$; see block ① in Fig. 4. Then, in Section 4.3, we determine the temporal order among subtasks in every sub-NBA.

4.2.1 Sorting the pairs of initial and accepting vertices by path length: As required by condition (b) in Definition 3.8, every restricted accepting run in $\mathcal{A}_{\text{relax}}$ contains one pair of initial and accepting vertices. In what follows, we sort all pairs of initial and accepting vertices in $\mathcal{A}_{\text{relax}}$ in an ascending order so that the pair of initial and accepting vertices connected by a restricted accepting run with the shortest length appears first. Then in Section 4.2.2, we extract a sub-NBA from $\mathcal{A}_{\text{relax}}$ for each pair in this ascending order. Intuitively, the sub-NBAs corresponding to restricted accepting runs of shorter length generally will contain fewer subtasks to be completed.

4.2.1.1 Computation of the shortest simple prefix path: Given a pair of an initial vertex v_0 and an accepting vertex v_{accept} in $\mathcal{A}_{\text{relax}}$, we first compute the shortest simple path from v_0 to v_{accept} in terms of the number of edges/subtasks, where a simple path does not contain any repeating vertices, as per condition (a) in Definition 3.8 that excludes cycles from restricted accepting runs. This step corresponds to the prefix part of a restricted accepting run. To this end, we first remove all other initial vertices and accepting vertices from $\mathcal{A}_{\text{relax}}$. This will not affect the restricted accepting runs in $\mathcal{A}_{\text{relax}}$ associated with the pair v_0 and v_{accept} due to condition

(b) in Definition 3.8. Then, depending on whether the initial vertex v_0 has a self-loop, we proceed as follows.

(1) If v_0 does not have a self-loop, i.e., $\gamma(v_0) = \perp$: We remove all outgoing edges v_0 in $\mathcal{A}_{\text{relax}}$ with label γ , if the initial robot locations do not satisfy the corresponding edge label γ_ϕ (including the negative literals) in \mathcal{A}_ϕ . We emphasize that we need to check satisfaction of γ_ϕ in the NBA \mathcal{A}_ϕ instead of satisfaction of γ in the relaxed NBA $\mathcal{A}_{\text{relax}}$, since if initial robot locations cannot enable an edge starting from v_0 in \mathcal{A}_ϕ , there is no reason to consider this edge in any NBA.

(2) If v_0 has a self-loop, i.e., $\gamma(v_0) \neq \perp$: We check whether the initial robot locations satisfy $\gamma_\phi(v_0)$ in the NBA \mathcal{A}_ϕ . If yes, we do nothing; otherwise, we proceed as in case (1) in this part and remove the self-loop of v_0 as well as all its outgoing edges in $\mathcal{A}_{\text{relax}}$ if the initial robot locations do not satisfy the corresponding edge label γ_ϕ in \mathcal{A}_ϕ .

Next, the shortest simple path connecting v_0 and v_{accept} can be found using Dijkstra's algorithm. Note that if a vertex is both an initial and accepting vertex, we treat it once as the initial vertex and once as the accepting vertex, although it appears twice in the shortest simple path.

4.2.1.2 Computation of the shortest simple prefix cycle: Next, we compute the shortest simple cycle around v_{accept} in $\mathcal{A}_{\text{relax}}$, where repeating vertices only appear at the beginning and at the end of the simple cycle. This step corresponds to the suffix part of a restricted accepting run, which is conducted in the original NBA $\mathcal{A}_{\text{relax}}$. If v_{accept} in $\mathcal{A}_{\text{relax}}$ has a self-loop, then the length of the shortest simple cycle is 0. Otherwise, similar to steps in Section 4.2.1.1 used to find the shortest simple prefix path, we first remove all other accepting vertices from $\mathcal{A}_{\text{relax}}$ and then remove all initial vertices (including v_0) if they do not have self-loops. In this way, the only vertex that does not have a self-loop is the accepting vertex v_{accept} . This will not affect those restricted accepting runs that are related to v_0 and v_{accept} due to conditions (b) and (c) in Definition 3.8.

Finally, the length associated with the pair v_0 and v_{accept} is equal to the total length of the shortest simple prefix path and the shortest simple prefix cycle connecting these vertices in $\mathcal{A}_{\text{relax}}$. By default, if no simple path or cycle exists for the pair v_0 and v_{accept} , the length is infinite, which means there is no restricted accepting run for this pair. We repeat this process for all pairs of initial and accepting vertices in $\mathcal{A}_{\text{relax}}$ and sort them in ascending order in terms of the total length. As discussed before, we plan first for pairs with shorter length since they contain fewer subtasks to be completed.

4.2.2 Extraction of the sub-NBA $\mathcal{A}_{\text{subtask}}$: For every pair of vertices v_0 and v_{accept} in $\mathcal{A}_{\text{relax}}$ connected by a simple path of finite total length in the above ascending order, our goal is to determine time-stamped task allocation plans for all robots that induce the simple prefix path and simple suffix cycle in $\mathcal{A}_{\text{relax}}$ connecting v_0 and v_{accept} . To do this, we extract one sub-NBA from the NBA $\mathcal{A}_{\text{relax}}$ that we can use to construct the prefix part of the plan and one that we can use to construct the suffix part of the plan, respectively. Here, we discuss the sub-NBA for the prefix part. The sub-NBA for the suffix part is similar and is discussed in Appendix A.3.

Given the pair of vertices v_0 and v_{accept} , we construct a prefix sub-NBA $\mathcal{A}_{\text{subtask}}$ by the following three steps. First,

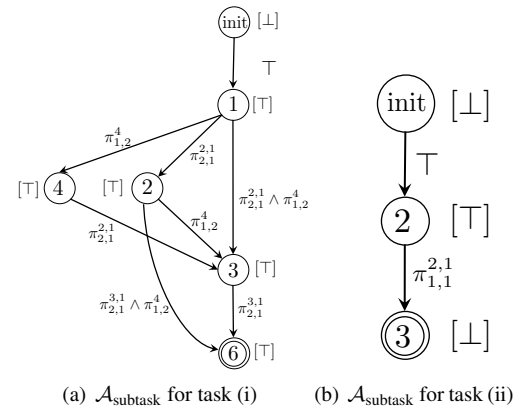


Figure 6. Sub-NBA $\mathcal{A}_{\text{subtask}}$ for the prefix part of tasks (i) and (ii) in Example 1, obtained from the NBA $\mathcal{A}_{\text{relax}}$ in Fig. 5.

we follow exactly the same steps in Section 4.2.1.1 that computes the shortest simple prefix path to prune the NBA $\mathcal{A}_{\text{relax}}$. Next, we remove all outgoing edges from v_{accept} if $v_{\text{accept}} \neq v_0$, because we focus on the prefix part. Finally, let \mathcal{V}_s denote the set that contains all remaining vertices in $\mathcal{A}_{\text{relax}}$ that belong to some path connecting v_0 and v_{accept} . Then, we construct a sub-NBA $\mathcal{A}_{\text{subtask}} = (\mathcal{V}_s, \mathcal{E}_s)$ from $\mathcal{A}_{\text{relax}}$ that includes all edges that connect the vertices in \mathcal{V}_s . The sub-NBA $\mathcal{A}_{\text{subtask}}$ contains prefix parts of all restricted accepting runs associated with the pair v_0 and v_{accept} .

Example 1. continued (Sub-NBA $\mathcal{A}_{\text{subtask}}$) The sub-NBA $\mathcal{A}_{\text{subtask}}$ for the prefix parts of plans associated with tasks (i) and (ii) are shown in Fig. 6. For task (i), given the pair v_{init} and v_6 in the relaxed NBA $\mathcal{A}_{\text{relax}}$ in Fig. 5(a), the total length is $3 + 0 = 3$ (edges $(v_{\text{init}}, v_3), (v_{\text{init}}, v_4), (v_{\text{init}}, v_5)$ were removed since v_{init} does not have a self-loop and all robots initially located inside region ℓ_1 do not satisfy their labels; see Fig. 1). The NBA $\mathcal{A}_{\text{subtask}}$, shown in Fig. 6(a) is obtained by removing edges $(v_{\text{init}}, v_3), (v_{\text{init}}, v_4), (v_{\text{init}}, v_5), (v_5, v_3), (v_5, v_6)$ and vertex v_5 from $\mathcal{A}_{\text{relax}}$. For task (ii), given the pair v_{init} and v_{init} , there is no cycle leading back to v_{init} , so the total length is infinite and there is no corresponding sub-NBA $\mathcal{A}_{\text{relax}}$. The total length for the pair v_{init} and v_3 is $2 + 2 = 4$. The NBA $\mathcal{A}_{\text{subtask}}$ is shown in Fig. 6(b), where edges (v_{init}, v_1) and (v_1, v_2) are removed since v_{init} does not have a self-loop and initial robot locations do not satisfy their labels.

Example 1. continued (Subtasks in $\mathcal{A}_{\text{subtask}}$) The sub-NBA $\mathcal{A}_{\text{subtask}}$ is composed of subtasks that need to be satisfied in specific orders to reach the accepting vertex. For instance, the path $v_{\text{init}}, v_1, v_4, v_3, v_6$ in Fig. 5(a) requires that first $\langle 1, 2 \rangle$ visits the control room ℓ_4 , then $\langle 2, 1 \rangle$ visit the office building ℓ_2 and finally the same two robots of type 1 drop off the mail at the delivery site ℓ_3 . By definition of task (i), the temporal order between these subtasks specifies that the time when $\langle 1, 2 \rangle$ visits the control room ℓ_4 is independent from the time when $\langle 2, 1 \rangle$ pick up the mail at the building ℓ_2 , and that $\langle 1, 2 \rangle$ visiting ℓ_4 and $\langle 2, 1 \rangle$ visiting ℓ_2 should occur prior to $\langle 2, 1 \rangle$ visiting the delivery site ℓ_3 .

4.2.3 Pruning the sub-NBA $\mathcal{A}_{\text{subtask}}$: Observe that the sub-NBA $\mathcal{A}_{\text{subtask}}$ in Fig. 6(a) still constitutes a large portion

of $\mathcal{A}_{\text{relax}}$ in Fig. 5(a), which is common in practice, since there are typically many more edges than vertices in $\mathcal{A}_{\text{relax}}$. However, some edges/subtasks are “redundant” in that they can be decomposed into more elementary edges/subtasks. Therefore, in what follows, we further prune the NBA $\mathcal{A}_{\text{subtask}}$ by removing such redundant edges.

Recall Definition 3.6 where subtasks are defined by their edge labels and starting vertex labels. Next we define the notion of equivalent subtasks.

Definition 4.1. (Equivalent subtasks). *Subtasks (v_1, v_2) and (v'_1, v'_2) in an NBA \mathcal{A} are equivalent, denoted by $(v_1, v_2) \sim (v'_1, v'_2)$, if $\gamma(v_1) = \gamma(v'_1)$, $\gamma(v_1, v_2) = \gamma(v'_1, v'_2)$ and they are not in the same path that connects the same pair of initial and accepting vertices.*

The last condition in Definition 4.1 is necessary since two subtasks in the same path mark different progress towards completing a task, even if they have identical labels. Recall that in task (i) in Example 1, certain regions can be visited in parallel. To capture the parallel visits, we define the following two properties over vertices in $\mathcal{A}_{\text{subtask}}$, namely, the independent diamond (ID) property adapted from Stefanescu (2006) and the sequential triangle (ST) property over vertices; see also Fig. 7.

Definition 4.2. (Independent diamond property). *Given four different vertices v_1, v_2, v_3, v_4 in the NBA $\mathcal{A}_{\text{subtask}}$, we say that these four vertices satisfy the ID property if*

- (a) $\gamma(v_1) = \gamma(v_2) = \gamma(v_4)$;
- (b) $v_1 \xrightarrow{\gamma} v_2 \xrightarrow{\gamma'} v_3$;
- (c) $v_1 \xrightarrow{\gamma'} v_4 \xrightarrow{\gamma} v_3$;
- (d) $v_1 \xrightarrow{\gamma \wedge \gamma'} v_3$;
- (e) $\gamma_\phi(v_3) = \top$ if $v_3 = v_{\text{accept}}$.

Intuitively, if vertices v_1, v_2, v_3 , and v_4 in $\mathcal{A}_{\text{subtask}}$ satisfy the ID property (see Fig. 7(a)), then conditions (a)-(c) in Definition 4.2 that the subtasks $(v_1, v_2) \sim (v_4, v_3)$ and $(v_1, v_4) \sim (v_2, v_3)$ in $\mathcal{A}_{\text{subtask}}$ are equivalent, while conditions (b)-(d) in Definition 4.2 state that their order is arbitrary, i.e., one can proceed the other or they can occur simultaneously. We refer to (v_1, v_3) as the *composite* subtask and (v_1, v_2) , (v_1, v_4) as the *elementary* subtasks. Although both can lead to vertex v_3 , composite subtasks are “redundant”, since elementary subtasks can be executed independently and, therefore, their labels are easier to satisfy, compared to composite tasks that need to be executed simultaneously and, therefore, more conditions need to hold so that their labels are satisfied. Note that we conduct the \top -check in condition (e) in Definition 4.2 on the NBA \mathcal{A}_ϕ so that condition (f) in Definition 3.8 is satisfied which means that the set of restricted accepting runs is not affected if the edge (v_1, v_3) is removed. This result is formally shown in Lemma C.5 in Appendix C. In words, if $\gamma_\phi(v_3) \neq \top$ with $v_3 = v_{\text{accept}}$, and if a restricted accepting run traverses edges (v_1, v_{accept}) and $(v_{\text{accept}}, v_{\text{next}})$ where $v_{\text{accept}} \neq v_{\text{next}}$, then condition (f) in Definition 3.8 states that $\gamma_\phi(v_1, v_{\text{accept}}) \Rightarrow \gamma_\phi(v_{\text{accept}}, v_{\text{next}})$. However $\gamma_\phi(v_2, v_{\text{accept}})$ and $\gamma_\phi(v_4, v_{\text{accept}})$ may not imply $\gamma_\phi(v_{\text{accept}}, v_{\text{next}})$ since they are subformulas of $\gamma_\phi(v_1, v_{\text{accept}})$. Therefore, removing the composite edge

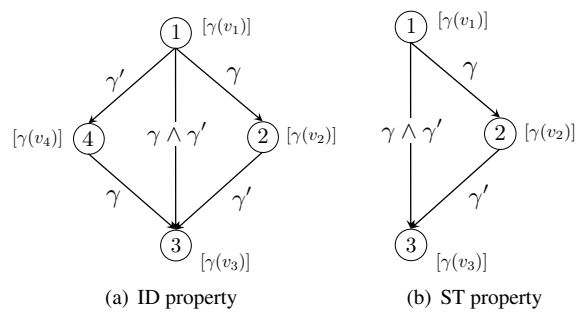


Figure 7. Independent diamond and sequential triangle properties.

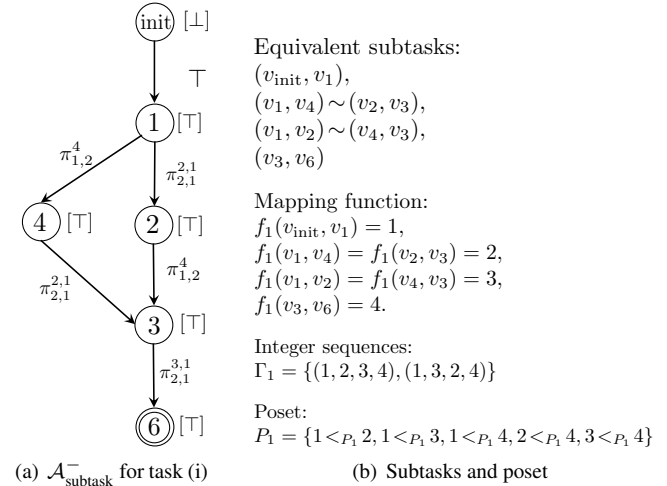


Figure 8. The NBA $\mathcal{A}_{\text{subtask}}^-$ and corresponding subtasks.

(v_1, v_{accept}) risks emptying the set of restricted accepting runs.

Definition 4.3. (Sequential triangle property). *Given three different vertices v_1, v_2, v_3 in the NBA $\mathcal{A}_{\text{subtask}}$, we say that these three vertices v_1, v_2, v_3 satisfy the ST property if*

- (a) $v_1 \xrightarrow{\gamma} v_2 \xrightarrow{\gamma'} v_3$;
- (b) $v_1 \xrightarrow{\gamma \wedge \gamma'} v_3$;
- (c) $\gamma_\phi(v_3) = \top$ if $v_3 = v_{\text{accept}}$.

If vertices v_1, v_2 , and v_3 in $\mathcal{A}_{\text{subtask}}$ satisfy the ST property (see Fig. 7(b)), then conditions (a) and (b) in Definition 4.3 state that subtask (v_1, v_2) should be satisfied no later than (v_2, v_3) . Note that if vertices v_1, v_2, v_3, v_4 satisfy the ID property, then v_1, v_2, v_3 and v_1, v_4, v_3 satisfy the ST property. Using these two properties, we remove all edges from $\mathcal{A}_{\text{subtask}}$ associated with composite subtasks and denote by $\mathcal{A}_{\text{subtask}}^-$ the resulting pruned $\mathcal{A}_{\text{subtask}}$. A composite subtask can be an elementary subtask of another composite subtask at a higher layer. Thus, removing composite subtasks is vital for reducing the size of $\mathcal{A}_{\text{subtask}}$. Similar to pruning \mathcal{A}_ϕ to get \mathcal{A}_ϕ^- , the feasibility of Problem 1 is not compromised by pruning composite subtasks from the NBA $\mathcal{A}_{\text{subtask}}$, as shown in Lemma C.5.

Example 1. continued (ID and ST properties and NBA $\mathcal{A}_{\text{subtask}}^-$) *In the NBA $\mathcal{A}_{\text{subtask}}$ for task (i), shown in Fig. 6(a), the vertices v_1, v_2, v_3, v_4 satisfy the ID property and the*

vertices v_2, v_3, v_6 ($\gamma_\phi(v_6) = \top$ in Fig. 2(a)) satisfy the ST property. Thus we delete (v_1, v_3) and (v_2, v_6) . The resulting $\mathcal{A}_{\text{subtask}}^-$ is shown in Fig. 8(a). The NBA $\mathcal{A}_{\text{subtask}}^-$ of task (ii) is the same as $\mathcal{A}_{\text{subtask}}$ since there are no composite subtasks.

4.3 Inferring the temporal order between subtasks in $\mathcal{A}_{\text{subtask}}^-$

In this section, we infer the temporal relation between subtasks in the pruned NBA $\mathcal{A}_{\text{subtask}}^- = (\mathcal{V}_s, \mathcal{E}_s)$; see also block ② in Fig. 4. For this, we rely on partially ordered sets introduced in Section 2.2. Specifically, let Θ denote the set that collects all simple paths connecting v_0 and v_{accept} in $\mathcal{A}_{\text{subtask}}^-$. We focus on simple paths since condition (a) in Definition 3.8 excludes cycles. Given a simple path $\theta \in \Theta$, let $\mathcal{T}(\theta)$ denote the set of subtasks in θ . We say that two simple paths θ_1 and θ_2 have the same set of subtasks if $\mathcal{T}(\theta_1) = \mathcal{T}(\theta_2)$. Then we partition Θ into subsets of simple paths that contain the same set of subtasks, that is, $\Theta = \cup_e \Theta_e$ where $\mathcal{T}(\theta_1) = \mathcal{T}(\theta_2)$ for all $\theta_1, \theta_2 \in \Theta_e$ and $e_1 \neq e_2$. The reason for this partition is that we want to map simple paths in $\mathcal{A}_{\text{subtask}}^-$ to posets, and the set of linear extensions generated by a poset has the same set of elements.

Given a subset Θ_e of simple paths in the partition, with a slight abuse of notation, let $\mathcal{T}(\Theta_e)$ denote the set of corresponding subtasks. Let the function $f_e : \mathcal{T}(\Theta_e) \rightarrow [| \mathcal{T}(\Theta_e) |]$ map each subtask to a distinct positive integer. Note that two different subtasks in two different subsets Θ_e and $\Theta_{e'}$ may be mapped to the same integer; however, we treat these two subsets separately. Using f_e , we can map every path in Θ_e to a sequence of integers, denoted by S_e . Let Γ_e collect all sequences of integers for all paths in Θ_e , so $|\Theta_e| = |\Gamma_e|$. Moreover, all sequences on integers in Γ_e are permutations of each other and we denote this base set by $X_e = [| \Theta_e |]$. For every sequence $S_e \in \Gamma_e$, let $S_e[i]$ denote its i -th entry. We define a linear order $L_{X_e} = (X_e, <_L)$ such that $S_e[i] <_L S_e[j]$ if $i < j$. In other words, the subtask $S_e[i]$ should be completed prior to $S_e[j]$. Then, let Ξ_e collect all linear orders over X_e that can be defined from sequences in Γ_e . A poset $P_e = (X_e, <_{P_e})$ containing the maximum number of linear orders in Ξ_e can be found using the algorithm proposed in Heath and Nema (2013) for the partial cover problem, where the order represents the precedence relation. Note that Ξ_e may not be identical to $\mathcal{L}(P_e)$, the set of all linear extensions of P_e . Thus, after obtaining poset P_e , each of the remaining linear orders in Ξ_e that are not covered by P_e are treated as separate totally ordered sets, that are posets as well. In this way, we do not discard any posets.

Finally, given a partition $\{\Theta_e\}$ and a corresponding set of posets $\{P_e\}$, we sort $\{P_e\}$ lexicographically first in descending order in terms of the width of posets and then in ascending order in terms of the height. Recall that the width of a poset is the cardinality of its maximal antichain, and its height is the cardinality of its maximal chain; see Section 2.2. Intuitively, the wider a poset is, the more temporally independent subtasks it contains. The shorter a poset is, the fewer subtasks it has. We consider first wider posets since they impose less restrictions on the high-level plans compared to shorter posets. Every linear extension of

subtasks in a poset produces a simple path connecting v_0 and v_{accept} in $\mathcal{A}_{\text{subtask}}^-$.

Example 1. continued (Temporal constraints) For task (i), there are two simple paths in $\mathcal{A}_{\text{subtask}}^-$ leading to v_6 and all have the same set of four edges, thus, $\Theta_1 = \{v_{\text{init}}, v_1, v_4, v_3, v_6; v_{\text{init}}, v_1, v_2, v_3, v_6\}$; see Fig 8(a). The design of equivalent subtasks, mapping function, integer sequence and the poset are shown in Fig. 8(b). The temporal relation implies that subtasks (v_1, v_4) and (v_1, v_2) are independent, which agrees with our observation. For task (ii), the NBA $\mathcal{A}_{\text{subtask}}^-$ in Fig. 6(b) only has one path of two subtasks that generates a totally ordered set where every two subtasks are comparable.

Remark 4.4. If the size of sub-NBA $\mathcal{A}_{\text{subtask}}^-$ is still large, leading to large number of simple paths, we can select a fixed number of simple paths, similar to finding a fixed number of runs in Kloetzer and Mahulea (2020). This will not severely compromise the diversity of the selected simple paths since a lot of simple paths are combinations of the same set of elementary subtasks.

5 Design of High-Level Task Allocation Plans and Low-Level Executable Paths

In this section, we synthesize plans that satisfy the LTL specification ϕ by first generating a time-stamped task allocation plan that respects the temporal order between subtasks that need to be satisfied in order to satisfy the specification, and then obtaining a low-level executable path that also satisfies the negative literals that we removed from $\mathcal{A}_{\text{relax}}$ in Section 4.1. In what follows, we discuss the synthesis of a prefix path; a similar process is used to synthesize the suffix path in Appendix A.3. Specifically, to synthesize high-level prefix plans, we iterate over the sorted set of posets $\{P_{\text{pre}}\}$, where P_{pre} is a poset corresponding to a simple prefix path in $\mathcal{A}_{\text{subtask}}^-$ and, for every poset in $\{P_{\text{pre}}\}$ we formulate a MILP to assign robots to tasks and determine a high-level plan, i.e., a sequence of time-stamped waypoints, that the robots need to visit to satisfy the subtasks in the corresponding simple path in $\mathcal{A}_{\text{subtask}}^-$; see blocks ③–⑤ in Fig. 4. Note that, given a poset $P \in \{P_{\text{pre}}\}$, every element in the corresponding base set X_P is an integer associated with an edge/subtask in the NBA $\mathcal{A}_{\text{subtask}}^-$. Since a solution to the proposed MILP is effectively a linear extension of the poset P , the corresponding plan sequentially satisfies the vertex and edge labels of all subtasks in $\mathcal{A}_{\text{subtask}}^-$ associated with the elements in X_P . Therefore, this plan produces a simple path in $\mathcal{A}_{\text{subtask}}^-$ that connects v_0 and v_{accept} . To obtain the low-level executable path, for every subtask in this simple path, we formulate a generalized multi-path robot planning problem that considers the negative literals that were removed from $\mathcal{A}_{\text{relax}}$ in Section 4.1; see blocks ⑥ and ⑦ in Fig. 4.

5.1 Formulation of the MILP

In this section, we propose a MILP inspired by the vehicle routing problem (VRP) with temporal constraints (Bredström and Rönnqvist 2008) to obtain a high-level plan that induces a simple path in $\mathcal{A}_{\text{subtask}}^-$ connecting v_0 and v_{accept} ; see blocks ③–④ in Fig. 4. In the VRP, a fleet of vehicles

traverses a given set of customers such that all vehicles depart from and return to the same depot, and each customer is visited by exactly one vehicle. Typically, a weighted graph is built with vertices corresponding to the customers and the depot, edges corresponding to the paths the vehicles can travel along, and edge weights representing the travel cost, e.g., energy and time. Then, a MILP can be formulated to solve the problem. Compared to the VRP with temporal constraints (Bredström and Rönnqvist 2008), the LTL-MRTA problem is significantly more complicated. First, robots are not required to return to their initial locations. Instead, there may exist robots that need to execute the task forever corresponding to the “always” LTL operator. Second, there may exist labeled regions that do not need to be visited at all and others that need to be visited exactly once, more than once, or even infinitely many times. Finally, visits of regions and the associated visiting times are subject to logical constraints induced by the NBA $\mathcal{A}_{\text{subtask}}^-$.

To formulate the proposed MILP, we first construct a routing graph $\mathcal{G} = (\mathcal{V}_\mathcal{G}, \mathcal{E}_\mathcal{G})$ where each vertex represents an initial robot location or a specific region that is associated with a specific literal in a specific label of a subtask in X_P . Each vertex/region in $\mathcal{V}_\mathcal{G}$ is visited by at most one robot. Simultaneous visits of multiple vertices in $\mathcal{V}_\mathcal{G}$ by a fleet of robots satisfy a literal, a clause, or a label in $\mathcal{A}_{\text{subtask}}^-$. The time of visits reflects the temporal relation among subtasks. The construction of the routing graph is detailed in Appendix A.1. Then, the proposed MILP contains five types of constraints that include routing constraints, scheduling constraints, logical constraints, temporal constraints, and transition constraints; see Appendix A.2. The solution of this MILP provides a sequences of edges in the routing graph \mathcal{G} along which robots need to move to drive transitions in $\mathcal{A}_{\text{subtask}}^-$ from v_0 to v_{accept} . The feasibility of the proposed MILP and the properties of the resulting solutions are analyzed in Lemmas C.9 and C.10 in Appendix C.

5.2 Construction of the robot prefix plans

Given the solution to the MILP discussed in Section 5.1, we first define a time axis that includes the sorted completion times of all subtasks in X_P . This time axis produces a linear extension of the poset P and the plan generated by this linear extension satisfies the vertex and edge labels in a given simple path in $\mathcal{A}_{\text{subtask}}^-$. Next, we define a time-stamped task allocation plan for each robot that can be used to generate low-level paths satisfying the specification ϕ . This process corresponds to block ⑤ in Fig. 4.

5.2.1 Time axis: The progress made in $\mathcal{A}_{\text{subtask}}^-$ is directly linked to the satisfaction of edge labels which, by condition (d) in Definition 3.8, implies the satisfaction of their end vertex labels, excluding v_{accept} . Therefore, we collect the completion times of all subtasks in X_P (the time when edges are enabled) and sort them in an ascending order to form a single increasing time axis, denoted by \vec{t} . We note that there are no identical time instants in the time axis since, by construction, the solution to the MILP described in Section 5.1 is a simple path in $\mathcal{A}_{\text{subtask}}^-$ and subtasks in any simple path are completed at different times.

5.2.2 High-level robot plans: Next we extract a high-level plan for each robot, which is a sequence of waypoints that

the robots need to visit to complete the subtasks in X_P along with the time instants of these visits. Specifically, for each robot $[r, j]$, let $p_{r,j}$ denote its corresponding high-level plan and let $t_{r,j}$ denote its timeline. Consider also a vertex $v_0^* \in \mathcal{V}_{\text{init}}$ in the routing graph \mathcal{G} that is associated with the initial location of robot $[r, j]$ and let v_1^* be the first vertex returned by the solution to the MILP such that $x_{v_0^* v_1^* r} = 1$, where $x_{v_0^* v_1^* r} \in \{0, 1\}$ is a routing variable which is 1 if robot r traverses the edge $(v_0^*, v_1^*) \in \mathcal{E}_\mathcal{G}$; see Appendix A.2. Note that robot r can only travel along one outgoing edge of v_0^* . Note also that each vertex in the routing graph \mathcal{G} is associated with a label captured in the mapping $\mathcal{M}_{\text{lits}}^\mathcal{V}$; see Appendix A.1 for more details on the mapping functions used in this paper. If the label associated with v_1^* is a vertex label, then we proceed to the next vertex v_2^* returned by the solution to the MILP such that $x_{v_1^* v_2^* r} = 1$, until a vertex $v^* \in \mathcal{V}_\mathcal{G}$ associated with an edge label is found. Then, the region associated with this vertex v^* , captured by the mapping $\mathcal{M}_\mathcal{L}^\mathcal{V}(v^*)$, constitutes the first waypoint robot r needs to visit to complete a subtask. We add this region $\mathcal{M}_\mathcal{L}^\mathcal{V}(v^*)$ to the plan $p_{r,j}$. Next, the visit time $t_{v^* r}^-$ (scheduling variable denoting the time when robot r arrives at vertex v^* ; see Appendix A.2) indicates the completion time of the associated subtask that is captured by the mapping $\mathcal{M}_e^\mathcal{V}(v^*)$. We add the time $t_{v^* r}^-$ to the timeline $t_{r,j}$. Since each time instant on the time axis \vec{t} corresponds to the completion of one subtask, this visit time $t_{v^* r}^-$ corresponds to the time instant on \vec{t} that the subtask $\mathcal{M}_e^\mathcal{V}(v^*)$ is completed. Continuing this process, we can construct for robot $[r, j]$ a sequence of waypoints and the corresponding timeline whose time instants appear on the time axis \vec{t} . Given this high-level plan $\{p_{r,j}\}$, we can design low-level executable paths that reconsider the negative literals that were originally removed from the NBA $\mathcal{A}_{\text{relax}}$.

Example 1. continued (Time-stamped task allocation plan)
After solving the MILP for the workspace in Fig. 1, the high-level plans and the associated timelines for robots are as follows: $p_{2,1} = p_{3,1} = \{\ell_2, \ell_3\}$, $t_{2,1} = t_{3,1} = \{4, 12\}$, $p_{2,2} = \{\ell_4\}$, $t_{2,2} = \{8\}$. That is, robots [2, 1] and [3, 1] visit the office building ℓ_2 at time instant 4, then robot [2, 2] visits the control room ℓ_4 at time instant 8, and finally robots [2, 1] and [3, 1] visit the delivery site ℓ_3 at time instant 12. The remaining robots remain idle. Observe that the lengths of the plans differ since every robot may undertake different number of subtasks. The induced simple path in $\mathcal{A}_{\text{subtask}}^-$ in Fig. 8(a) is $v_{\text{init}}, v_1, v_2, v_3, v_6$. The associated time axis is $\vec{t} = \{0, 4, 8, 12\}$, one time instant per subtask. In words, the subtask (v_{init}, v_1) is completed at time instant 0 and the subtask (v_1, v_2) is completed at time instant 4, which corresponds to the event that robots [2, 1] and [3, 1] visit the office building ℓ_2 at time instant 4.

5.3 Design of low-level prefix paths

In this section we discuss the correction stage that reintroduces the negative literals to the NBA and corrects the high-level plans designed in Section 5.2 (if needed) so that they satisfy the specification ϕ ; see also blocks ⑥ and ⑦ in Fig. 4. To this end, we first find the simple path in the NBA $\mathcal{A}_{\text{subtask}}^-$ connecting v_0 and v_{accept} using the time axis and the time-stamped task allocation plan. To satisfy the

specification ϕ , for every subtask in the simple path, we formulate a generalized multi-robot path planning (GMRPP) problem. Each GMRPP is essentially a generalization of the multi-robot point-to-point navigation problem, whose goal is to determine a collection of executable paths that allow the robots to complete the current subtask (by enabling the edge label at the end while respecting the starting vertex en route) and automatically activate the next subtask, since the satisfaction of the edge label leads to the satisfaction of the starting vertex of the next subtask. The details can be found in Appendix B, that also discusses different implementations of the proposed GMRPP (see Appendix B.4) that depend on whether all or a subset of robots are allowed to move during the execution of the current subtask, since not all robots are responsible for the completion of this subtask, and whether the completion times of subtasks are disjoint or partially overlapping. Finally, the feasibility of the proposed GMRPP is analyzed Lemma C.11 in Appendix C.

5.4 Obtaining the best prefix-suffix path

After obtaining the prefix path corresponding to a poset $P \in \{P_{\text{pre}}\}$ for the given pair v_0 and v_{accept} , next we find the suffix path around v_{accept} . For this, we can follow a similar process as this described in Sections 5.1–5.3 to find the prefix path for poset $P \in \{P_{\text{pre}}\}$, with the difference that now we treat the accepting vertex v_{accept} as both the initial vertex v_0 and the accepting vertex v_{accept} . This is because the suffix path is essentially a loop, i.e., the final locations in the suffix path are identical to the initial locations in the suffix path, which are also the final locations in the prefix path; see Appendix A.3 for more details.

Specifically, given the pair v_0 and v_{accept} , we solve one MILP for each poset $P' \in \{P_{\text{ suf}}\}$ to obtain a corresponding suffix path; these MILPs can be infeasible if there are no feasible paths that induce simple paths corresponding to the poset P' . Then, among all suffix paths for all posets $P' \in \{P_{\text{ suf}}\}$ we select the one with the lowest cost. This best suffix path corresponds to the prefix path generated from a poset $P \in \{P_{\text{pre}}\}$ for the given pair v_0 and v_{accept} . Combining this suffix path with the corresponding prefix path we obtain the best total path associated with the poset P for the given pair v_0 and v_{accept} . Then, using cost function (2), we select the best total path over all posets in $\{P_{\text{pre}}\}$ for the given pair v_0 and v_{accept} . Finally, by iterating over all pairs of initial and accepting vertices with finite total length, we can obtain the best total path. We highlight that our method can terminate anytime once a feasible path is found, but running the algorithm longer can lead to more optimal feasible paths. Note also that by iterating over the pairs v_0 and v_{accept} and the corresponding posets in the ascending order discussed in Section 4.3, it is more likely that the first solutions we obtain have low cost since they involve fewer subtasks that need to be accomplished. This observation is also validated numerically in Section 7.

Example 1. continued (Low-level paths) When generating low-level paths for task (i), we also consider collision avoidance. Fig. 9 shows an array of three key frames where different subtasks are completed. Observe that task (i) is completed at time 15, longer than 12 given by the timestamped task allocation plan since the high-level plan uses

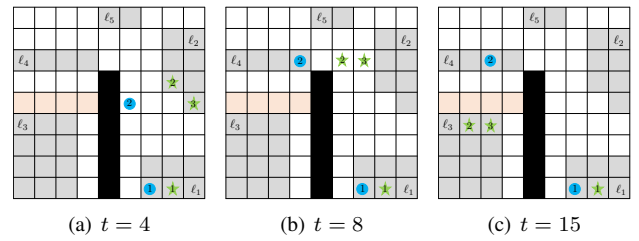


Figure 9. Key frames demonstrating the execution of low-level paths that satisfy task (i). The initial configuration is shown in Fig. 1. Fig. 9(a) shows that at time instant 4, robots [2, 1] and [3, 1] reach the office building ℓ_2 , while robot [2, 2] is on the way to the control room ℓ_4 . Fig. 9(b) shows at time instant 8, robot [2, 2] reaches the control room ℓ_4 while robots [2, 1] and [3, 1] head towards the delivery site ℓ_3 . Finally, they reach ℓ_3 in Fig. 9(c) at time instant 15. Robots [1, 1] and [1, 2] remain idle throughout the process.

the shortest travel time between regions and does not consider collision avoidance.

6 Theoretical Analysis

In this section, we analyze the completeness and soundness of our method. First we show that, with mild assumptions, our method is complete for LTL^0 specifications.

Theorem 6.1. (Completeness). Consider a discrete workspace satisfying Assumption 3.5, a team of n robots of m types and a valid specification $\phi \in LTL^0$. Assume also that there exists a path $\tau = \tau^{\text{pre}}[\tau^{\text{ suf}}]^\omega$ that induces a restricted accepting run $\rho = \rho^{\text{pre}}[\rho^{\text{ suf}}]^\omega = v_0, \dots, v_{\text{prior}}, v_{\text{accept}} [v_{\text{next}}, \dots, v'_{\text{prior}}, v_{\text{accept}}]^\omega$ in the pre-processed NBA \mathcal{A}_ϕ and satisfies Assumption 3.11. Then, the proposed synthesis method can find a robot path $\tilde{\tau} = \tilde{\tau}^{\text{pre}}[\tilde{\tau}^{\text{ suf}}]^\omega$ that satisfies the specification ϕ .

The key idea in the proof of Theorem 6.1 is to first show that feasible paths still exist in $\mathcal{A}_{\text{subtask}}^-$ and then use this fact to show feasibility of the MILP and GMRPP problems. The detailed proof can be found in Appendix C. We emphasize that the completeness result in Theorem 6.1 is ensured for LTL^0 rather than LTL^χ formulas. This is because task allocations captured by induced atomic propositions in the prefix part may not lead to feasible allocations in the suffix part. However, when the LTL^χ specification can be satisfied by finite-length paths, such as co-safe LTL (Kupferman and Vardi 2001) or LTL_f (De Giacomo and Vardi 2013), then our method is complete also for LTL^χ specifications; This is shown in Proposition C.8 in Appendix C.3 as part of the proof of Theorem 6.1.

Remark 6.2. We note that the path $\tilde{\tau}$ constructed by our approach may not satisfy Assumption 3.11 that requires that robots close their suffix loops at the same time the NBA \mathcal{A}_ϕ transitions to v_{accept} . However, in our method, when the NBA \mathcal{A}_ϕ transitions to v_{accept} , only those robots involved in the completion of the last subtask in the prefix part return to regions corresponding to their initial locations. Thereafter, trajectories are closed.

The following statement shows the soundness of our method, which is a direct consequence of Theorem 6.1.

Corollary 6.3. (Soundness). Consider a discrete workspace, a team of n robots of m types and a valid specification $\phi \in LTL^X$. Then, the path returned by the GMRPP satisfies the specification ϕ . Also, the specific implementation of the GMRPP is not important.

7 Numerical Experiments

In this section we present three case studies, implemented in Python 3.6.3 on a computer with 2.3 GHz Intel Core i5 and 8G RAM, that illustrate the correctness and scalability of our method. The MILP is solved using Gurobi (Gurobi Optimization 2018) with big-M $M_{\max} = 10^5$. First, we compare with the optimal solution to examine the suboptimality of our proposed method when the NBA can be captured by one poset (thus, only one solution). Second, we generate multiple solutions for specifications with multiple posets, and compare the cost of the first solution corresponding to the widest poset to that of the subsequent solutions. We observe that the quality of the first solution obtained for the widest poset is generally very good. Finally, we compare our method to the approach proposed in Sahin et al. (2019b) for large workspaces and numbers of robots and show that our method outperforms the approach in Sahin et al. (2019b) in terms of optimality and scalability. We note that in the implementation of our method, we ignore constraints (27)-(28) in the MILP in Appendix A.2.6 which facilitate the transition between the prefix and suffix parts (see Appendix A.2.6) and adopt a single step approach to close the robot suffix loops (see Appendix A.3.2.4). We emphasize that the sets of restricted accepting runs of all specifications $\phi_1 - \phi_{10}$ considered in the following simulations, are nonempty, which shows that this assumption is not restrictive in practice.

7.1 Case study I: Suboptimality

In this case study, we examine the quality of the paths constructed for the two tasks in the Example 1. Observe that in Fig. 8(a), a unique poset corresponds to the sub-NBA $\mathcal{A}_{\text{subtask}}^-$ for task (i). A similar observation can be made for the sub-NBA $\mathcal{A}_{\text{subtask}}^-$ in Fig. 6(b) for task (ii).

To measure the suboptimality of our solution in terms of path length (number of transitions between different cells), we need access to the optimal cost. However, due to the complexity of the LTL-MRTA problem, it is computationally expensive to get this optimal cost. For instance, for the 9-by-9 workspace in Fig. 9, the product transition system composed of 5 robots has $(9^2)^5 = 9^{10}$ states. Therefore, we take the following task-specific approach to get the shortest path length, without considering collision avoidance between robots. In the workspace shown in Fig. 9, we randomly generate the initial locations of all robots that are at the right side of the vertical obstacles with x -coordinate larger than 4. No robots are located inside region ℓ_2 . Task (i) can be satisfied by finite-length paths, whose sub-NBA $\mathcal{A}_{\text{subtask}}^-$ is shown in Fig. 8(a). Using a brute-force approach, we first select two robots of type 1 that have the shortest paths from their initial locations to region ℓ_2 and then to region ℓ_3 . Next, we select one robot of type 2 that has the shortest path from its initial location to region ℓ_4 . The optimal cost is the sum of these three path lengths. Note that we did not consider

Table 1. Statistics on the optimal cost and solutions returned by our method. Column “NoCol+Seq” represents the case where collision avoidance is ignored and robots move sequentially, and column “Col+Sim” incorporates collision avoidance and simultaneous execution. The notation J^* denotes the optimal cost without considering collision avoidance. The number of trials out of 50 trials where the cost cost is equivalent to the optimal cost J^* are shown inside the parentheses.

task	J^*	NoCol+Seq		Col+Sim	
		cost	horizon	cost	horizon
(i)	27.2 ± 3.1	28.0 ± 3.3 (30)	18.8 ± 3.0	30.3 ± 3.2	14.9 ± 1.7
(ii)	18.7 ± 1.2	21.6 ± 2.8 (4)	23.2 ± 2.8	22.0 ± 3.0	23.8 ± 2.8

the temporal relation between robots since they can go and stop along the shortest paths. Similarly, for task (ii), we select the robot of type 1 that has the shortest path from its initial location to region ℓ_2 , then to region ℓ_3 and finally back to region ℓ_2 .

Next, given the same randomly generated initial robot locations, we implement our proposed method in the following two different ways. First, we implement GMRPP without collision avoidance and with sequential execution (see Appendix B.2.1). Using sequential execution, only robots participating in the subtask under consideration are assigned target regions and the rest of the robots just move out of their way, whereas in the case of the simultaneous execution (see Appendix B.4.2), multiple subtasks can be undertaken at the same time, and robots that do not participate in the current subtasks simultaneously move towards their target points for subsequent subtasks. Second, we implement GMRPP with collision avoidance (see Appendix B.4.1) and with simultaneous execution. Both implementations employ the full execution (see Appendix B.2.1), in which all robots are allowed to move. Note that in the partial execution (see Appendix B.4.3), only necessary robots participating in the current subtask are allowed to move and the remaining robots are treated as obstacles. Table 1 shows statistical results on the path costs and path time horizons, averaged over 50 trials.

Without considering collision avoidance, the cost returned by our method is close to the optimal cost, especially for task (i) that only requires paths of finite length. Out of 50 trials, there are 30 trials in which our method can identify the exact optimal solutions. For task (ii), the additional cost arises from planning separately for the prefix and suffix parts. In the prefix part, the robot can visit the cell in region ℓ_2 that is the closest to its initial location, however, it may incur additional cost to return to this cell in the suffix part. The costs when considering collision avoidance are also close to the optimal cost, indicating that often robots follow the shortest path. As for the path horizon, observe that, for task (i), simultaneous execution results in shorter horizons since one robot of type 2 can move towards region ℓ_4 while two robots of type 1 leave from their initial locations for region ℓ_2 . Nonetheless, for task (ii), the horizon remains almost the same, since the corresponding subtasks cannot be executed in parallel by the same robot.

Table 2. Results for specifications $\phi_3 - \phi_8$, where N_{pair} is the number of pairs of initial and accepting vertices, $|\mathcal{A}|$, $|\mathcal{A}_\phi|$, $|\mathcal{A}_{\text{subtask}}^{\text{-,pre}}|$ and $|\mathcal{A}_{\text{subtask}}^{\text{-,suf}}|$ are the size of the NBA before and after pre-processing, for the prefix and suffix parts from which the first solutions are obtained, respectively. The symbol “—” means that only one solution found for ϕ_3 and ϕ_4 , and less than or equal to 5 solutions found for ϕ_5 .

Task	N_{pair}	$ \mathcal{A} $	$ \mathcal{A}_\phi $	$ \mathcal{A}_{\text{subtask}}^{\text{-,pre}} $	$ \mathcal{A}_{\text{subtask}}^{\text{-,suf}} $	$N_{\text{sol}} = 1$		$N_{\text{sol}} = 5$		$N_{\text{sol}} = 10$	
						cost	time(sec)	cost	time(sec)	cost	time(sec)
ϕ_3	8	(20, 142)	(20, 49)	(3, 2)	(5, 5)	56.2±4.2	2.0±0.3	—	—	—	—
ϕ_4	4	(10, 57)	(10, 31)	(3, 2)	(3, 3)	46.0±4.5	1.7±0.6	—	—	—	—
ϕ_5	2	(11, 31)	(11, 25)	(10, 19)	(3, 3)	17.6±6.2	0.7±0.2	17.6±6.2	3.4±0.8	—	—
ϕ_6	1	(4, 9)	(4, 8)	(4, 5)	(4, 5)	30.6±9.2	1.7±0.8	24.9±6.1	5.0±1.9	24.9±6.1	5.3±2.0
ϕ_7	3	(24, 140)	(24, 104)	(22, 57)	(9, 18)	49.3±9.5	3.8±2.5	49.3±9.5	4.4±2.5	49.3±9.5	5.6±2.5
ϕ_8	4	(15, 83)	(15, 41)	(8, 13)	(8, 14)	45.9±6.8	1.5±0.2	45.9±6.8	7.3±0.6	45.9±6.8	17.7±1.4

7.2 Case study II: Quality of the first solution

Common to the two specifications in the first case study is that the sub-NBA $\mathcal{A}_{\text{subtask}}^-$ for the prefix and suffix parts can be concisely captured by one poset, which may not be the case for most specifications. Here, we consider various specifications that can produce many posets and examine the quality of the first solutions obtained for the widest poset (see Section 4.3) by comparing to subsequent solutions obtained for subsequent posets. We use the same workspace and robot team as in Example 1. The considered specifications are as follows:

$$\begin{aligned}\phi_3 &= \square \diamond (\pi_{2,1}^{2,1} \wedge \diamond (\pi_{2,1}^{3,1} \wedge \diamond (\pi_{2,1}^{4,1} \wedge \diamond \pi_{2,1}^{5,1}))), \\ \phi_4 &= \square \diamond (\pi_{2,1}^{2,1} \wedge \diamond \pi_{2,1}^{3,1}) \wedge \square (\pi_{1,1}^{5,2} \implies \bigcirc (\pi_{1,1}^{5,2} \cup \pi_{1,2}^4)) \\ &\quad \wedge \square \neg \pi_{2,1}^4, \\ \phi_5 &= \diamond (\pi_{1,2}^{4,1} \wedge \bigcirc (\pi_{1,2}^{4,1} \cup \pi_{2,1}^3)) \wedge \square \diamond (\pi_{1,2}^{4,1} \wedge \diamond \pi_{1,2}^{3,1}), \\ \phi_6 &= \square \diamond (\pi_{1,1}^{3,1} \vee \pi_{1,1}^{5,1}) \wedge \square \diamond \pi_{1,1}^{2,1} \wedge \square \diamond (\pi_{2,2}^3 \vee \pi_{2,2}^5) \\ &\quad \wedge \square \neg \pi_{2,1}^4 \wedge \square \neg \pi_{2,2}^4, \\ \phi_7 &= \square \diamond (\pi_{1,2}^4 \wedge \bigcirc (\diamond \neg \pi_{1,2}^4)) \wedge \square \diamond (\pi_{1,1}^5 \wedge \bigcirc (\diamond \neg \pi_{1,1}^5)) \\ &\quad \wedge \diamond (\pi_{3,1}^3 \wedge \pi_{2,2}^3), \\ \phi_8 &= \square \diamond (\pi_{2,2}^{4,1} \wedge \diamond (\pi_{2,2}^{2,1} \wedge \diamond \pi_{2,2}^{5,1})) \wedge \neg \pi_{1,2}^2 \cup \pi_{2,2}^{4,1} \\ &\quad \wedge \neg \pi_{1,2}^5 \cup \pi_{2,2}^{4,1} \wedge (\square \diamond \pi_{2,1}^5 \vee \square \diamond \pi_{2,1}^3),\end{aligned}$$

where (a) ϕ_3 requires that the same two robots of type 1 meet first at regions ℓ_2 , then ℓ_3 , next ℓ_4 , and finally at ℓ_5 , repeating this process infinitely often; (b) ϕ_4 requires that the same two robots of type 1 meet at region ℓ_2 and then ℓ_3 infinitely many times. Also, every time one robot of type 1 visits region ℓ_5 , it should stay there until one robot of type 2 visits region ℓ_4 . Finally, at most one robot of type 1 should be at region ℓ_4 at any time; (c) ϕ_5 requires that one robot of type 2 visits region ℓ_4 and stays there until two robots of type 1 reach region ℓ_3 . This type 2 robot should visit regions ℓ_4 and then ℓ_3 infinitely many times; (d) ϕ_6 requires that the same robot of type 1 visits regions ℓ_3 or ℓ_5 infinitely many times and this robot visits region ℓ_2 infinitely many times, while two robots of type 2 meet at regions ℓ_3 or ℓ_5 infinitely many times. Finally, at most one robot of any type can be present at region ℓ_4 ; (e) ϕ_7 requires that one robot of type 2 periodically visits region ℓ_4 while one robot of type 1 periodically visits region ℓ_5 . All robots must eventually meet at region ℓ_3 ; (f) ϕ_8 requires that two robots of type 2 meet at region ℓ_4 , then ℓ_2 and next ℓ_5 , repeating this infinitely many times with the restriction that no robots of type 2 reach regions ℓ_2 and ℓ_5 .

before two robots of type 2 meet at region ℓ_4 for the first time. Ultimately, two robots of type 1 should meet at region ℓ_5 or ℓ_3 infinitely often.

These specifications involve various operators and are representative of commonly used complex tasks in robotics applications. For example, ϕ_3 can capture surveillance and data gathering tasks (Smith et al. 2011; Guo and Zavlanos 2017), and the subformula $\square \diamond (\pi_{1,1}^{3,1} \vee \pi_{1,1}^{5,1})$ in ϕ_6 can specify intermittent connectivity tasks where robots are required to meet at communication regions infinitely often (Kantaros and Zavlanos 2017a; Kantaros et al. 2019; Khodayi-mehr et al. 2019). Furthermore, subformula $\square \neg \pi_{2,2}^4$ in ϕ_5 can be used to represent collision avoidance among robots and $\neg \pi_{1,2}^2 \cup \pi_{2,2}^{4,1}$ in ϕ_8 can prioritize certain subtasks to others.

We executed our method 20 times for each specification. In each trial, we randomly generated initial robot locations inside the label-free cells such that no two robots occupy the same cell. We considered collision avoidance, as well as full and simultaneous execution. In Table 2, we report the number of pairs of initial and accepting vertices in the NBA \mathcal{A}_ϕ before pre-processing, the size (number of vertices and edges) of the NBA \mathcal{A}_ϕ before and after pre-processing, and the size of the sub-NBA $\mathcal{A}_{\text{subtask}}^-$ for the prefix and suffix parts from which the first solutions are obtained. We terminate our method until all solutions or the first 10 solutions are generated, whichever comes first. We record the smallest cost achieved by the first solution, after the first 5 and 10 solutions along with the runtimes.

In Table 2, we observe that the size of sub-NBA $\mathcal{A}_{\text{subtask}}^-$ is dramatically reduced compared to the size of NBA before pre-processing, especially for specifications ϕ_3 , ϕ_7 and ϕ_8 , considerably reducing the computation times. It takes less than 20 seconds to get 10 solutions for specification ϕ_8 . Except for specification ϕ_6 , the first solution returned by our method is also the lowest cost solution. For specification ϕ_6 , the best solution corresponds to one of the first 5 posets. This is because our optimization-based method sorts the set of posets in part according to their height so that posets with smaller numbers of subtasks are considered first (see Section 4.3). Therefore, we can terminate our method only after a few solutions have been obtained, which is especially important when the complexity of the planning problem increases, as in the next case study.

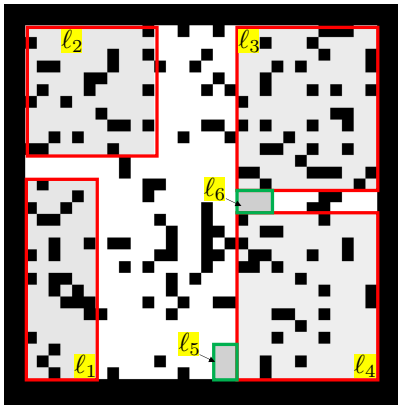


Figure 10. Grid world from Sahin et al. (2019b)

7.3 Case study III: Scalability

In this case study, we examine the scalability of our proposed method with respect to the size of the workspace and the number of robots. Specifically, we first compare our method to the Bounded-Model-Checking-based (BMC) method in Sahin et al. (2019b) and then, we examine the effect of full or partial execution on the performance.

7.3.1 Comparison with the BMC method: Similar to our method, Sahin et al. (2019b) also adopt a hierarchical framework, which improves the scalability of their algorithms (Sahin et al. 2017b, 2019a). For the purpose of comparison, we borrow the workspace used in Sahin et al. (2019b), a 30-by-30 grid world containing 6 regions $\ell_i, i = 1, \dots, 6$; shown in Fig. 10. At each trial, 20% of cells are randomly selected as obstacles. We consider a team of n robots of the same type whose initial locations are randomly sampled inside region ℓ_1 . The specification we consider is given by Sahin et al. (2019b):

$$\begin{aligned}\phi_9 = & \square\Diamond\pi_{n,1}^2 \wedge \square\Diamond\pi_{n/2,1}^3 \wedge \square\Diamond\pi_{n/2,1}^4 \\ & \wedge \neg\pi_{1,1}^4 \mathcal{U} (\pi_{1,1}^5 \wedge \pi_{1,1}^6),\end{aligned}$$

which requires (a) all robots to meet at region ℓ_2 infinitely often, (b) at least half of the robots to meet at regions ℓ_3 and ℓ_4 , respectively, infinitely often, and (c) robots should not visit region ℓ_4 until at least one robot is inside region ℓ_5 and one robot is inside region ℓ_6 at the same time. We vary the number of robots n from 4 to 30, which produces a product transition system that has up to $(30 \times 30)^{30} \approx 10^{90}$ states.

The size of the NBA is independent from the number of robots. The NBA \mathcal{A}_ϕ has one pair of initial and accepting vertices, 5 vertices and 10 edges (excluding self-loops). The sub-NBA $\mathcal{A}_{\text{subtask}}^-$ for the prefix part has 5 vertices and 5 edges and for the suffix part has 4 vertices and 5 edges. In the implementation of our method, we employ the full and simultaneous execution. We record runtimes and cost of the first feasible solutions, where the cost is the sum of the cost of the prefix and suffix parts. Both methods consider collision avoidance. The horizon increases by 10 when no solution exists for the GMRPP, until the considered horizon exceeds the initial horizon by 100. The source code for Sahin et al. (2019b) can address robots of the same type, and is available at Sahin (2019). The statistical results averaged over 10 trials are shown in Table 3.

Table 3. Results with respect to the number of robots

n	Our method		BMC method	
	cost	time(sec)	cost	time(sec)
4	270.6±4.4	62.4±1.4	944.4±21.2	76.5±13.8
8	513.0±30.2	124.9±9.2	1819.0±149.9	334.9±153.9
12	794.6±11.1	187.4±9.1	2217.0±163.8	704.3±178.0
16	1080.2±14.7	502.0±225.4	2725.8±149.2	1135.8±123.7
30	2509.4±168.9	4072.1±985.4	—	—

Observe in Table 3 that our method outperforms the BMC method both in terms of runtimes and optimality of the solutions. Specifically, as the number of robots increases, the runtime of our method is about half the runtime of the BMC method but the cost returned by our method is about 1/3 of the cost of the solutions obtained using the BMC method. The reason is that we optimize the cost at both the high level and the low level, while the BMC method only considers feasibility. For $n = 30$ robots, the BMC method did not produce a solution within 2 hours. Furthermore, the efficiency of the low-level path planner has significant impact on the runtime. In our method, the number of times that the path planner is invoked is the same or smaller than the number of subtasks in the simple path extracted from the high-level plan (see Appendix B.1). On the other hand, the BMC method abstracts the given environment by aggregating states with the same observation, where transitions between abstract states are defined by whether they share the same boundary. Then, each transition in the high-level plan obtained by the BMC method is converted into one instance of multi-robot path planning problem. Obviously, the number of transitions in the BMC method is larger than the number of subtasks in our method, since each subtask may take multiple transitions.

7.3.2 Full vs. partial GMRPP execution: We use the same workspace as in Fig. 10 and consider a team of n homogeneous robots that are subject to the specification:

$$\begin{aligned}\phi_{10} = & \Diamond(\pi_{3,1}^5 \vee \pi_{3,1}^6) \wedge \square\Diamond(\pi_{n/2,1}^{2,1} \wedge \Diamond\pi_{n/2,1}^{4,1}) \\ & \wedge \square\Diamond\pi_{n/4,1}^3 \wedge \square\neg\pi_{4,1}^6,\end{aligned}$$

which requires that (a) at least 3 robots eventually meet at either region ℓ_5 or ℓ_6 , (b) a fleet of at least half robots meet at region ℓ_2 and then the same robots meet at region ℓ_4 , infinitely often, (c) at least a quarter robots meet at region ℓ_3 infinitely often, and (d) always no more than 3 robots can be present at region ℓ_6 at the same time.

Before pre-processing, there are two pairs of initial and accepting vertices in the NBA \mathcal{A}_ϕ that contains 8 vertices and 27 edges. After pre-processing, the NBA \mathcal{A}_ϕ has 8 vertices and 20 edges. For the first pair of initial and accepting vertices, the sub-NBA $\mathcal{A}_{\text{subtask}}^-$ associated with the prefix part has 7 vertices and 10 edges, and the sub-NBA associated with suffix part has 5 vertices and 7 edges. We compare the performance of our method for the full and partial execution in the GMRPP problem and for an increasing number of robots up to 32. The results averaged over 10 trials are shown in Table 4. It can be seen that our method with partial execution in the GMRPP problem takes less time than with full execution. This advantage becomes more significant as the number of robots increases since in this case, a larger

Table 4. Results with respect to the number of robots.

n	Full execution		Partial execution	
	cost	time(sec)	cost	time(sec)
4	181.4±17.7	89.5±5.0	180.4±20.1	65.8±10.1
8	356.6±16.0	198.9±12.3	354.2±15.2	129.3±4.9
12	573.5±63.3	350.7±25.4	554.3±49.4	192.5±10.4
16	774.2±59.0	561.0±44.4	763.0±50.7	278.9±8.9
32	1560.4±160.7	1886.8±696.0	1524.6±30.6*	778.1±134.9

* 3 out of 10 trials failed.

number of robots that do not participate in the current subtask can remain idle and can be treated as obstacles in the GMRPP. For example, the subtask requiring that at least 3 robots meet at region ℓ_5 or ℓ_6 , only involves 3 robots no matter how large the robot team is. On the other hand, the full execution of the GMRPP problem results in slightly larger cost which suggests that even though all robots are allowed to move, those robots that do not participate in the specific subtask rarely move because our method optimizes the cost. Observe that for the partial execution of the GMRPP problem and for 32 robots, no solutions are generated in 3 out of 10 trials. This is due to the fact that robots treated as obstacles affect the obstacle-free workspace and, therefore, may make the GMRPP infeasible. Thus, the partial execution of the GMRPP problem can be more effective in large workspaces with few robots, where a few idle robots do not significantly alter the obstacle-free environment.

8 Conclusion

In this work, we consider the problem of allocating tasks, expressed as global LTL specifications, to teams of heterogeneous mobile robots. This problem cannot be solved using existing model checkers since all possible allocations of robots to tasks can result in LTL formulas that are prohibitively long. We proposed a hierarchical approach to solve this problem that first solves an MILP to obtain a high-level time-stamped allocation of robots to tasks and then formulates a sequence of multi-robot path planning problems to obtain the low-level executable paths. We proved that, with mild assumptions, the proposed method is complete and we provided extensive simulations that showed that our method outperforms the state-of-the-art BMC method in terms of optimality and scalability. Scalability of our method is primarily due to a clever relaxation of the NBA that captures the LTL specification, that involves removing the negative literals. This relaxation is motivated by “lazy collision checking” methods for point-to-point navigation, and significantly simplifies the high-level planning problem as constraint violation is not considered during planning and instead it is only checked during execution when needed. To the best of our knowledge, this is the first time that “lazy collision checking” methods are used and shown to be effective for high-level planning tasks.

Acknowledgements

This work is supported in part by ONR under agreement #N00014-18-1-2374 and by AFOSR under the award #FA9550-19-1-0169.

References

- Baier C and Katoen JP (2008) *Principles of model checking*. MIT press Cambridge.
- Banks C, Wilson S, Coogan S and Egerstedt M (2020) Multi-agent task allocation using cross-entropy temporal logic optimization. In: *2020 IEEE International Conference on Robotics and Automation (ICRA)*. IEEE, pp. 7712–7718.
- Biere A, Heljanko K, Junttila T, Latvala T and Schuppan V (2006) Linear encodings of bounded LTL model checking. *arXiv preprint cs/0611029*.
- Bredström D and Rönnqvist M (2008) Combined vehicle routing and scheduling with temporal precedence and synchronization constraints. *European journal of operational research* 191(1): 19–31.
- Camacho A, Icarte RT, Klassen TQ, Valenzano R and McIlraith SA (2019) LTL and beyond: Formal languages for reward function specification in reinforcement learning. In: *Proceedings of the 28th International Joint Conference on Artificial Intelligence (IJCAI)*. pp. 6065–6073.
- Camacho A, Triantafillou E, Muise CJ, Baier JA and McIlraith SA (2017) Non-deterministic planning with temporally extended goals: Ltl over finite and infinite traces. In: *AAAI*. pp. 3716–3724.
- Chen Y, Ding XC, Stefanescu A and Belta C (2011) Formal approach to the deployment of distributed robotic teams. *IEEE Transactions on Robotics* 28(1): 158–171.
- Cimatti A, Clarke E, Giunchiglia E, Giunchiglia F, Pistore M, Roveri M, Sebastiani R and Tacchella A (2002) Nusmv 2: An opensource tool for symbolic model checking. In: *International Conference on Computer Aided Verification*. Springer, pp. 359–364.
- De Giacomo G and Vardi MY (2013) Linear temporal logic and linear dynamic logic on finite traces. In: *Twenty-Third International Joint Conference on Artificial Intelligence*.
- Fainekos GE, Kress-Gazit H and Pappas GJ (2005) Temporal logic motion planning for mobile robots. In: *IEEE International Conference on Robotics and Automation (ICRA)*. Barcelona, Spain, pp. 2020–2025.
- Faruq F, Parker D, Lacerda B and Hawes N (2018) Simultaneous task allocation and planning under uncertainty. In: *2018 IEEE/RSJ International Conference on Intelligent Robots and Systems (IROS)*. IEEE, pp. 3559–3564.
- Gastin P and Oddoux D (2001) Fast LTL to Büchi automata translation. In: *International Conference on Computer Aided Verification*. Springer, pp. 53–65.
- Gini ML (2017) Multi-robot allocation of tasks with temporal and ordering constraints. In: *AAAI*. pp. 4863–4869.
- Gombolay M, Wilcox R and Shah J (2013) Fast scheduling of multi-robot teams with temporospatial constraints .
- Guo M and Dimarogonas DV (2015) Multi-agent plan reconfiguration under local LTL specifications. *The International Journal of Robotics Research* 34(2): 218–235.
- Guo M and Zavlanos MM (2017) Distributed data gathering with buffer constraints and intermittent communication. In: *2017 IEEE International Conference on Robotics and Automation (ICRA)*. IEEE, pp. 279–284.
- Gurobi Optimization L (2018) Gurobi optimizer reference manual. URL <http://www.gurobi.com>.

- Hauser K (2015) Lazy collision checking in asymptotically-optimal motion planning. In: *2015 IEEE International Conference on Robotics and Automation (ICRA)*. IEEE, pp. 2951–2957.
- Heath LS and Nema AK (2013) The poset cover problem. *Open Journal of Discrete Mathematics* 3(03): 101.
- Jones AM, Leahy K, Vasile CI, Sadradinni S, Serlin Z, Tron R and Belta C (2019) Scalable and Robust Deployment of Heterogeneous Teams from Temporal Logic Specifications. In: *International Symposium on Robotics Research (ISRR)*. Hanoi, Vietnam.
- Jones EG, Dias MB and Stentz A (2011) Time-extended multi-robot coordination for domains with intra-path constraints. *Autonomous robots* 30(1): 41–56.
- Kantaros Y, Guo M and Zavlanos MM (2019) Temporal logic task planning and intermittent connectivity control of mobile robot networks. *IEEE Transactions on Automatic Control* 64(10): 4105–4120.
- Kantaros Y and Zavlanos MM (2015a) Intermittent connectivity control in mobile robot networks. In: *49th Asilomar Conference on Signals, Systems and Computers*. Pacific Grove, CA, USA, pp. 1125–1129.
- Kantaros Y and Zavlanos MM (2015b) Intermittent connectivity control in mobile robot networks. In: *2015 49th Asilomar Conference on Signals, Systems and Computers*. IEEE, pp. 1125–1129.
- Kantaros Y and Zavlanos MM (2016) Distributed communication-aware coverage control by mobile sensor networks. *Automatica* 63: 209–220.
- Kantaros Y and Zavlanos MM (2017a) Distributed intermittent connectivity control of mobile robot networks. *IEEE Transactions on Automatic Control* 62(7): 3109–3121.
- Kantaros Y and Zavlanos MM (2017b) Sampling-based control synthesis for multi-robot systems under global temporal specifications. In: *2017 ACM/IEEE 8th International Conference on Cyber-Physical Systems (ICCPs)*. IEEE, pp. 3–14.
- Kantaros Y and Zavlanos MM (2018a) Distributed optimal control synthesis for multi-robot systems under global temporal tasks. In: *Proceedings of the 9th ACM/IEEE International Conference on Cyber-Physical Systems*. IEEE Press, pp. 162–173.
- Kantaros Y and Zavlanos MM (2018b) Sampling-based optimal control synthesis for multirobot systems under global temporal tasks. *IEEE Transactions on Automatic Control* 64(5): 1916–1931.
- Kantaros Y and Zavlanos MM (2018c) Temporal logic optimal control for large-scale multi-robot systems: 10^{400} states and beyond. In: *2018 IEEE Conference on Decision and Control (CDC)*. IEEE, pp. 2519–2524.
- Kantaros Y and Zavlanos MM (2020) Stylus*: A temporal logic optimal control synthesis algorithm for large-scale multi-robot systems. *The International Journal of Robotics Research* 39(7): 812–836.
- Karaman S and Frazzoli E (2011) Linear temporal logic vehicle routing with applications to multi-uav mission planning. *International Journal of Robust and Nonlinear Control* 21(12): 1372–1395.
- Khodayi-mehr R, Kantaros Y and Zavlanos MM (2019) Distributed state estimation using intermittently connected robot networks. *IEEE Transactions on Robotics* 35(3): 709–724.
- Kloetzer M, Ding XC and Belta C (2011) Multi-robot deployment from LTL specifications with reduced communication. In: *2011 50th IEEE Conference on Decision and Control and European Control Conference*. IEEE, pp. 4867–4872.
- Kloetzer M and Mahulea C (2020) Path planning for robotic teams based on LTL specifications and petri net models. *Discrete Event Dynamic Systems* 30(1): 55–79.
- Korsah GA, Stentz A and Dias MB (2013) A comprehensive taxonomy for multi-robot task allocation. *The International Journal of Robotics Research* 32(12): 1495–1512.
- Kupferman O and Vardi MY (2001) Model checking of safety properties. *Formal Methods in System Design* 19(3): 291–314.
- Lacerda B and Lima PU (2019) Petri net based multi-robot task coordination from temporal logic specifications. *Robotics and Autonomous Systems* 122: 103289.
- LaValle SM (2006) *Planning algorithms*. Cambridge university press.
- Leahy K, Jones A, Schwager M and Belta C (2015) Distributed information gathering policies under temporal logic constraints. In: *2015 54th IEEE Conference on Decision and Control (CDC)*. IEEE, pp. 6803–6808.
- Leahy K, Zhou D, Vasile CI, Oikonomopoulos K, Schwager M and Belta C (2016) Persistent surveillance for unmanned aerial vehicles subject to charging and temporal logic constraints. *Autonomous Robots* 40(8): 1363–1378.
- Loizou SG and Kyriakopoulos KJ (December 2004) Automatic synthesis of multi-agent motion tasks based on LTL specifications. In: *43rd IEEE Conference on Decision and Control (CDC)*, volume 1. The Bahamas, pp. 153–158.
- Luckcuck M, Farrell M, Dennis LA, Dixon C and Fisher M (2019) Formal specification and verification of autonomous robotic systems: A survey. *ACM Computing Surveys (CSUR)* 52(5): 1–41.
- Luo X, Kantaros Y and Zavlanos MM (2019) An abstraction-free method for multi-robot temporal logic optimal control synthesis. *arXiv preprint arXiv:1909.00526*.
- Luo X and Zavlanos M (2019) Transfer planning for temporal logic tasks. In: *Proc. of the 58th IEEE Conference on Decision and Control*. France, Nice.
- Michael N, Zavlanos MM, Kumar V and Pappas GJ (2008) Distributed multi-robot task assignment and formation control. In: *2008 IEEE International Conference on Robotics and Automation*. IEEE, pp. 128–133.
- Moarref S and Kress-Gazit H (2017) Decentralized control of robotic swarms from high-level temporal logic specifications. In: *2017 International Symposium on Multi-robot and Multi-agent Systems (MRS)*. IEEE, pp. 17–23.
- Nunes E, Manner M, Mitiche H and Gini M (2017) A taxonomy for task allocation problems with temporal and ordering constraints. *Robotics and Autonomous Systems* 90: 55–70.
- Russell S and Norvig P (2002) Artificial intelligence: a modern approach .
- Saha I, Ramaithitima R, Kumar V, Pappas GJ and Seshia SA (2014) Automated composition of motion primitives for multi-robot systems from safe LTL specifications. In: *2014 IEEE/RSJ International Conference on Intelligent Robots and Systems*. IEEE, pp. 1525–1532.
- Sahin YE (2019) <https://github.com/sahiny/cltl-hierarchical> .

- Sahin YE, Nilsson P and Ozay N (2017a) Provably-correct coordination of large collections of agents with counting temporal logic constraints. In: *Proceedings of the 8th International Conference on Cyber-Physical Systems*. ACM, pp. 249–258.
- Sahin YE, Nilsson P and Ozay N (2017b) Synchronous and asynchronous multi-agent coordination with cLTL+ constraints. In: *2017 IEEE 56th Annual Conference on Decision and Control (CDC)*. IEEE, pp. 335–342.
- Sahin YE, Nilsson P and Ozay N (2019a) Multirobot coordination with counting temporal logics. *IEEE Transactions on Robotics*.
- Sahin YE, Ozay N and Tripakis S (2019b) Multi-agent coordination subject to counting constraints: A hierarchical approach. In: *Distributed Autonomous Robotic Systems*. Springer, pp. 265–281.
- Sánchez G and Latombe JC (2003) A single-query bi-directional probabilistic roadmap planner with lazy collision checking. In: *Robotics research*. Springer, pp. 403–417.
- Schillinger P, Bürger M and Dimarogonas DV (2018a) Decomposition of finite LTL specifications for efficient multi-agent planning. In: *Distributed Autonomous Robotic Systems*. Springer, pp. 253–267.
- Schillinger P, Bürger M and Dimarogonas DV (2018b) Simultaneous task allocation and planning for temporal logic goals in heterogeneous multi-robot systems. *The International Journal of Robotics Research* 37(7): 818–838.
- Schillinger P, Bürger M and Dimarogonas DV (2019) Hierarchical LTL-task mdps for multi-agent coordination through auctioning and learning. *The International Journal of Robotics Research*.
- Shoukry Y, Nuzzo P, Balkan A, Saha I, Sangiovanni-Vincentelli AL, Seshia SA, Pappas GJ and Tabuada P (2017) Linear temporal logic motion planning for teams of underactuated robots using satisfiability modulo convex programming. In: *2017 IEEE 56th Annual Conference on Decision and Control (CDC)*. IEEE, pp. 1132–1137.
- Smith SL, Tůmová J, Belta C and Rus D (2010) Optimal path planning under temporal logic constraints. In: *2010 IEEE/RSJ International Conference on Intelligent Robots and Systems*. IEEE, pp. 3288–3293.
- Smith SL, Tůmová J, Belta C and Rus D (2011) Optimal path planning for surveillance with temporal-logic constraints. *The International Journal of Robotics Research* 30(14): 1695–1708.
- Stefanescu A (2006) Automatic synthesis of distributed transition systems.
- Tumova J and Dimarogonas DV (2015) Decomposition of multi-agent planning under distributed motion and task LTL specifications. In: *2015 54th IEEE Conference on Decision and Control (CDC)*. IEEE, pp. 7448–7453.
- Tumova J and Dimarogonas DV (2016) Multi-agent planning under local LTL specifications and event-based synchronization. *Automatica* 70: 239–248.
- Ulusoy A, Smith SL, Ding XC, Belta C and Rus D (2013) Optimality and robustness in multi-robot path planning with temporal logic constraints. *The International Journal of Robotics Research* 32(8): 889–911.
- Vardi MY and Wolper P (1986) An automata-theoretic approach to automatic program verification. In: *1st Symposium in Logic in Computer Science (LICS)*. IEEE Computer Society.
- Yu J and LaValle SM (2016) Optimal multirobot path planning on graphs: Complete algorithms and effective heuristics. *IEEE Transactions on Robotics* 32(5): 1163–1177.
- Zavlanos MM and Pappas GJ (2007) Distributed formation control with permutation symmetries. In: *2007 46th IEEE Conference on Decision and Control*. IEEE, pp. 2894–2899.
- Zavlanos MM and Pappas GJ (2008) Dynamic assignment in distributed motion planning with local coordination. *IEEE Transactions on Robotics* 24(1): 232–242.
- Zavlanos MM, Spesivtsev L and Pappas GJ (2008) A distributed auction algorithm for the assignment problem. In: *2008 47th IEEE Conference on Decision and Control*. IEEE, pp. 1212–1217.

Appendix A Time-Stamped Task Allocation

In this section, we first construct a routing graph and then formulate the MILP problem discussed in Section 5.1 to obtain the time-stamped task allocation plan for the prefix part. Next, we present a similar process for the suffix part. Finally, we discuss extensions of the MILP to address problem-specific requirements.

A.1 Construction of the prefix routing graph

We first construct the vertex set and then the edge set of the routing graph \mathcal{G} . Both constructions consist of four layers that iterate over the edges, then the labels, then the clauses, and finally, the literals in $\mathcal{A}_{\text{subtask}}^-$. The outline of the algorithm is shown in Alg. 1. An illustrative graph for task (i) is shown in Fig. 11.

A.1.1 Construction of the vertex set: The vertex set $\mathcal{V}_{\mathcal{G}}$ consists of three types of vertices, namely, location vertices related to initial robot locations, literal vertices related to edge labels in the sub-NBA $\mathcal{A}_{\text{subtask}}^-$, and literal vertices related to vertex labels in the sub-NBA $\mathcal{A}_{\text{subtask}}^-$. Specifically, we construct the location vertices as follows.

A.1.1.1 Location vertices associated with initial robot locations: First we create n vertices, collected in the set $\mathcal{V}_{\text{init}} \subseteq \mathcal{V}_{\mathcal{G}}$ such that each vertex points to the initial location $s_{r,j}^0$ of robot $[r, j] \in \mathcal{K}_j, \forall j \in [m]$ [line 1, Alg. 1] (see blue dots in Fig. 11).

To obtain the set of literal vertices in $\mathcal{V}_{\mathcal{G}}$, we iterate over subtasks in X_P . Given a subtask $e = (v_1, v_2) \in X_P$, we construct vertices for the edge label $\gamma(v_1, v_2)$ and the starting vertex label $\gamma(v_1)$, if they are neither \top nor \perp . Specifically, we take the following steps.

A.1.1.2 Literal vertices associated with edge labels: If $\gamma(v_1, v_2) \neq \top$, we operate on $\gamma(v_1, v_2) = \bigvee_{p \in \mathcal{P}} \bigwedge_{q \in \mathcal{Q}_p} \pi_{i,j}^{k,\chi}$ starting by iterating over the clauses $\mathcal{C}_p^\gamma \in \text{cls}(\gamma)$ in the label, and then over the literals in each clause \mathcal{C}_p^γ [lines 2–6, Alg. 1]. The literal $\pi_{i,j}^{k,\chi} \in \text{lits}^+(\mathcal{C}_p^\gamma)$ implies that at least $\langle i, j \rangle$, i.e., i robots of type j , should visit the target region ℓ_k simultaneously. Hence, we create i vertices in $\mathcal{V}_{\mathcal{G}}$ all associated with region ℓ_k . If $\langle i, j \rangle$ visit these i vertices simultaneously, one robot per vertex, then $\pi_{i,j}^{k,\chi}$ is true. Note that if $\chi \neq 0$, the robots visiting these i vertices should be the same as those visiting

Algorithm 1: Construct the routing graph

Input: Poset P

- 1 Create the vertex set $\mathcal{V}_{\text{init}}$ for initial locations ; ▷ Create the vertex set
- 2 **for** $e = (v_1, v_2) \in X_P$ **do**
- 3 **if** $\gamma(v_1, v_2) \neq \top$ **then**
- 4 **for** $C_p^\gamma \in \text{cls}(\gamma)$ **do**
- 5 **for** $\pi_{i,j}^{k,\chi} \in \text{lits}^+(C_p^\gamma)$ **do**
- 6 | Create i vertices ;
- 7 **if** $\gamma(v_1) \neq \top, \perp$ **then**
- 8 | Create vertices by following lines 4-6 ; ▷ Create the edge set
- 9 **for** $e = (v_1, v_2) \in X_P$ **do**
- 10 **if** $\gamma(v_1, v_2) \neq \top$ **then**
- 11 **for** $C_p^\gamma \in \text{cls}(\gamma)$ **do**
- 12 **for** $\pi_{i,j}^{k,\chi} \in \text{lits}^+(C_p^\gamma)$ **do**
- 13 (i) Vertices of initial robot locations ;
- 14 (ii) Vertices of prior subtasks ;
- 15 (iii) Vertices associated with $\gamma(v_1)$;
- 16 **if** $\gamma(v_1) \neq \top, \perp$ **then**
- 17 **if** $S_2^e = \emptyset$ **then**
- 18 | Create edges by following lines 11-13 ;
- 19 **else if** $S_2^e \neq \emptyset$ **then**
- 20 | Create edges from vertices associated with subtasks in S_2^e ;
- 21 **if** $X_{\prec_P}^e = \emptyset$ **and** $X_{\parallel_P}^e \neq \emptyset$ **then**
- 22 | Create edges from vertices associated with initial robot locations ;

another i vertices associated with another literal with the same nonzero connector, which is ensured by the MILP formulation; see the red, yellow, and green dots in Fig. 11.

A.1.1.3 Literal vertices associated with starting vertex labels: After vertices in \mathcal{V}_G associated with the edge label $\gamma(v_1, v_2)$ of subtask e have been constructed, vertices in \mathcal{V}_G associated with the starting vertex label $\gamma(v_1)$ can be constructed in the same manner if $\gamma(v_1)$ is neither \top nor \perp [lines 7-8, Alg. 1].

Repeating steps in Appendices A.1.1.2 and A.1.1.3 for all subtasks in X_P completes the construction of the vertex set \mathcal{V}_G . Note that each vertex in $\mathcal{V}_G \setminus \mathcal{V}_{\text{init}}$ is associated with a literal of a certain subtask in X_P . Also, each literal of a certain subtask in X_P is associated with one or more vertices in $\mathcal{V}_G \setminus \mathcal{V}_{\text{init}}$, and the literal specifies the region and the robot type associated with these vertices. To capture this correspondence, let $\mathcal{M}_e^{\mathcal{V}} : \mathcal{V}_G \setminus \mathcal{V}_{\text{init}} \rightarrow X_P$ and $\mathcal{M}_{\text{lits}}^{\mathcal{V}} : \mathcal{V}_G \setminus \mathcal{V}_{\text{init}} \rightarrow \prod_{\text{lits}}$ map a vertex in $\mathcal{V}_G \setminus \mathcal{V}_{\text{init}}$ to its associated subtask and literal, respectively, where \prod_{lits} is the cartesian product $X_P \times \{0, 1\} \times \mathcal{P} \times \mathcal{Q}_p$, and 0, 1 represent the label type, 0 for vertex label and 1 for edge label. Furthermore, let $\mathcal{M}_{\mathcal{V}}^{\text{lits}} : \prod_{\text{lits}} \rightarrow 2^{\mathcal{V}_G}$ and $\mathcal{M}_{\mathcal{V}}^{\text{cls}} : \prod_{\text{cls}} \rightarrow 2^{\mathcal{V}_G}$ map a literal and clause to the associated vertices in \mathcal{V}_G , respectively, where \prod_{cls} is the cartesian product $X_P \times \{0, 1\} \times \mathcal{P}$. We also define $\mathcal{M}_{\mathcal{L}}^{\mathcal{V}} : \mathcal{V}_G \rightarrow \mathcal{L}$ and $\mathcal{M}_{\mathcal{K}}^{\mathcal{V}} : \mathcal{V}_G \rightarrow \{\mathcal{K}_j\}$ that map a vertex in \mathcal{V}_G to its associated region and robot type. Finally, if $\chi \neq 0$, we define $\mathcal{M}_{\gamma}^{\chi} : \mathbb{N}^+ \rightarrow 2^{X_P \times \{0, 1\}}$ to map χ to all labels in X_P that have literals with the same connector χ ,

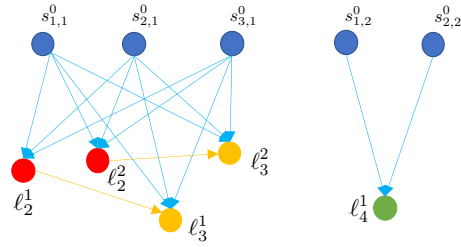


Figure 11. Routing graph \mathcal{G} for task (i). $s_{1,1}^0, s_{2,1}^0$ and $s_{3,1}^0$ are initial locations of three robots of type 1 and $s_{1,2}^0$ and $s_{2,2}^0$ are initial locations of two robots of type 2 (see case A.1.1.1). Red dots ℓ_2^1 and ℓ_2^2 correspond to the edge label $\pi_{2,1}^{2,1}$ of element 3, i.e., edge (v_1, v_2) in X_P ; see Fig. 8(b). Yellow dots ℓ_3^1, ℓ_3^2 correspond to the edge label $\pi_{2,1}^{3,1}$ of element 4, and green dot ℓ_4^1 corresponds to the edge label $\pi_{1,2}^{4,1}$ of element 2 (see Appendix A.1.1.2). No dots correspond to vertex labels since all vertex labels are either \top or \perp . The edges from ℓ_2^1 to ℓ_3^1 and from ℓ_2^2 to ℓ_3^2 are due to $3 <_P 4$.

which will be used in the MILP problem in Appendix A.2.5 to encode the constraint that some regions are visited by the same i robots of type j .

Example 1. continued (Mappings for task (i)) *The mappings in Fig. 11 associated with the vertex ℓ_2^1 are: $\mathcal{M}_e^{\mathcal{V}}(\ell_2^1) = (v_1, v_2) = 3$ and $\mathcal{M}_{\text{lits}}^{\mathcal{V}}(\ell_2^1) = ((v_1, v_2), 1, 1, 1)$ since the vertex ℓ_2^1 corresponds to the first literal $\pi_{2,1}^{2,1}$ of the first clause of the edge label of subtask (v_1, v_2) in X_P ; see also Fig. 8. $\mathcal{M}_{\mathcal{L}}^{\mathcal{V}}(\ell_2^1) = \ell_2$ and $\mathcal{M}_{\mathcal{K}}^{\mathcal{V}}(\ell_2^1) = \mathcal{K}_1$ since the literal $\pi_{2,1}^{2,1}$ requires two robots of type 1 to visit region ℓ_2 .*

Furthermore, the literal/clause-to-vertex mappings are: $\mathcal{M}_{\mathcal{V}}^{\text{lits}}(((v_1, v_2), 1, 1, 1)) = \mathcal{M}_{\mathcal{V}}^{\text{cls}}(((v_1, v_2), 1, 1, 1)) = \{\ell_2^1, \ell_2^2\}$; $\mathcal{M}_{\mathcal{V}}^{\text{lits}}(((v_1, v_4), 1, 1, 1)) = \mathcal{M}_{\mathcal{V}}^{\text{cls}}(((v_1, v_4), 1, 1, 1)) = \{\ell_4^1\}$ since the literal $\pi_{1,2}^{4,1}$, the first literal of the first clause of the edge label of subtask (v_1, v_4) , requires one robot to visit region ℓ_4 . Finally, the connector-to-label mapping is: $\mathcal{M}_{\gamma}^{\chi}(1) = \{((v_1, v_2), 1), ((v_3, v_6), 1)\}$ since the connector 1 appears in the edge label of subtask (v_1, v_2) and the edge label of subtask (v_3, v_6) .

A.1.2 Construction of the edge set: The edges in \mathcal{G} respect the partial order among subtasks captured by the poset P . We construct the edge set \mathcal{E}_G by following a similar procedure as that used to construct the vertex set \mathcal{V}_G . Specifically, we iterate over the elements in X_P . For every subtask $e = (v_1, v_2) \in X_P$, if $\gamma(v_1, v_2) \neq \top$, we first operate on the edge label $\gamma(v_1, v_2) = \bigvee_{p \in \mathcal{P}} \bigwedge_{q \in \mathcal{Q}_p} \pi_{i,j}^{k,\chi}$ starting by iterating over the clauses $C_p^\gamma \in \text{cls}(\gamma)$, and then over the literals in each clause C_p^γ [lines 9-15, Alg. 1]. Specifically, recall from Appendix A.1.1 that the literal $\pi_{i,j}^{k,\chi} \in \text{lits}^+(C_p^\gamma)$ corresponds to i vertices in \mathcal{V}_G that are associated with region ℓ_k that should be visited by i robots. In what follows, we identify three types of *leaving vertices* in \mathcal{V}_G from where i robots can depart to reach these i vertices that satisfy literal $\pi_{i,j}^{k,\chi}$.

A.1.2.1 Location vertices: The location vertices in $\mathcal{V}_{\text{init}}$ associated with robots of type j are leaving vertices. We add an edge from all initial vertices to every vertex associated with literal $\pi_{i,j}^{k,\chi}$ (see blue edges in Fig. 11). Intuitively, robots depart from initial locations to undertake certain subtasks. These edges are associated with a weight T^* that

is equal to the shortest travel time from the initial location to region ℓ_k and another weight d that is equal to the smallest traveling cost between the initial location and ℓ_k , which will be used in the MILP problem in Appendices A.2.2 and A.2.7 to encode the scheduling constraints and the objective.

A.1.2.2 Leaving vertices associated with prior subtasks: Let $X_{<_P}^e$, $X_{\prec_P}^e$ and $X_{\parallel_P}^e$ denote the sets that collect subtasks in X_P that are smaller than, covered by, and incomparable to subtask e , respectively (see Section 2.2). In words, $X_{<_P}^e$ contains subtasks in X_P that should be completed prior to e , $X_{\prec_P}^e \subseteq X_{<_P}^e$ contains subtasks in $X_{<_P}^e$ that can be completed right before e , and $X_{\parallel_P}^e$ contains subtasks independent from e . To find leaving vertices, we iterate over $S_1^e = X_{<_P}^e \cup X_{\parallel_P}^e$ that includes all subtasks that can be completed prior to e , respecting the partial order between subtasks. Given a subtask $e' = (v'_1, v'_2) \in S_1^e$, if its edge label $\gamma'(v'_1, v'_2) \neq \top$, we iterate over all clauses in γ' and then over all literals in each clause. Specially, given a clause $C_p^{\gamma'} \in \text{cls}(\gamma')$, for any literal $\pi_{i',j'}^{k',\chi'} \in \text{lits}^+(C_p^{\gamma'})$, if $j' = j$, then literal vertices in \mathcal{V}_G associated with this literal are leaving vertices. If further $i' = i$, we randomly create i one-to-one edges starting from these i vertices and ending at the i vertices associated with $\pi_{i,j}^{k,\chi}$ (see the orange edges in Fig. 11). Because there are exactly i robots of type j , it suffices to build i one-to-one edges. Furthermore, if $\chi = \chi' \neq 0$, then literals $\pi_{i,j}^{k,\chi}$ and $\pi_{i',j'}^{k',\chi'}$ must have the same number of vertices. Building i one-to-one edges can guarantee that the same i robots of type j satisfy these two literals. Otherwise, if $i' \neq i$, we add $i \times i'$ edges to \mathcal{E}_G by creating an edge from any vertex associated with $\pi_{i',j'}^{k',\chi'}$ to any vertex of $\pi_{i,j}^{k,\chi}$. Finally, since each region may span multiple cells, the weights T^* and d of these edges are set as the shortest travel time and lowest traveling cost from $\ell_{k'}$ to ℓ_k . After creating edges associated with the edge label $\gamma'(v'_1, v'_2)$ of e' , we identify leaving vertices among literal vertices in \mathcal{V}_G associated with the starting vertex label $\gamma(v'_1)$ of e' and build edges in the same manner.

A.1.2.3 Leaving vertices associated with $\gamma(v_1)$ of e : When the iteration over S_1^e is completed, we identify leaving vertices among literal vertices associated with the starting vertex label $\gamma(v_1)$ of the current subtask e by following the procedure in Appendix A.1.2.2 for the prior subtasks. This is because $\gamma(v_1)$ becomes true before $\gamma(v_1, v_2)$.

So far we have constructed three types of leaving vertices corresponding to the literal $\pi_{i,j}^{k,\chi}$ in $\text{lits}^+(C_p^{\gamma})$ of the edge label $\gamma(v_1, v_2)$ [lines 13–15, Alg. 1]. We continue constructing leaving vertices for all other literals in $\text{lits}^+(C_p^{\gamma})$ [line 12, Alg. 1] and clauses in $\text{cls}(\gamma)$ [line 11, Alg. 1]. After constructing all edges pointing to vertices associated with literals in the edge label $\gamma(v_1, v_2)$ of the current subtask e [line 10, Alg. 1], we construct edges pointing to vertices associated with literals in the starting vertex label $\gamma(v_1)$, by identifying leaving vertices among location vertices and literal vertices associated with prior subtasks. Specifically, let $S_2^e = X_{\prec_P}^e \cup X_{\parallel_P}^e$ be the set that collects all subtasks that can occur immediately prior to subtask e . The satisfaction of edge labels of subtasks in S_2^e can directly lead to the starting vertex v_1 of e . We consider the following cases.

(1) $S_2^e = \emptyset$: In this case, no subtask can be completed before subtask e , i.e., the subtask e should be the first one

among all in X_P to be completed. Thus, v_1 is identical to the initial vertex v_0 . In this case, we only identify location vertices as leaving vertices, as in Appendix A.1.2.1 [lines 18, Alg. 1].

(2) $S_2^e \neq \emptyset$: We identify leaving vertices associated with prior subtasks in S_2^e . Given a subtask $e' = (v'_1, v'_2) \in S_2^e$, we find all clauses $C_p^{\gamma'} \in \text{cls}(\gamma')$ in the edge label γ' of e' such that, for the considered clause $C_p^{\gamma} \in \text{cls}(\gamma)$ in the starting vertex label of subtask e , its corresponding clause $(C_p^{\gamma})_{\phi}$ in \mathcal{A}_{ϕ} is the subformula of their corresponding clauses $(C_p^{\gamma'})_{\phi}$ in \mathcal{A}_{ϕ} . Next, for each literal $\pi_{i,j}^{k,\chi} \in \text{lits}^+(C_p^{\gamma})$ we create i one-to-one edges, starting from those i vertices associated with the counterpart of literal $\pi_{i,j}^{k,\chi}$ in the found clause $C_p^{\gamma'} \in \text{cls}(\gamma')$ and ending at the i vertices associated with $\pi_{i,j}^{k,\chi}$ [lines 20, Alg. 1]. We create such one-to-one edges based on condition (d) in Definition 3.8 and condition (b) in Definition 3.10. That is, the edge label strongly implies its end vertex label, the satisfied clause in the edge label implies the satisfied clause in the end vertex label, and the fleet of robots satisfying the clause in the vertex label belongs to the fleet of robots satisfying the clause in the incoming edge label. This is also the reason why we consider prior subtasks in S_2^e rather than S_1^e as in Appendix A.1.2.2.

(3) $X_{\prec_P}^e = \emptyset$ and $X_{\parallel_P}^e \neq \emptyset$: In this case, the subtask e can be the first one among all to be completed. If so, its starting vertex label $\gamma(v_1)$ should be satisfied at the beginning. However, robots cannot depart from leaving vertices that are literal vertices (see case (2) in Appendix A.1.2.3), because these edges are enabled after subtask e . Therefore, for the vertex label $\gamma(v_1)$, we additionally identify leaving vertices pointing to initial robot locations, as in Appendix A.1.2.1 [lines 22, Alg. 1]. Note that, if $X_{\prec_P}^e \neq \emptyset$, there are no leaving vertices associated with initial locations since there exists a subtask that should be completed before e and, therefore, subtask e can not be the first one. When the iteration over all subtasks in X_P is over, we finish the construction of the edge set \mathcal{E}_G [line 9, Alg. 1].

Remark A.1. (Relaxation of strong implication in condition (d) in Definition 3.8). *Condition (d) in Definition 3.8 requires that an edge label strongly implies its end vertex label. This condition ensures both that the satisfaction of an edge label leads to the satisfaction of its end vertex label and that when constructing the routing graph \mathcal{G} , robots satisfying the positive subformula in an end vertex label belong to robots satisfying the corresponding edge label (see step (2) in Appendix A.1.2.3). This condition can be relaxed to requiring that an edge label implies its end vertex label (see Definition 3.7), which can still ensure that the satisfaction of an edge label implies the satisfaction of its end vertex label, so that the previous instance of GMRPP still activates the immediately following instance of GMRPP. The only change needed in this case is in the pre-processing steps in Section 3.4.2 where we need to remove all clauses in an end vertex label that are not a subformula of clauses in the corresponding edge label. This way, the edge label strongly implies the remaining clauses in its end vertex label.*

A.2 Construction of the prefix MILP

To formulate the proposed MILP, we define two types of variables: the routing variables $x_{uvr} \in \{0, 1\}$ and the scheduling variables $t_{vr}^-, t_{vr}^+ \in \mathbb{N}$, where $x_{uvr} = 1$ if robot $r \in \mathcal{M}_K^\mathcal{V}(v)$ traverses the edge $(u, v) \in \mathcal{E}_G$, and t_{vr}^-, t_{vr}^+ are times when robot r should arrive at and is allowed to leave from vertex $v \in \mathcal{V}_G$. We assume that robot r is still at vertex v at departure time t_{vr}^+ . Since the satisfaction of the edge label is instantaneous, if $v \in \mathcal{V}_G$ is associated with an edge label, we have $t_{vr}^- = t_{vr}^+$, which means that the robot is allowed to leave at the next time instant. As for the vertex label, we have $t_{vr}^- \leq t_{vr}^+$, which means that the robot should stay where it is to wait for the satisfaction of the corresponding edge label.

A.2.1 Routing constraints: These constraints are associated with vertices and restrict the flow of robots between connected vertices in \mathcal{V}_G . Specifically, $\forall v \in \mathcal{V}_G \setminus \mathcal{V}_{\text{init}}$, the constraint that v is visited by at most one robot of type $\mathcal{M}_K^\mathcal{V}(v)$ can be written as

$$\sum_{u:(u,v) \in \mathcal{E}_G} \sum_{r \in \mathcal{M}_K^\mathcal{V}(v)} x_{uvr} \leq 1, \quad (3)$$

which is not a strict equality since the clause that vertex v is associated with can be false. In this case, there is no need to visit this vertex. Moreover, the constraint that the inflow is no less than the outflow at any vertex $v \in \mathcal{V}_G \setminus \mathcal{V}_{\text{init}}$ can be written as

$$\sum_{w:(v,w) \in \mathcal{E}_G} x_{vwr} \leq \sum_{u:(u,v) \in \mathcal{E}_G} x_{uvr}, \quad \forall r \in \mathcal{M}_K^\mathcal{V}(v), \quad (4)$$

which states that robots can remain idle if they are not assigned a subtask. Then, $\forall v \in \mathcal{V}_{\text{init}}$, the initial conditions associated with constraint (4) are

$$\sum_{w:(v,w) \in \mathcal{E}_G} x_{vwr} \leq 1, \quad \text{if } r = r_v \in \mathcal{M}_K^\mathcal{V}(v), \quad (5a)$$

$$\sum_{w:(v,w) \in \mathcal{E}_G} x_{vwr} = 0, \quad \forall r \in \mathcal{M}_K^\mathcal{V}(v) \setminus \{r_v\}, \quad (5b)$$

where r_v refers to the specific robot at the initial location $\mathcal{M}_L^\mathcal{V}(v) = s^0$ if $v \in \mathcal{V}_{\text{init}}$.

A.2.2 Scheduling constraints: These constraints are also associated with vertices and capture the temporal relation on a vertex or between visits of two connected vertices. First, we require positivity of scheduling variables, $\forall v \in \mathcal{V}_G$, i.e.,

$$0 \leq t_{vr}^-, t_{vr}^+ \leq M_{\max} \sum_{u:(u,v) \in \mathcal{E}_G} x_{uvr}, \quad \forall r \in \mathcal{M}_K^\mathcal{V}(v), \quad (6)$$

where M_{\max} is a large positive integer. The constraint (6) implies that $t_{vr}^- = t_{vr}^+ = 0$ if vertex v is not visited by robot r . The initial condition associated with constraint (6) is

$$t_{vr}^- = t_{vr}^+ = 0, \quad \forall r \in \mathcal{M}_K^\mathcal{V}(v), \quad \forall v \in \mathcal{V}_{\text{init}}. \quad (7)$$

The scheduling constraints between visiting times of two connected vertices considering the travel time, $\forall r \in \mathcal{M}_K^\mathcal{V}(v)$, $\forall (u, v) \in \mathcal{E}_G$, are

$$t_{ur}^+ + (T_{uv}^* + 1)x_{uvr} \leq t_{vr}^- + M_{\max}(1 - x_{uvr}), \quad \text{if } u \parallel_P v, \quad (8a)$$

$$t_{ur}^+ + T_{uv}^*x_{uvr} \leq t_{vr}^- + M_{\max}(1 - x_{uvr}), \quad \text{otherwise}. \quad (8b)$$

where T_{uv}^* is the shortest travel time between regions that vertices u and v correspond to and $u \parallel_P v$ means that the subtask $\mathcal{M}_e^\mathcal{V}(u)$ is incomparable to $\mathcal{M}_e^\mathcal{V}(v)$, corresponding to the cases in Appendices A.1.2.2 and A.1.2.3. When $x_{uvr} = 1$, constraint (8a) becomes $t_{ur}^+ + T_{uv}^* + 1 \leq t_{vr}^-$ and constraint (8b) becomes $t_{ur}^+ + T_{uv}^* \leq t_{vr}^-$. Because $T_{uv}^* \geq 0$, constraints (8) ensure that t_{vr}^- should be no less than t_{ur}^+ if $x_{uvr} = 1$. Note that a cycle in \mathcal{G} must include a pair of incomparable vertices, since all comparable vertices constitute a chain. Constraint (8a) prevents cycles in \mathcal{G} where all vertices correspond to the same region. For instance, consider such a cycle $u_1, u_2, \dots, u_c, u_1$. Without constraint (8a), a solution with zero travel time satisfies constraints (3), (4) and (8b), resulting in $x_{u_1 u_2} = \dots = x_{u_c u_1} = 1$ for a robot r , without this robot actually visiting any vertex from its initial location. Constraint (8a) is functionally similar to the subtour elimination constraint in vehicle routing problems which prevents any solution that consists of a disconnected tour. We leverage a term 1 to ensure that time increases along the edge that connects incomparable vertices, thus preventing visiting of a cycle.

A.2.3 Logical constraints: These constraints associate vertices with subtasks and encode the logical relation between labels, clauses and literals, and the realization of literals. Given a subtask $e \in X_P$, every vertex or edge label $\gamma = \bigvee_{p \in \mathcal{P}} \bigwedge_{q \in \mathcal{Q}_p} \pi_{i_q, j_q}^{k_q, \chi_q}$ (neither \top nor \perp) is true as long as one of its clauses is true. To this end, we associate each clause $\mathcal{C}_p^\gamma \in \text{cls}(\gamma)$ with a binary variable b_p such that $b_p = 1$ if the p -th clause \mathcal{C}_p^γ is true. Hence, the label γ being true can be encoded as

$$\sum_{p \in \mathcal{P}} b_p = 1. \quad (9)$$

That is, one and only one clause is true, which is justified by condition (a) in Definition 3.10 which states that it is the same clause in a vertex label that is satisfied. The logical relation, between a clause and its literals, that the satisfaction of the clause is equivalent to the satisfaction of all its literals, is written as

$$\left[\sum_{q \in \mathcal{Q}_p} \sum_{v \in \mathcal{M}_V^{\text{lits}}(e, 0|1, p, q)} \sum_{u:(u,v) \in \mathcal{E}_G} \sum_{r \in \mathcal{M}_K^\mathcal{V}(v)} x_{uvr} \right] / \sum_{q \in \mathcal{Q}_p} i^q = b_p, \quad (10)$$

which connects the routing variables x_{uvr} with the logical variables b_p . In words, if $b_p = 1$, then every vertex associated with the p -th clause should be visited by one robot. Let

$$z_q = \sum_{v \in \mathcal{M}_V^{\text{lits}}(e, 0|1, p, q)} \sum_{u:(u,v) \in \mathcal{E}_G} \sum_{r \in \mathcal{M}_K^\mathcal{V}(v)} x_{uvr}$$

be the inner summation in (10). If $b_p = 1$, then all literals in $\text{lits}^+(\mathcal{C}_p^\gamma)$ are true. In this case, for the q -th literal $\pi_{i_q, j_q}^{k_q, \chi_q} \in \text{lits}^+(\mathcal{C}_p^\gamma)$, all i^q vertices in $\mathcal{M}_V^{\text{lits}}(e, 0|1, p, q)$ should be visited, so $\sum_{u:(u,v) \in \mathcal{E}_G} \sum_{r \in \mathcal{M}_K^\mathcal{V}(v)} x_{uvr} = 1$ for each vertex $v \in \mathcal{M}_V^{\text{lits}}(e, 0|1, p, q)$, and therefore $z_q = i^q$, and the left side of constraint (10) becomes

$$\sum_{q \in \mathcal{Q}_p} z_q / \sum_{q \in \mathcal{Q}_p} i^q = \sum_{q \in \mathcal{Q}_p} i^q / \sum_{q \in \mathcal{Q}_p} i^q = 1 = b_p.$$

If $b_p = 0$, all x_{uvr} in constraint (10) equal 0, which implies that no vertices need to be visited for false clauses. Combining constraints (6) and (10), $\sum_{r \in \mathcal{M}_{\mathcal{K}}^{\mathcal{V}}(v)} t_{vr}^-$ equals 0 if the clause that v is associated with is false. That is, a robot remains idle if it is not responsible for the satisfaction of any clause.

Note that the logical relation in constraint (10) only requires that some vertices should be visited at some point in time to satisfy all literals. Next, we formulate the synchronization constraint requiring that, if γ is an edge label and the p -th clause C_p^γ is true, all vertices in $\mathcal{M}_{\mathcal{V}}^{\text{cls}}(e, 1, p)$ should be visited at the same time since the satisfaction of edge labels is instantaneous. We define the pairwise vertex set induced from the clause C_p^γ as $\mathcal{V}_{\gamma, p}^{\text{sync}} = \{(u, v) \mid u, v \in \mathcal{M}_{\mathcal{V}}^{\text{cls}}(e, 1, p), u \neq v\}$. If $b_p = 1$, visiting any pair in $\mathcal{V}_{\gamma, p}^{\text{sync}}$ simultaneously is written as

$$\sum_{r \in \mathcal{M}_{\mathcal{K}}^{\mathcal{V}}(u)} t_{ur}^- = \sum_{r \in \mathcal{M}_{\mathcal{K}}^{\mathcal{V}}(v)} t_{vr}^-, \quad \forall (u, v) \in \mathcal{V}_{\gamma, p}^{\text{sync}}. \quad (11)$$

When $b_p = 0$, constraint (11) also holds since both sides equal 0.

A.2.4 Temporal constraints: These constraints capture the temporal orders between subtasks. We first introduce the notions of the activation and completion time of a subtask. Then, given a subtask e , there are three types of temporal constraints associated with the activation and completion times (see Definition A.2 below), for the subtask e or between subtasks.

Definition A.2. (Activation and completion time of a subtask or its starting vertex label). *Given a subtask $e = (v_1, v_2)$, we define its activation time (equivalently, the activation time of its starting vertex label) as the time instant when its vertex label $\gamma(v_1)$ becomes true. Similarly, we define the completion time of a subtask (equivalently, the completion time of its starting vertex label) as the time instant when its edge label $\gamma(v_1, v_2)$ becomes true (or the last time its starting vertex label $\gamma(v_1)$ is true). The span of a subtask (or its starting vertex label) is the time interval starting from the activation time and ending at the completion time.*

A.2.4.1 Temporal constraints associated with one subtask: These constraints capture the relation that the completion time of a subtask should lie in the span of its starting vertex label, or exactly one time step after the completion of its starting vertex label. Intuitively, the “avoid” part of a subtask should be maintained until the “reach” part is realized.

For this, we define the auxiliary variable t_e to denote the completion time of the subtask e , i.e., time when its edge label becomes true. We have

$$t_e = \sum_{p \in \mathcal{P}} \sum_{r \in \mathcal{M}_{\mathcal{K}}^{\mathcal{V}}(v_p)} t_{vr}^-, \quad (12)$$

where v_p is randomly selected from $\mathcal{M}_{\mathcal{V}}^{\text{cls}}(e, 1, p)$ due to constraints (9) and (11) that require that only one clause of an edge label is true and all associated vertices are visited at the same time.

When the starting vertex v_1 has a self-loop, and its label $\gamma(v_1)$ is not \top (if this is not the case, there are no vertices

in \mathcal{G} associated with $\gamma(v_1)$), the temporal relation, $\forall C_p^\gamma \in \text{cls}(\gamma(v_1))$ and $\forall v \in \mathcal{M}_{\mathcal{V}}^{\text{cls}}(e, 0, p)$, can be written as

$$\sum_{r \in \mathcal{M}_{\mathcal{K}}^{\mathcal{V}}(v)} t_{vr}^- \leq t_e \leq \sum_{r \in \mathcal{M}_{\mathcal{K}}^{\mathcal{V}}(v)} t_{vr}^+ + 1 + M_{\max}(1 - b_p). \quad (13)$$

If $b_p = 0$, then by constraint (10) no robot visits vertex v , so $\sum_{r \in \mathcal{M}_{\mathcal{K}}^{\mathcal{V}}(v)} t_{vr}^- = 0 \leq t_e$, i.e., the left inequality in (13) holds. The right inequality in (13) holds trivially. Only when $b_p = 1$, i.e., when the p -th clause in the vertex label is true, does constraint (13) become active. Note that constraint (13) implies that the span of a subtask is not necessarily equal to the span of its starting vertex label. On the other hand, when the starting vertex v_1 does not have a self-loop, v_1 is identical to the initial vertex v_0 . Recall that in Section 4.1 we remove all vertices without self-loops except for the initial and accepting vertices. Hence, in $\mathcal{A}_{\text{subtask}}^-$, only v_0 and v_{accept} are allowed not to have self-loops but v_{accept} cannot be the starting vertex. Therefore, $v_1 = v_0$. If $\gamma(v_0) = \perp$, constraint (13) implies that the edge label of subtask e should be satisfied at time instant 0, i.e.,

$$t_e = 0, \quad \text{if } \gamma(v_0) = \perp. \quad (14)$$

A.2.4.2 Temporal constraints associated with the completion of two sequential subtasks: These constraints impose the precedence relation that subsequent subtasks should be completed after prior subtasks are completed. Given the current subtask e , we collect its prior subtasks in the set $X_{\prec_P}^e$ rather than a larger set $X_{\leq_P}^e$ (defined in Appendix A.1.2.2). That is, we consider subtasks that are covered by e due to the transitivity property of the partial order. If $X_{\prec_P}^e$ is nonempty, we iterate over subtasks in it. Given $e' \in X_{\prec_P}^e$, we can capture the requirement that the subtask e' is completed before the current subtask e by the constraint

$$t_{e'} + 1 \leq t_e, \quad \forall e' \in X_{\prec_P}^e, \quad (15)$$

where the term 1 excludes the case where two edge labels become true simultaneously, violating the precedence relation.

A.2.4.3 Temporal constraints associated with the completion of the current subtask and the activation of the subtask immediately following it: These constraints capture the precedence relation that the current subtask e should be completed at most one time step before the subtask immediately following it is activated. Otherwise, progress in the sub-NBA induced from the poset P will be trapped at subtask e if there is no subtask immediately after it is activated. To capture this requirement, we define $|X_P| \cdot |X_P - 1|$ auxiliary binary variables $b_{ee'}$ for any two different subtasks $e, e' \in X_P$, such that $b_{ee'} = 1$ if subtask e' occurs immediately after subtask e . Furthermore, we define the set $S_3^e = X_{\succ_P}^e \cup X_{\parallel_P}^e$ that collects all subtasks whose activation can immediately follow the completion of subtask e . In what follows, we proceed based on whether $X_{\succ_P}^e \neq \emptyset$.

(1) $X_{\succ_P}^e \neq \emptyset$: In this case, there must exist a subtask that occurs after e . Then, the constraint that there exists a subtask in S_3^e that occurs immediately after e can be written as

$$\sum_{e' \in S_3^e} b_{ee'} = 1. \quad (16)$$

If the subtask e' indeed occurs immediately after subtask e , then it should be completed after subtask e , that is,

$$t_e + 1 \leq t_{e'} + M_{\max}(1 - b_{ee'}), \forall e' \in S_3^e. \quad (17)$$

To establish the transition between subtasks, the subtask e' that occurs immediately after subtask e should be activated at most one time step after the completion of e . That is, $\forall e' = (v'_1, v'_2) \in S_3^e, \forall \mathcal{C}_p^{\gamma(v'_1)} \in \text{cls}(\gamma(v'_1)), \forall v \in \mathcal{M}_{\mathcal{V}}^{\text{cls}}(e', 0, p)$, we have

$$\sum_{r \in \mathcal{M}_{\mathcal{K}}^{\mathcal{V}}(v)} t_{vr}^- \leq t_e + 1 + M_{\max}(1 - b_{ee'}). \quad (18)$$

If the p -th clause in the vertex label $\gamma(v'_1)$ is true, constraint (18) requires that the associated vertices are visited at most one time step after the completion of e . Otherwise if the p -th clause is false, the left side of (18) becomes 0 and the constraint (18) holds trivially. If $\gamma(v'_1) = \top$, the subtask e' can be viewed as being activated at time instant 0. Thus, constraint (18) is satisfied trivially.

(2) $X_{\prec_P}^e = \emptyset$: In this case, if subtask e is completed after the subtasks in $X_{\parallel_P}^e$, then it is the last subtask to be completed in X_P . Thus, there is no subtask to be activated any more. Otherwise, if subtask e is not the last subtask, then there exists a subtask that occurs after e , same as in case (1).

To determine whether subtask e is the last subtask, we define $|X_P| \cdot |X_P - 1|$ auxiliary binary variables $b_e^{e'}$ for any two different subtasks $e, e' \in X_P$, such that $b_e^{e'} = 1$ if and only if $t_e > t_{e'}$, i.e., if and only if subtask e is completed after e' . This implication can be written as, $\forall e, e' \in X_P$ and $e \neq e'$,

$$b_e^{e'} + b_{e'}^e = 1, \quad (19a)$$

$$M_{\max}(b_e^{e'} - 1) \leq t_e - t_{e'} \leq M_{\max}b_e^{e'} - 1. \quad (19b)$$

Constraints (19) require that no two subtasks are completed at the same time and that $b_e^{e'} = 1$ if and only if $t_e > t_{e'}$. Assume $t_e = t_{e'}$. From constraint (19b), we get $b_e^{e'} = b_{e'}^e = 1$, which violates constraint (19a). Although independent subtasks can occur simultaneously, constraint (19) requires that they occur serially so that the solution to the MILP gives rise to a simple path in $\mathcal{A}_{\text{subtask}}^-$ that is a linear extension of the poset P . When $t_e > t_{e'}$, the right side of constraint (19b) implies $b_e^{e'} = 1$; when $t_e < t_{e'}$, the left side of constraint (19b) implies $b_e^{e'} = 0$.

Furthermore, we define $z = |X_{\parallel_P}^e|$. Observe that, for $e' \in X_{\parallel_P}^e$, the term $z - \sum_{e' \in X_{\parallel_P}^e} b_e^{e'} = 0$ if e is the last completed task; otherwise it is positive. If subtask e is not the last subtask, there should be a subtask in $X_{\parallel_P}^e$ that occurs immediately after e . This requirement can be written as

$$\sum_{e' \in X_{\parallel_P}^e} b_{ee'} \leq 1, \quad (20a)$$

$$z - \sum_{e' \in X_{\parallel_P}^e} b_e^{e'} - M_{\max} \sum_{e' \in X_{\parallel_P}^e} b_{ee'} \leq 0, \quad (20b)$$

$$\sum_{e' \in X_{\parallel_P}^e} b_{ee'} - M_{\max}(z - \sum_{e' \in X_{\parallel_P}^e} b_e^{e'}) \leq 0. \quad (20c)$$

If subtask e is completed after all subtasks in $X_{\parallel_P}^e$, then $z - \sum_{e' \in X_{\parallel_P}^e} b_e^{e'} = 0$, and constraint (20c) gives

$\sum_{e' \in X_{\parallel_P}^e} b_{ee'} = 0$, i.e., there is no subtask that follows e immediately. Constraint (20a) becomes $0 \leq 1$ and (20b) becomes $0 \leq 0$. Both hold trivially. Otherwise, if subtask is not the last subtask, i.e., if $z - \sum_{e' \in X_{\parallel_P}^e} b_e^{e'} > 0$, then constraints (20a) and (20b) give $\sum_{e' \in X_{\parallel_P}^e} b_{ee'} = 1$. Constraint (20c) holds trivially. Finally, after determining the subtask e' that occurs immediately after e , we impose the same constraints as (17) and (18).

Note that constraints (16)-(20) in (1) and (2) ensure that, for a subtask in X_P , except for the last one, there exists another subtask that immediately follows it. However, it is possible that two different subtasks are followed by the same subtask, which cannot be excluded by constraint (16). To avoid this situation, next we impose the constraint that except for the first subtask to be completed in X_P , each subtask can only immediately follow one subtask. Combined with constraints (16)-(20), we guarantee the one-to-one correspondence between any two consecutive subtasks in a linear extension. Recall that $S_2^e = X_{\prec_P}^e \cup X_{\parallel_P}^e$. We proceed based on whether $X_{\prec_P}^e = \emptyset$ or not.

(3) $X_{\prec_P}^e \neq \emptyset$: In this case, subtask e cannot be the first subtask to be completed, that is, it has to immediately follow one subtask in S_2^e . This requirement is captured by the constraint

$$\sum_{e' \in S_2^e} b_{e'e} = 1. \quad (21)$$

(4) $X_{\prec_P}^e = \emptyset$: In this case, $X_{\prec_P}^e = \emptyset$, so there is no subtask prior to e . Recall that the binary variable $b_e^{e'} = 1$ if subtask e is completed after e' and no two subtasks are completed at the same time. Therefore, $b_e^{e'} = 0$ if e is completed prior to e' , and further the term $\sum_{e' \in X_{\parallel_P}^e} b_e^{e'} = 0$ if e is the first completed task; otherwise it is positive. Then, the constraint that each subtask in $X_{\parallel_P}^e$, except the first one, immediately follows another subtask can be written as

$$\sum_{e' \in X_{\parallel_P}^e} b_{e'e} \leq 1, \quad (22a)$$

$$\sum_{e' \in X_{\parallel_P}^e} b_e^{e'} - M_{\max} \sum_{e' \in X_{\parallel_P}^e} b_{e'e} \leq 0, \quad (22b)$$

$$\sum_{e' \in X_{\parallel_P}^e} b_{e'e} - M_{\max} \sum_{e' \in X_{\parallel_P}^e} b_e^{e'} \leq 0. \quad (22c)$$

When e is the first subtask, i.e., when $\sum_{e' \in X_{\parallel_P}^e} b_e^{e'} = 0$, then constraints (22b) and (22c) give $\sum_{e' \in X_{\parallel_P}^e} b_{e'e} = 0$. Otherwise, if e is not the first subtask, i.e., if $\sum_{e' \in X_{\parallel_P}^e} b_e^{e'} > 0$, then constraints (22a) and (22b) give $\sum_{e' \in X_{\parallel_P}^e} b_{e'e} = 1$; same as (21).

A.2.4.4 Temporal constraints associated with the activation of the first subtask: We analyzed the temporal constraints on the completion of the current subtask and the activation of subsequent subtasks above. However, if the subtask e is the first subtask to be completed, there is no subtask whose completion activates e , which should be activated at the beginning. To determine the first subtask in X_P , let P_{\max} be the set that collects subtasks that can be

the first ones to be completed, which are referred to as the maximal elements in a poset P . An element in a poset P is a maximal element if there is no larger element in P than itself. That is, for any subtask $e \in P_{\max}$, we have $X_{\prec_P}^e = \emptyset$. If the first completed subtask $e = (v_1, v_2)$ has a self-loop and the vertex label is not \top (it is activated at the beginning if $\gamma(v_1) = \top$), we require that the vertex label $\gamma(v_1)$ be activated at time 0, which implies that the associated vertices in \mathcal{G} should be visited at time 0, i.e., $\forall e \in P_{\max}, \forall \mathcal{C}_p^{\gamma(v_1)} \in \text{cls}(\gamma(v_1)), \forall v \in \mathcal{M}_{\mathcal{V}}^{\text{cls}}(e, 0, p)$,

$$\sum_{r \in \mathcal{M}_{\mathcal{K}}^{\mathcal{V}}(v)} t_{vr}^- \leq M_{\max} \left(\sum_{e' \in P_{\max} \setminus \{e\}} b_e^{e'} + 1 - b_p \right). \quad (23)$$

Only when e is the first subtask to be completed, i.e., when $\sum_{e' \in P_{\max} \setminus \{e\}} b_e^{e'} = 0$ and when the associated clause is true, i.e., when $b_p = 1$, should the vertices associated with the p -th clause be visited by robots at time 0, i.e., $\sum_{r \in \mathcal{M}_{\mathcal{K}}^{\mathcal{V}}(v)} t_{vr}^- \leq 0$. When $|P_{\max}| = 1$, constraint (23) will be reduced to $\sum_{r \in \mathcal{M}_{\mathcal{K}}^{\mathcal{V}}(v)} t_{vr}^- \leq M_{\max}(1 - b_p)$. Note that if the vertex label $\gamma(v_1)$ has no self-loop, then v_1 is identical to v_0 . We have discussed this case in constraint (14).

Recall that in cases (2) and (3) in Appendix A.1.2.3 when constructing the edges for vertex labels of subtasks in P_{\max} (a subtask e is in P_{\max} if $X_{\prec_P}^e = \emptyset$), their leaving vertices fall into two categories, location vertices and literal vertices associated with immediately preceding subtasks. To satisfy condition (b) in Definition 3.10 that the satisfied clause in the edge label implies the satisfied clause in the end vertex label and the same fleet of robots satisfy these two clauses, we require that the starting vertex label of the first completed subtask in P_{\max} should be satisfied by robots coming from location vertices in $\mathcal{V}_{\text{init}}$, and the starting vertex label of the remaining subtasks in P_{\max} should be satisfied by robots coming from literal vertices associated with edge labels of immediately prior subtasks. To this end, we first define an auxiliary binary variable b_e^\prec such that $b_e^\prec = 1$ if and only if subtask e is the first subtask in P_{\max} . Then, we define the following constraints

$$\sum_{e' \in P_{\max} \setminus \{e\}} b_e^{e'} - M_{\max}(1 - b_e^\prec) \leq 0 \quad (24a)$$

$$1 - b_e^\prec - M_{\max} \sum_{e' \in P_{\max} \setminus \{e\}} b_e^{e'} \leq 0. \quad (24b)$$

Only when e is the first subtask, i.e., when $\sum_{e' \in P_{\max} \setminus \{e\}} b_e^{e'} = 0$, does constraint (24) give $b_e^\prec = 1$. Then, for any clause in the starting vertex label of e , the constraints specifying which categories of leaving vertices robots should come from can be written as, $\forall \mathcal{C}_p^\gamma \in \text{cls}(\gamma)$,

$$\sum_{q \in \mathcal{Q}_p} \sum_{v \in \mathcal{M}_{\mathcal{V}}^{\text{cls}}(e, 0, p, q)} \sum_{u: (u, v) \in \mathcal{E}_{\mathcal{G}}} \sum_{r \in \mathcal{M}_{\mathcal{K}}^{\mathcal{V}}(v)} x_{uvr} \leq M_{\max}(1 - b_e^\prec), \quad (25a)$$

$$\sum_{q \in \mathcal{Q}_p} \sum_{v \in \mathcal{M}_{\mathcal{V}}^{\text{cls}}(e, 0, p, q)} \sum_{u: (u, v) \in \mathcal{E}_{\mathcal{G}}} \sum_{r \in \mathcal{M}_{\mathcal{K}}^{\mathcal{V}}(v)} x_{uvr} \leq M_{\max} b_e^\prec. \quad (25b)$$

When subtask e is the first one to be completed in P_{\max} , i.e., when $b_e^\prec = 1$, then constraint (25a), combined with

constraint (10), states that robots should come from location vertices in $\mathcal{V}_{\text{init}}$. However, when subtask e is not the first subtask to be completed in P_{\max} , i.e., when $b_e^\prec = 0$, then constraint (25b) requires that robots should come from literal vertices associated with immediately prior subtasks.

A.2.5 Same- $\langle i, j \rangle$ constraints: Next, we encode the constraint that some subtasks are executed by the same i robots of type j , which are indicated by the same nonzero connector χ . Given a nonzero connector χ , we can identify all vertex or edge labels that have literals with the same connector χ by the mapping $\mathcal{M}_{\gamma}^{\chi}(\chi)$. In an edge label $(e, 1) \in \mathcal{M}_{\gamma}^{\chi}(\chi)$ or a vertex label $(e, 0) \in \mathcal{M}_{\gamma}^{\chi}(\chi)$, each clause has at most one literal $\pi_{i,j}^{k,\chi}$ with connector χ and it is associated with i vertices in \mathcal{G} . We enumerate these i vertices and denote the b -th vertex by v_k^b . Then for any two labels $\gamma, \gamma' \in \mathcal{M}_{\gamma}^{\chi}(\chi)$ and any two clauses $\mathcal{C}_p^\gamma \in \text{cls}(\gamma)$ and $\mathcal{C}_{p'}^{\gamma'} \in \text{cls}(\gamma')$ that have literals $\pi_{i,j}^{k,\chi}$ and $\pi_{i,j}^{k',\chi}$, respectively, the constraint that the corresponding literals are satisfied by the same i robots of type j , $\forall b \in [i]$ and $\forall r \in \mathcal{K}_j$, can be written as

$$\begin{aligned} & \sum_{u: (u, v_k^b) \in \mathcal{E}_{\mathcal{G}}} x_{uv_k^b r} + M_{\max}(b_p - 1) \\ & \leq \sum_{u: (u, v_{k'}^{b'}) \in \mathcal{E}_{\mathcal{G}}} x_{uv_{k'}^{b'} r} + M_{\max}(1 - b_{p'}), \end{aligned} \quad (26a)$$

$$\begin{aligned} & \sum_{u: (u, v_k^b) \in \mathcal{E}_{\mathcal{G}}} x_{uv_k^b r} + M_{\max}(b_{p'} - 1) \\ & \leq \sum_{u: (u, v_k^b) \in \mathcal{E}_{\mathcal{G}}} x_{uv_k^b r} + M_{\max}(1 - b_p), \end{aligned} \quad (26b)$$

where $v_{k'}^{b'}$ is the b -th vertex associated with $\pi_{i,j}^{k',\chi}$. Only when $b_p = b_{p'} = 1$, does (26) become active. Then, $\sum_{u: (u, v_k^b) \in \mathcal{E}_{\mathcal{G}}} x_{uv_k^b r} = \sum_{u: (u, v_{k'}^{b'}) \in \mathcal{E}_{\mathcal{G}}} x_{uv_{k'}^{b'} r}$, i.e., two b -th vertices v_k^b and $v_{k'}^{b'}$ are visited by the same robot r .

A.2.6 Constraints associated with the transition between the prefix and suffix parts: Since we synthesize plans for the prefix and suffix parts separately, to ensure that the final locations of the prefix part seamlessly transition to the suffix part, we impose constraints on the final locations of the prefix part, which are determined by the satisfied clause in the edge label of the subtask that is the last one to be completed.

To this end, we first find the set of subtasks, denoted by P_{\min} , in the poset P that can be the last ones to be completed, which are referred to as the minimal elements in a poset. An element in a poset P is a minimal element if there is no smaller element in P than itself. Then, we iterate over subtasks in P_{\min} when formulating the MILP each time selecting a different subtask $e \in P_{\min}$ to be the last one, which can be written as

$$b_e^{e'} = 1, \quad \forall e' \in X_P \setminus \{e\}. \quad (27)$$

After selecting the last subtask to be completed, we next select one clause in its edge label γ that needs to be satisfied. We iterate over all clauses in the edge label of the last subtask each time selecting a different clause $\mathcal{C}_p^\gamma \in \text{cls}(\gamma)$ to be true, i.e.,

$$b_p = 1. \quad (28)$$

If a path for Problem 1 cannot be detected when e is the last subtask in the prefix part and its p -th clause is set to be true, then we continue iterating over clauses in the edge label of e . If a path for Problem 1 cannot be detected after iterating over clauses in the selected edge label, we select another subtask in P_{\min} to be the last one and repeat the same process.

Remark A.3. Assuming there is a feasible path τ to Problem 1, the constraints (27)-(28) on the final locations of the prefix part allow us to identify the same clause satisfied by the final locations of the prefix part as that satisfied by the assumed feasible path τ . This ensures the feasibility of the suffix part and the completeness of our method; see also Theorem 6.1. Note that the constraints (27)-(28) are necessary for establishing the completeness of our proposed method. However, there may exist multiple solutions to Problem 1, and it will be computationally inefficient to try all possibilities for the last subtasks and the corresponding clauses. We found that often in practice, omitting constraints (27)-(28) did not make Problem 1 infeasible. Therefore, constraints (27)-(28) can be initially omitted from the formulation of the MILP.

A.2.7 MILP objective: The objective is to minimize the weighted sum of the travel cost and travel time, i.e.,

$$\min \alpha \sum_{(u,v) \in \mathcal{E}_G} \sum_{r \in \mathcal{M}_{\mathcal{K}}^{\mathcal{V}}(v)} d_{uv} x_{uvr} + (1 - \alpha) \sum_{e \in X_P} t_e, \quad (29)$$

where α is a user-specified parameter and d_{uv} is the travel cost, e.g., travel distance. Compared to Problem 1, objective (29) involves optimization of time. In practice, we observed that without optimizing time, some scheduling variables can take large values, which impacts the generation of the low-level path. Note that travel cost, e.g., travel distance, and travel time are typically non-conflicting objectives.

A.3 Construction of the robot suffix path

In this section, we construct the robot path for the suffix part. We assume that the high-level plan found in Section 5.2 for the prefix part has been used to generate low-level paths as in Appendix B, which induces a run in \mathcal{A}_ϕ connecting v_0 and v_{accept} . Thus, the final robot locations of the prefix part are known. In what follows, we proceed depending on whether the vertex v_{accept} has a self-loop or not. If the vertex v_{accept} has a self-loop, we first examine whether the final locations of the prefix part satisfy its label $\gamma_\phi(v_{\text{accept}})$. If yes, we conclude that the prefix path we have found also satisfies the specification ϕ . Otherwise, we remove this self-loop since it does not contribute to the identification of the suffix paths. By treating the final locations of the prefix paths as the initial robot locations of the suffix paths, the suffix paths aim to drive the progress in \mathcal{A}_ϕ back to vertex v_{accept} and send robots to the initial locations of the suffix part to close the trajectories. The basic idea is to view the simple cycle around v_{accept} as a simple path, by treating the accepting vertex at the beginning of this simple path as the initial vertex v_0 and the other accepting vertex at the end as the goal to be reached. Then, starting from the NBA \mathcal{A}_ϕ^- in Section 4.1, we can follow a procedure similar to the prefix part to obtain paths for the suffix part.

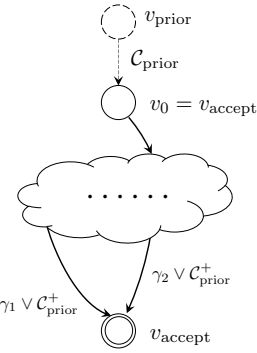


Figure 12. $\mathcal{A}_{\text{subtask}}^-$ for the suffix part when v_{accept} does not have a self-loop, where γ_1, γ_2 and γ_3 are edge labels and C_{prior}^+ is positive subformula that is satisfied by final robot locations of the prefix part; see Appendix A.3.2.

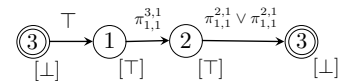


Figure 13. $\mathcal{A}_{\text{subtask}}^-$ for task (ii) obtained from Fig. 5(b). A clause $\pi_{1,1}^{2,1}$ is added to the edge label $\gamma(v_2, v_3)$; see Appendix A.3.2.

A.3.1 Extracting subtasks and inferring the temporal order from the NBA

A.3.1.1 Extraction of sub-NBA $\mathcal{A}_{\text{subtask}}$ from $\mathcal{A}_{\text{relax}}$: First, based on the NBA \mathcal{A}_ϕ^- we obtain the relaxed NBA $\mathcal{A}_{\text{relax}}$, as in Section 4.1. Then, to obtain the sub-NBA $\mathcal{A}_{\text{subtask}}$, similar to finding the shortest simple cycle around v_{accept} in Section 4.2.1.2, we remove all other accepting vertices from $\mathcal{A}_{\text{relax}}$ and all initial vertices if they do not have self-loops. Let $\gamma_\phi(v_{\text{prior}}, v_{\text{accept}})$ denote the edge label corresponding to the last completed subtask in the prefix part. After generating the low-level paths for the prefix part, the final robot locations of the prefix part satisfy $\gamma_\phi(v_{\text{prior}}, v_{\text{accept}})$ (see Fig. 3). Next, since v_{accept} does not have a self-loop, we remove all outgoing edges from v_{accept} (acting as v_0) from $\mathcal{A}_{\text{relax}}$ if $\gamma_\phi(v_{\text{prior}}, v_{\text{accept}})$ does not imply its edge label in \mathcal{A}_ϕ . Also, we remove all incoming edges to v_{accept} (acting as v_{accept}) from $\mathcal{A}_{\text{relax}}$ if the corresponding edge label in \mathcal{A}_ϕ is not implied by $\gamma_\phi(v_{\text{prior}}, v_{\text{accept}})$. By condition (f) in Definition 3.8, these edges do not appear in any restricted accepting run if the corresponding prefix part traverses the edge $(v_{\text{prior}}, v_{\text{accept}})$. Also, if the set of restricted accepting runs is nonempty, there exist accepting vertices in $\mathcal{A}_{\text{relax}}$ that have outgoing edges and incoming edges for which this implication holds. Note that the implication check is conducted in \mathcal{A}_ϕ . Finally, we follow a similar process as that described in Section 4.2.2 to extract a sub-NBA $\mathcal{A}_{\text{subtask}}$ from $\mathcal{A}_{\text{relax}}$ for the pair v_{accept} (acting as v_0) and v_{accept} . The structure of $\mathcal{A}_{\text{subtask}}$ is shown in Fig. 12 where v_0 does not have a self-loop. We also depict the vertex v_{prior} in the prefix part for better understanding. Then, we prune $\mathcal{A}_{\text{subtask}}$ to obtain the NBA $\mathcal{A}_{\text{subtask}}^-$, as in Section 4.2.3.

Example 1. continued ($\mathcal{A}_{\text{subtask}}^-$ for the suffix part) The suffix part for task (i) only consists of the accepting vertex v_{accept} . The sub-NBA $\mathcal{A}_{\text{subtask}}^-$ associated with the suffix part for task (ii) is a cycle v_3, v_1, v_2, v_3 ; see Fig. 13.

A.3.1.2 Inferring temporal order between subtasks in $\mathcal{A}_{\text{subtask}}^-$: We collect all simple cycles around v_{accept} in the set Θ . Because the initial robot locations for the suffix part satisfy $\gamma_\phi(v_{\text{prior}}, v_{\text{accept}})$, they also satisfy the label of the last edge in every simple cycle $\theta \in \Theta$ since edges in $\mathcal{A}_{\text{relax}}$ whose labels are not implied by $\gamma_\phi(v_{\text{prior}}, v_{\text{accept}})$ are removed from $\mathcal{A}_{\text{relax}}$ when constructing $\mathcal{A}_{\text{subtask}}$. By following such a simple cycle θ , not only the transition is driven back to v_{accept} , but further robots are able to return to their initial locations to close the trajectories. Finally, we infer a set of posets $\{P_{\text{suf}}\}$ from simple cycles in Θ and sort them as Section 4.3.

A.3.2 Finding the suffix path on $\mathcal{A}_{\text{subtask}}^-$: Similar to the prefix part, we find the suffix path that, combined with the prefix path, satisfies the specification by iterating over the set of posets $\{P_{\text{suf}}\}$. By condition (c) in Definition 3.10, robots need to return to their initial locations to close the suffix loop and drive the transition in \mathcal{A}_ϕ back to v_{accept} . To ensure that our method is complete, we achieve these two goals separately. First, those robots participating in the satisfaction of the positive subformula in $\gamma_\phi(v_{\text{prior}}, v_{\text{next}})$ return to regions corresponding to their initial locations of the suffix part (not necessarily returning to their initial locations), and at the same time drive the transition in \mathcal{A}_ϕ back to v_{accept} . Then, all robots return to their initial locations of the suffix part while not violating the specification ϕ . We also discuss how to achieve these two goals above at the same time in Appendix A.3.2.4.

To achieve the first step, we find the satisfied clause, denoted by $\mathcal{C}_{\text{prior}}$, in the edge label $\gamma_\phi(v_{\text{prior}}, v_{\text{next}})$; we denote by $\mathcal{C}_{\text{prior}}^+$ and $\mathcal{C}_{\text{prior}}^-$ the positive and negative subformulas in $\mathcal{C}_{\text{prior}}$, respectively. Next, we find the set P_{\min} of subtasks in X_P that can be the last one to be completed. For each subtask $e = (v_1, v_2) \in P_{\min}$, we augment its edge label $\gamma(v_1, v_2)$ with the clause $\mathcal{C}_{\text{prior}}^+$, i.e., $\gamma(v_1, v_2) = \gamma(v_1, v_2) \vee \mathcal{C}_{\text{prior}}^+$; see also Fig. 12. If $e \in P_{\min}$ is the last subtask to be completed, we require that the clause $\mathcal{C}_{\text{prior}}^+$ is satisfied. We say that $\mathcal{C}_{\text{prior}}^+$ is satisfied if those robots involved in satisfying $\mathcal{C}_{\text{prior}}^+$ in the prefix part return to regions including their initial locations. For instance, in Fig. 13 that shows $\mathcal{A}_{\text{subtask}}^-$ for task (ii) in Example 1, we augment the label of the last edge with the clause $\mathcal{C}_{\text{prior}}^+ = \pi_{1,1}^{2,1}$, which is the clause in the last edge label of the prefix part; see Fig. 6(b). Combined with the negative subformula $\mathcal{C}_{\text{prior}}^-$, if $\mathcal{C}_{\text{prior}}^+ \wedge \mathcal{C}_{\text{prior}}^-$ is satisfied, the original edge label $\gamma_\phi(v_1, v_2)$ will also be satisfied since, by condition (f) in Definition 3.8, the label $\gamma_\phi(v_{\text{prior}}, v_{\text{accept}})$ implies the original edge label $\gamma_\phi(v_1, v_2)$ (acting as $\gamma_\phi(v'_{\text{prior}}, v_{\text{accept}})$; see Fig. 3). In this way, robots return to regions that contain their initial locations and at the same time drive the transition in $\mathcal{A}_{\text{subtask}}^-$ back to v_{accept} . In what follows, we first construct the routing graph and formulate the MILP for the first step, and then design low-level paths so that the robots can return to their initial locations while satisfying the specification ϕ .

A.3.2.1 Construction of the routing graph: Given the poset P , we build a routing graph $\mathcal{G} = (\mathcal{V}_G, \mathcal{E}_G)$ following almost the same steps as in Appendix A.1. The only differences are related to the augmented clause $\mathcal{C}_{\text{prior}}^+$. When building the vertex set \mathcal{V}_G , each time we encounter a literal $\pi_{i,j}^{k,\chi}$ in $\text{lits}^+(\mathcal{C}_{\text{prior}}^+)$, we create i vertices and let each

vertex point to the region ℓ_k . Also, we build a one-to-one correspondence between vertices and robots satisfying this literal in the prefix part since these robots need to return to their initial regions. We emphasize that each such vertex is associated with a single robot instead of a type of robots. The mappings are created as in Appendix A.1.1.

When building the edge set \mathcal{E}_G , there are no outgoing edges from vertices associated with the literals in $\mathcal{C}_{\text{prior}}^+$ since these are the vertices where the robots will be located at the final moment. To construct the incoming edges to these vertices we treat $\mathcal{C}_{\text{prior}}^+$ as a regular clause in an edge label but with one exception. Recall in Appendix A.1.2.2 that identifies the leaving vertices associated with prior subtasks. In this case, when the number of leaving vertices is the same as the number of end vertices, we randomly create one-to-one edges between leaving vertices and end vertices since all robots visiting these leaving vertices belong to the same type. However, here we create edges from all leaving vertices to each vertex associated with literal $\pi_{i,j}^{k,\chi}$ in $\mathcal{C}_{\text{prior}}^+$ since each vertex associated with this literal is only allowed to be visited by a specific robot of a specific type.

A.3.2.2 Formulation of the MILP problem: To find a high-level plan, we formulate a MILP based on the routing graph \mathcal{G} by following a similar process as in the case of the prefix part, but with the exception that at the end, some robots need to return to their initial regions. The MILP formulation for the suffix part results in the same constraints as (3)-(26) in Appendix A.2 with the following two exceptions.

(1) *Returning to initial regions:* The first exception results from the requirement that while driving transition back to v_{accept} , robots need to return to regions corresponding to their initial locations. To this end, we define binary variables b_e for each subtask in P_{\min} that can be the last one to be completed, such that b_e equaling 1 implies the satisfaction of the augmented clause $\mathcal{C}_{\text{prior}}^+$; see Fig. 12. First, we require that one and only one b_e can be true, i.e.,

$$\sum_{e \in P_{\min}} b_e = 1. \quad (30)$$

If $b_e = 0$ for a subtask e in P_{\min} , then one of the remaining clauses in the edge label of e must be satisfied according to constraint (9), which is reduced to the case where $\mathcal{C}_{\text{prior}}^+$ does not exist.

Next, we encode the constraint that when completing the last subtask in P_{\min} , robots must return to their respective regions. Recall that in Appendix A.2 we defined the binary variable $b_e^{e'} = 1$ which equals 1 if subtask e is completed after e' , i.e., $t_e > t_{e'}$. To determine this last satisfied subtask in P_{\min} , we define $z = |P_{\min}| - 1$. Then, for any $e \in P_{\min}$, the term $\sum_{e' \in P_{\min} \setminus \{e\}} b_e^{e'} - z = 0$ if e is the last subtask to be completed. Thus, the requirement that some robots return to their respective regions to complete the last subtask can be written as

$$\begin{aligned} 1 + M_{\max} \left(\sum_{e' \in P_{\min} \setminus \{e\}} b_e^{e'} - z \right) &\leq b_e \\ &\leq 1 + M_{\max} \left(z - \sum_{e' \in P_{\min} \setminus \{e\}} b_e^{e'} \right), \end{aligned} \quad (31)$$

for any subtask $e \in P_{\min}$. Only when e is the last subtask in P_{\min} , does $b_e = 1$ come into effect.

Given a subtask $e = (v_1, v_2) \in P_{\min}$, similar to constraint (10), the following constraint states that when $b_e = 1$, i.e., when subtask e is the last one to be completed, each vertex in \mathcal{G} associated with clause $\mathcal{C}_{\text{prior}}^+$ of $\gamma(v_1, v_2)$ will be visited by a specific robot, for the q -th literal $\pi_{i^q, j^q}^{k^q, \chi^q}$ in $\mathcal{C}_{\text{prior}}^+$,

$$\left[\sum_{v \in \mathcal{M}_{\mathcal{V}}^{\text{its}}(e, 1, p_e, q)} \sum_{u: (u, v) \in \mathcal{E}_{\mathcal{G}}} \sum_{r_v = \mathcal{M}_{\mathcal{K}}^{\mathcal{V}}(v)} x_{uvr} \right] / i^q = b_e, \quad (32)$$

where p_e is the index of the clause $\mathcal{C}_{\text{prior}}^+$ in $\gamma(v_1, v_2)$ and robot r_v is the specific robot that should visit vertex v .

(2) *same- $\langle i, j \rangle$ constraints*: The second exception relates to the same- $\langle i, j \rangle$ constraints in Appendix A.2.5. The goal is to ensure that the same i robots of type j satisfy those atomic propositions with the same non-zero connectors that appear both in the prefix and suffix NBA. Specifically, after solving the MILP for the prefix part, for any connector $\chi \neq 0$ that appears in the specification ϕ , we check whether any literal that includes this connector was involved in the prefix part. If yes, then these literals with the same nonzero connector should be satisfied by the same $\langle i, j \rangle$. We denote by $\mathcal{K}^\chi \subseteq \mathcal{K}_j$ the set of $\langle i, j \rangle$ that make these literals true and by r^b the b -th robot in the enumerated set \mathcal{K}^χ . When dealing with the suffix part, for any label $\gamma \in \mathcal{M}_{\mathcal{V}}^{\mathcal{X}}(\chi)$ where literals with connector χ appear and any clause $\mathcal{C}_p^\gamma \in \text{cls}(\gamma)$ that has literal $\pi_{i,j}^{k,\chi}$, the constraint that this literal is satisfied by the same $\langle i, j \rangle$ can be written as

$$\sum_{u: (u, v_k^b) \in \mathcal{E}_{\mathcal{G}}} x_{uv_k^b r^b} = b_p, \quad \forall r^b \in \mathcal{K}^\chi, \quad (33)$$

where v_k^b is the b -th vertex in the set of vertices in the routing graph \mathcal{G} that are associated with literal $\pi_{i,j}^{k,\chi}$. If the clause \mathcal{C}_p^γ is true, i.e., if $b_p = 1$, then the b -th vertex v_k^b is visited by the b -th robot $r^b \in \mathcal{K}^\chi$. On the other hand, if $\mathcal{K}^\chi = \emptyset$, that is, if literals that share this χ do not appear in the prefix part, we turn to constraint (26) to impose the same- $\langle i, j \rangle$ constraints.

By condition (f) in Definition 3.8, there is a clause \mathcal{C}' in the edge label $\gamma(v'_{\text{prior}}, v_{\text{accept}})$ that is a subformula of $\mathcal{C}_{\text{prior}}$. Therefore, some robots returning to regions corresponding to their initial locations will enable the positive subformula in \mathcal{C}' of $\gamma(v'_{\text{prior}}, v_{\text{accept}})$ and, at the same time ensure that any positive literal in the clause \mathcal{C}' with nonzero connector uses the same group of robots as the literal in the clause $\mathcal{C}_{\text{prior}}^+$ of $\gamma(v'_{\text{prior}}, v_{\text{accept}})$ with the same connector. In other words, when robots head back to their initial locations, the same- $\langle i, j \rangle$ constraints over the last completed subtask are satisfied automatically. Robots can safely return to their initial locations without violating the same- $\langle i, j \rangle$ constraints.

A.3.2.3 Closing the suffix loops: After solving the MILP for the first step for the suffix part, we utilize the method in Appendix B to obtain low-level paths that drive the transition in \mathcal{A}_ϕ back to v_{accept} , and at the same time ensure that robots involved in $\mathcal{C}_{\text{prior}}^+$ return to regions corresponding to their initial locations of the suffix part. Note that to generate the low-level paths for the last completed subtask $(v'_{\text{prior}}, v_{\text{accept}})$, we need to satisfy the augmented clause $\mathcal{C}_{\text{prior}}$ in the edge label $\gamma_\phi(v'_{\text{prior}}, v_{\text{accept}})$. By conditions (d)

and (f) in Definition 3.8, we have $\gamma_\phi(v_{\text{prior}}, v_{\text{accept}}) \implies \gamma_\phi(v_{\text{accept}}, v_{\text{next}})$ and $\gamma_\phi(v_{\text{accept}}, v_{\text{next}}) \implies_s \gamma_\phi(v_{\text{next}})$, thus the initial locations of the suffix part satisfy the edge label $\gamma_\phi(v_{\text{accept}}, v_{\text{next}})$ and the vertex label $\gamma_\phi(v_{\text{next}})$; so do the final locations in the low-level paths that enable $\gamma_\phi(v'_{\text{prior}}, v_{\text{accept}})$ since they satisfy $\mathcal{C}_{\text{prior}}$. Next, to close the suffix loop, robots return to their initial locations starting from the final locations in the low-level paths, while satisfying the clause $\mathcal{C}_{\text{prior}}$ en route, thus satisfying $\gamma_\phi(v_{\text{next}})$. Because those robots involved in $\mathcal{C}_{\text{prior}}^+$ have returned to their initial regions, and by Assumption 3.5 each region spans consecutive cells, they can return to their initial locations by traveling inside these regions. In this way, the NBA \mathcal{A}_ϕ remains at vertex v_{next} , thus the specification ϕ is not violated. The problem of finding the path that travels inside the regions can be formulated as a generalized multi-robot path planning problem; see Appendix B.2.

Remark A.4. *Closing the suffix loops in two steps is important to show the completeness of our proposed method. In a single step approach where robots return to their initial locations in the suffix part at the same time that the NBA \mathcal{A}_ϕ transitions to v_{accept} , the robots return to their initial locations to satisfy the last subtask $(v'_{\text{prior}}, v_{\text{accept}})$. However, it is possible that the initial locations violate the vertex label $\gamma_\phi(v'_{\text{prior}})$ of the last subtask. In this case, once the robots reach regions corresponding to their initial locations (not necessarily reaching initial locations), the edge label of the last subtask is satisfied and the last subtask has to be completed since its vertex label is violated. Nonetheless, it is possible that, at this moment, robots have not reached their initial locations inside these regions if some regions cover multiple cells. Therefore, this single-step approach may fail in this case. In practice such scenario rarely occurs. In fact, a single step approach generally works well in practice. Nevertheless, the proposed two-step method allows to guarantee completeness of our approach.*

A.3.2.4 Returning to initial locations in one step: To ensure that the robots returning to their initial locations and progressing towards the accepting vertex v_{accept} in the NBA \mathcal{A}_ϕ is made in one step, we first define a positive atomic proposition π_{init} which is true if all robots return to their initial locations at the end of the suffix paths. Then, we replace $\mathcal{C}_{\text{prior}}^+$ on the edge label of the last subtasks with π_{init} ; see Fig. 12. If π_{init} is satisfied, the original edge label $\gamma_\phi(v'_{\text{prior}}, v_{\text{accept}})$ in \mathcal{A}_ϕ will also be satisfied since the initial robot locations satisfy $\mathcal{C}_{\text{prior}}$ in $\gamma_\phi(v_{\text{prior}}, v_{\text{accept}})$ and $\gamma_\phi(v_{\text{prior}}, v_{\text{accept}}) \implies \gamma_\phi(v'_{\text{prior}}, v_{\text{accept}})$. We adopt the first step in Appendix A.3.2 with all exceptions related to the difference between π_{init} and $\mathcal{C}_{\text{prior}}^+$. That is, π_{init} requires all robots to return to their initial locations, whereas $\mathcal{C}_{\text{prior}}^+$ in the suffix part requires only those robots participating in the satisfaction of $\mathcal{C}_{\text{prior}}^+$ in the prefix part to return to regions corresponding to their initial locations.

Recall that the vertex set $\mathcal{V}_{\text{init}} \subseteq \mathcal{V}_{\mathcal{G}}$ contains vertices pointing to the initial robot locations. When building vertices in $\mathcal{V}_{\mathcal{G}}$ for the literal π_{init} , we create a copy of vertices in $\mathcal{V}_{\text{init}}$ and associate these vertices with the literal π_{init} , so that each vertex points to one single cell which is the initial location of a specific robot. The incoming edges of these vertices are constructed by treating π_{init} as a regular clause (single

literal with connector $\chi = 0$) of an edge label. Specifically, given a subtask $e \in P_{\min}$, let robot r_v denote the specific robot that should visit vertex v associated with its literal π_{init} . We identify all vertices in \mathcal{V}_G that are associated with robots of the same type as r_v and are related to initial locations (see Appendix A.1.2.1), prior subtasks of e (see Appendix A.1.2.2) or vertex labels of the same subtask (see Appendix A.1.2.3). Then, we create an edge from each one of these vertices to vertex r_v . No outgoing edges exist for these vertices. The remaining steps to build the routing graph are the same as those in Appendix A.3.2.1.

When formulating the MILP, the only difference is in the constraint (32), that is, π_{init} is true if and only if each vertex in \mathcal{G} that is associated with π_{init} is visited by a specific robot among the whole fleet of n robots, i.e.,

$$\left[\sum_{v \in \mathcal{M}_{\mathcal{V}}^{\text{lits}}(e, 1, p_e, 1)} \sum_{u:(u,v) \in \mathcal{E}_G} x_{uvr_v} \right] / n = b_e, \quad (34)$$

where robot r_v is the specific robot that should visit vertex v . Note that robots returning to their initial locations in one step does not guarantee the completeness of our proposed method, as discussed in Remark A.4.

A.4 Extensions of the MILP

One advantage of the proposed MILP for the prefix and suffix parts is that it is associated with each subtask individually, which allows us to impose additional constraints on certain subtasks to address problem-specific requirements. In this section, we present possible extensions of the LTL $^\chi$ formula and introduce variations to the MILP formulation by considering more interesting constraints.

A.4.1 Requiring specific robots to participate in a subtask: Given an atomic proposition $\pi_{i,j}^{k,\chi}$ that appears in the LTL $^\chi$ formula, we can require that a specific subset of robots, denoted by $\mathcal{K}'_j \subseteq \mathcal{K}_j$, participates or not in the satisfaction of this formula. Suppose the set of vertices in \mathcal{G} that are associated with this literal is $\mathcal{M}_{\mathcal{V}}^{\text{lits}}(e, 0|1, p, q)$. Then for each specific robot $r \in \mathcal{K}'_j$, we have

$$\sum_{u:(u,v) \in \mathcal{E}_G} x_{uvr} = I, \quad \forall v \in \mathcal{M}_{\mathcal{V}}^{\text{lits}}(e, 0|1, p, q) \quad (35)$$

where $I \in \{0, 1\}$. We set I to 1 if we require every robot in \mathcal{K}'_j to participate in the satisfaction of $\pi_{i,j}^{k,\chi}$ (where $|\mathcal{K}'_j| \leq i$) and $I = 0$ if no robot in \mathcal{K}'_j should be involved.

A.4.2 Managing the number of participating robots: When completing the task specified by the LTL $^\chi$ formula, it may be desirable to dispatch as few robots as possible to keep the whole system at a small scale. On the other hand, we may want to dispatch as many robots as possible to enhance the efficiency. This requirement can be handled by adding another term to the MILP objective in (29) as follows

$$\begin{aligned} \min \quad & \alpha_1 \sum_{(u,v) \in \mathcal{E}_G} \sum_{r \in \mathcal{M}_{\mathcal{K}}^{\text{V}}(v)} d_{uv} x_{uvr} + \alpha_2 \sum_{e \in X_P} t_e \\ & \pm \alpha_3 \sum_{v \in \mathcal{V}_{\text{init}}} \sum_{w:(v,w) \in \mathcal{E}_G} x_{vw r_v}, \end{aligned} \quad (36)$$

where $\alpha_1 + \alpha_2 + \alpha_3 = 1$, r_v is the specific robot at vertex $v \in \mathcal{V}_{\text{init}}$, and the final term captures the number of robots that leave their initial locations, equivalent to the number of robots that are assigned to the desired subtasks. The positive sign in the last term in objective (36) corresponds to the case where fewer robots are needed while the negative sign corresponds to the case where more diverse robots are needed.

A.4.3 Prohibiting the use of the same robots: In Definition 3.4 of the LTL $^\chi$ formula, we handled the requirement that two atomic propositions with the same nonzero connector must be satisfied by the same fleet of robots. Alternatively, we can impose the restriction that some atomic propositions involving the same robot type but different nonzero connectors must be satisfied by two disjoint fleets of robots. For instance, the formula $\Diamond \pi_{1,1}^{1,1} \wedge \Diamond \pi_{2,1}^{2,2}$ requires that the robots that visit region ℓ_1 are different from those two robots that visit region ℓ_2 . Given such two atomic propositions that need to be satisfied by different robots, suppose the sets of vertices in \mathcal{G} that are associated with these two literals are $\mathcal{M}_{\mathcal{V}}^{\text{lits}}(e, 0|1, p, q)$ and $\mathcal{M}_{\mathcal{V}}^{\text{lits}}(e', 0|1, p', q')$. Then, $\forall r \in \mathcal{K}_j$, this requirement can be written as

$$\begin{aligned} \sum_{v \in \mathcal{M}_{\mathcal{V}}^{\text{lits}}(e, 0|1, p, q)} \sum_{u:(u,v) \in \mathcal{E}_G} x_{uvr} + \\ \sum_{v \in \mathcal{M}_{\mathcal{V}}^{\text{lits}}(e', 0|1, p', q')} \sum_{u:(u,v) \in \mathcal{E}_G} x_{uvr} \leq 1. \end{aligned} \quad (37)$$

Constraint (37) states that robot r of type j can visit at most one vertex among the vertices that are associated with these two literals.

Appendix B Design of Low-Level Paths that Satisfy the Original LTL Task

This section presents the correction stage that concretizes the high-level plan obtained in Section 5.2 to satisfy the specification ϕ ; see also blocks (6) and (7) in Fig. 4. We first find a simple path from the NBA $\mathcal{A}_{\text{subtask}}^-$ that connects v_0 and v_{accept} , based on the time axis and the time-stamped task allocation plan, and then find the counterpart of this simple path from the NBA \mathcal{A}_ϕ . To satisfy the specification ϕ , while following the high-level plan, we formulate a sequence of generalized multi-robot path planning (GMRPP) problems to design low-level executable paths.

B.1 Extraction of the simple path from the sub-NBA $\mathcal{A}_{\text{subtask}}^-$

Recall that each distinct time instant on the time axis \vec{t} obtained in Section 5.2 has a one-to-one correspondence with subtasks in the set X_P , and the sorted time axis generates a linear extension of subtasks in X_P that induces a simple path in $\mathcal{A}_{\text{subtask}}^-$ that connects v_0 and v_{accept} . In this section, we proceed along the time axis \vec{t} to extract this simple path using a graph-search version of the backtracking search algorithm, which is a variant of the depth-first search (Russell and Norvig 2002). In our graph-search method, each vertex is searched at most once. The outline of this algorithm is shown in Alg. 2.

Algorithm 2: Extract the simple path from $\mathcal{A}_{\text{subtask}}^-$

```

Input: time axis  $\vec{t}$ , sub-NBA  $\mathcal{A}_{\text{subtask}}^-$ 
1  $v_1 = v_0, c = 0, \text{frontier} = \{(v_1, c)\}, \text{explored} = \emptyset$ 
  while  $v_1 \neq v_{\text{accept}}$  do
2   Remove  $(v_1, c)$  from  $\text{frontier}$  and add  $v_1$  to  $\text{explored}$ ;
3   Obtain the subtask  $e' = (v'_1, v'_2)$  that is associated
     with  $\vec{t}(c+1)$ ;
4   for  $(v_1, v_2) \in \mathcal{A}_{\text{subtask}}^-$  do
5     if  $\gamma(v_1, v_2) = \gamma(v'_1, v'_2)$  and  $\gamma(v_1) = \gamma(v'_1)$ 
        then
6       Determine (1) essential clause, (2)
         essential robots, (3) negative clause, and
         (4) sequence of vertices leading to  $v_2$ ;
7       if  $v_2$  not in  $\text{frontier}$  and  $\text{explored}$  then
8         | Add  $(v_2, c+1)$  to  $\text{frontier}$ ;
9   return the simple path leading to  $v_1$ ;

```

To this end, we define $c \in \mathbb{N}$ as the *global counter* which keeps track of the progress made along the time axis \vec{t} . Specifically, c is the index of the subtask that has been completed most recently. Therefore, $\vec{t}(c+1)$ is the completion time of the subtask, denoted by $e' = (v'_1, v'_2)$, that is the next one to be completed. Let v_1 denote the vertex in $\mathcal{A}_{\text{subtask}}^-$ that is the most recently reached. The set frontier is a last-in-first-out queue that stores vertices that are available for expansion and the set explored stores vertices that have been expanded. At each iteration, among all subtasks with the starting vertex v_1 , we find the one (v_1, v_2) that is equivalent to subtask e' [line 5, Alg 2]. Then, after time instant $\vec{t}(c+1)$, vertex v_2 becomes the most recently reached vertex. We next increase the global counter by 1 and add it to frontier , a last-in-first-out queue [line 8, Alg. 2]. The iteration will terminate when the accepting vertex v_{accept} is reached.

When a subtask (v_1, v_2) in $\mathcal{A}_{\text{subtask}}^-$ is matched with the subtask e' that is completed at $\vec{t}(c+1)$, we keep track of the following information: (1) the exact clauses that are satisfied in the vertex label $\gamma(v_1)$ and edge label $\gamma(v_1, v_2)$ since only one clause in each label is true by constraint (9) in the MILP, (2) the subset of robots that participate in the satisfaction of each literal in these clauses, (3) the negative subformula in \mathcal{A}_ϕ that is in conjunction with the satisfied clause found in (1) but is replaced with \top during the relaxation stage in Section 4.1, and (4) the sequence of vertices in $\mathcal{A}_{\text{subtask}}^-$ that have been visited up to vertex v_2 . This information will be used to formulate the generalized multi-robot path planning problems later. In what follows, we discuss (1)-(3) in further detail and omit step (4) since it is straightforward.

(1) *Essential clauses:* Given the edge label or vertex label $\gamma = \bigvee_{p \in \mathcal{P}} \bigwedge_{q \in \mathcal{Q}_p} \pi_{i,j}^{k,\chi}$ of subtask (v_1, v_2) that is neither \top nor \perp , we refer to the unique satisfied clause as the *essential clause* and denote it by γ^+ . Recall that in Appendix A.2.3 we define a binary variable b_p representing the truth of the p -th clause in a given label; see constraint (9). Thus, we find the essential clause by locating the clause $\mathcal{C}_p^\gamma \in \text{cls}(\gamma)$ such

that $b_p = 1$. On the other hand, when the vertex or edge label is \top , by default, we define the essential clause as \top .

(2) *Essential robots:* We refer to the set of robots whose collective behavior satisfies the positive literals in the essential clause as the *essential robots*. Recall in Appendix A.2 that the binary variable x_{uvr} represents robot r visiting a vertex v in the routing graph \mathcal{G} . For the q -th literal $\pi_{i,j}^{k,\chi}$ in the essential clause \mathcal{C}_p^γ of a vertex or edge label of subtask (v_1, v_2) , we determine its essential robots by locating the associated x_{uvr} whose value is 1. That is, for each associated vertex $v \in \mathcal{M}_V^{\text{lits}}(e, 0|1, p, q)$, we identify the robot $r \in \mathcal{M}_K^V(v)$ such that $\exists (u, v) \in \mathcal{E}_G$, making $x_{uvr} = 1$. On the other hand, if the essential clause is \top , there are no essential robots.

(3) *Negative clause:* The collective behavior of essential robots satisfies the essential clauses in $\mathcal{A}_{\text{subtask}}^-$. For an essential clause that is not \top , there exists a unique clause in the NBA \mathcal{A}_ϕ that only differs from the essential clause in that it may contain the conjunction of the negative literals that were removed during the relaxation stage. We refer to this conjunction of negative literals as the *negative clause* and denote it by γ^- , which will be satisfied by the low-level paths. By default, we define the negative clause as \top , if the corresponding clause in \mathcal{A}_ϕ does not have negative literals. Finally, the conjunction $\gamma^+ \wedge \gamma^-$ of an essential clause and its corresponding negative clause constitutes a *complete clause* in \mathcal{A}_ϕ .

When the vertex label $\gamma(v_1)$ or edge label $\gamma(v_1, v_2)$ of subtask (v_1, v_2) in $\mathcal{A}_{\text{subtask}}^-$ is \top , the associated essential clause is also \top . However, the negative clause may not be \top , which happens when there exists a clause in the corresponding label in \mathcal{A}_ϕ that only includes negative literals. Note that by condition (b) in Definition 3.10, the complete clause of the vertex v_1 is implied by the complete clause of the edge that is immediately preceding the current subtask (v_1, v_2) . If the label is the edge label $\gamma(v_1, v_2)$, we randomly select one among the clauses that only include negative literals. Otherwise, if the label is the vertex label $\gamma(v_1)$, and further if the current subtask is not the first one, we select one as the negative clause (acting as the complete clause), that is implied by the complete clause in the edge that is immediately preceding the current subtask (v_1, v_2) . We can obtain this edge since in step (4) we keep track of the sequence of vertices that lead to vertex v_2 . This ensures that when the edge label (v_1, v_2) is enabled due to the satisfaction of its complete clause, the complete clause in its end vertex label can be satisfied automatically. On the other hand, if the current subtask is indeed the first one, we randomly select a negative clause that is satisfied by the initial robot locations.

B.2 Generalized multi-robot path planning

Leveraging the correspondence between the NBA \mathcal{A}_ϕ and the sub-NBA $\mathcal{A}_{\text{subtask}}^-$, we can find the counterpart in \mathcal{A}_ϕ of the simple path in $\mathcal{A}_{\text{subtask}}^-$ obtained in Appendix B.1. We denote by θ_ϕ this counterpart, which corresponds to a sequence of temporally sequential subtasks. Our goal is to find a collection of executable paths that induce the simple path θ_ϕ in \mathcal{A}_ϕ ; see also block 7 in Fig. 4. To achieve this, we formulate the execution of each subtask in θ_ϕ into a *generalized multi-robot path planning problem (GMRPP)*. Compared to traditional multi-robot path planning that,

given an initial robot configuration, designs paths to reach the target configuration, the GMRPP imposes additional constraints on the intermediate configurations.

Observe that given the completion time of two consecutive subtasks on the time axis \vec{t} , we can obtain the tightest span of the second subtask's vertex label; see Definition A.2. Specifically, the activation time of the second subtask's vertex label is at most one time step after the completion time of the first subtask; see also constraint (18) in Appendix A.2 that captures the temporal relation between two subtasks. On the other hand, the completion time of the vertex label of the second subtask is at most one time step before the completion time of the second subtask; see also constraint (13) in Appendix A.2 that captures the temporal relation for the same subtask. To design the low-level paths, we let each robot visit waypoints in its individual plan $p_{r,j}$ sequentially, possibly at different time instants than those in its timeline $t_{r,j}$. This is because the individual timeline is obtained using the shortest travel time between regions (see scheduling constraints in Appendix A.2.2) and omitting collision avoidance between robots, but the relative temporal relations with other robots are kept. Also, we maintain the tightest span of the vertex label of the considered subtask between completion time of two consecutive subtasks.

To this end, for each robot $[r, j] \in \mathcal{R}$, we define a *local counter* $\zeta_{r,j} \in \mathbb{N}$ that keeps track of how much progress has been made along the individual plan $p_{r,j}$. Specifically, $\zeta_{r,j} = a$ indicates that the a -th waypoint in the plan $p_{r,j}$ is the one visited by robot $[r, j]$ most recently. Furthermore, recall that the global clock c monitors the index of the most recently completed subtask along the time axis \vec{t} , which also captures the execution progress along the simple path θ_ϕ since a one-to-one correspondence exists between time instants in \vec{t} and subtasks in θ_ϕ . In what follows, we provide the ingredients for the construction of GMRPP.

B.2.1 Ingredients of GMRPP: Consider a subtask $e = (v_1, v_2)$ generated by the simple path θ_ϕ that is the next one to be completed. Let γ_1^+ and γ_1^- denote the essential and negative clauses associated with the vertex label $\gamma_\phi(v_1)$, respectively. Similarly, we define $\gamma_{1,2}^+$ and $\gamma_{1,2}^-$ for the edge label $\gamma_\phi(v_1, v_2)$. The goal of a GMRPP is to determine a collection of executable paths such that robots complete the current subtask (by satisfying the complete clause $\gamma_1^+ \wedge \gamma_{1,2}^-$ at the end while respecting the complete clause $\gamma_1^+ \wedge \gamma_1^-$ en route) and automatically activate the next subtask after completion since the complete clause $\gamma_{1,2}^+ \wedge \gamma_{1,2}^-$ implies the complete clause associated with the starting vertex of the next subtask. We refer to γ_1^- as the *running constraint* and $\gamma_{1,2}^-$ as the *terminal constraint*. Next, we determine three types of robots that are directly involved in the execution of the current subtask e .

(1) *Essential robots associated with constraint γ_1^+ :* We collect essential robots associated with essential clauses in γ_1^+ in the set \mathcal{R}_1 , where robots need to remain at certain target regions.

(2) *Essential robots associated with target $\gamma_{1,2}^+$:* We collect essential robots associated with the essential clause

$\gamma_{1,2}^+$ in the set $\mathcal{R}_{1,2}$, where robots need to reach certain target regions.

(3) *Robots associated with running and terminal constraints γ_1^- and $\gamma_{1,2}^-$:* The robots, in this case, are different from the previous two types since they are related to negative clauses γ_1^- or $\gamma_{1,2}^-$. These robots, unless they are involved in the first two cases, navigate without specific targets, only to satisfy the bound imposed by the negative literals on the number of certain types of robots in some regions. We collect them in the set \mathcal{R}^- , which contains all robots that belong to certain types involved in γ_1^- or $\gamma_{1,2}^-$, i.e., $\mathcal{R}^- = \{\mathcal{K}_j : \neg \pi_{i,j}^k \in \text{lits}^-(\gamma_1^- \vee \gamma_{1,2}^-)\}$.

Let $\mathcal{R}_e = \mathcal{R}_1 \cup \mathcal{R}_{1,2} \cup \mathcal{R}^-$ denote the set that collects all robots directly involved in the current subtask, and $\mathcal{R}_0 = \mathcal{R} \setminus \mathcal{R}_e$ collects the remaining robots. To formulate the GMRPP, we define by X_I and X_G the sets of initial and target locations, respectively, such that $X_I(r, j) \in S$ and $X_G(r, j) \subseteq S$ are the initial and target locations of robot $[r, j] \in \mathcal{R}$. Specifically, the initial robot locations are where the robots are at the end of the subtask immediately preceding e . The target region of robot $[r, j] \in \mathcal{R}_{1,2}$ is determined by its associated literal in $\gamma_{1,2}^+$, which is also given by $p_{r,j}(\zeta(r, j) + 1)$. Similarly, the target region of robot $[r, j] \in \mathcal{R}_1$ can also be determined by its associated literal in γ_1^+ . There are no specific target locations for robots in $\mathcal{R}^- \cup \mathcal{R}_0$.

Finally, let $\tau'_{r,j}$ denote the path segment of robot $[r, j] \in \mathcal{R}$, where $\tau'_{r,j}(t)$ denotes the robot location at time t for $t = 0, \dots, T$, where time instants 0 and T correspond to the completion time of the immediately preceding subtask and the current subtask, respectively. Next, the generalized multi-robot path planning problem, adapted from [Yu and LaValle \(2016\)](#), is defined as follows.

Definition B.1. (Generalized multi-robot path planning). *Given a discrete workspace E , a set of robots $\mathcal{R} = \mathcal{R}_e \cup \mathcal{R}_0$ where $\mathcal{R}_e = \mathcal{R}_1 \cup \mathcal{R}_{1,2} \cup \mathcal{R}^-$, a set of initial locations X_I , a set of target regions X_G , the running constraint γ_1^- , the terminal constraint $\gamma_{1,2}^-$, and the horizon T , find a collection of path segments $\tau'_{r,j}$ for all robots $[r, j] \in \mathcal{R}$ such that (i) every robot $[r, j] \in \mathcal{R}_{1,2}$ starts from the initial location and arrives at the target region at time instant T , i.e., $\tau'_{r,j}(0) = X_I(r, j)$ and $\tau'_{r,j}(T) \in X_G(r, j)$, $\forall [r, j] \in \mathcal{R}_{1,2}$; (ii) every robot $[r, j] \in \mathcal{R}_1$ remains in the target region for all time except 0 and T , i.e., $\tau'_{r,j}(0) = X_I(r, j)$ and $\tau'_{r,j}(t) \in X_G(r, j)$ for all $t = 1, \dots, T - 1$; and (iii) the paths $\{\tau'_{r,j}\}, \forall [r, j] \in \mathcal{R}^-$, satisfy the running constraint γ_1^- for all times except at 0 and T , and also satisfy the terminal constraint $\gamma_{1,2}^-$ at time instant T .*

Fig. 14 illustrates the time relation within one instance of GMRPP. The paths do not need to satisfy γ_1^+ and γ_1^- at time instants 0 and T since the tightest span of the vertex label of the current subtask can be one time step after the completion of the immediately preceding subtask, which is indicated by time 0, and one time step before the completion of the current subtask, which is indicated by time T . In Appendix B.3, we discuss how to solve the GMMPP with horizon T . The paths returned by this GMRPP complete the subtasks (v_1, v_2) and meanwhile activate the vertex label of v_2 , i.e., the next subtask.

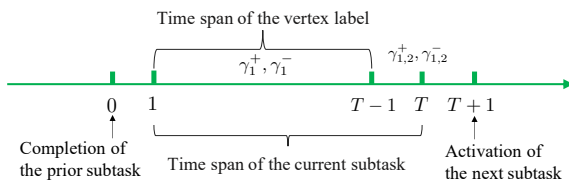


Figure 14. The time relation within one GMRPP. The essential and negative clauses are aligned with the time instants when they should be satisfied.

Remark B.2. In the formulation of the GMRPP, we did not take into account collision avoidance between robots, which will be addressed in Appendix B.4.1.

Remark B.3. Note that subtasks are executed sequentially as discussed above since we only assign target regions to those robots $\mathcal{R}_1 \cup \mathcal{R}_{1,2}$ directly involved in the current subtask e. Thus, we refer to this as the sequential execution. However, robots that participate in subsequent subtasks can move together with the robots that participate in the current subtask e by heading toward some “intermediate” targets, so that after the current subtask e is completed, these robots associated with subsequent subtasks have already traveled part of their routes towards finishing their respective subtasks. We will present this simultaneous execution in Appendix B.4.2.

Remark B.4. We refer to the execution of the subtask e discussed above as the full execution since it mobilizes all robots in the workspace. However, most times not all robots need to move for one specific subtask since only a subset of robots are responsible for the satisfaction of this subtask. In Appendix B.4.3 we discuss a partial execution where only necessary robots in \mathcal{R}_e , are allowed to move and the rest of the robots stay put. The partial execution shares most similarity with the full execution.

B.2.2 Sequential GMRPP solutions to find low-level paths that induce the simple path θ_ϕ : The GMRPP algorithm to design executable paths under the full execution is outlined in Alg. 3. We initialize all local counters and the global clock to 0 [line 1, Alg. 3]. The algorithm terminates when iteration over the subtasks in the simple path θ_ϕ is finished [line 2, Alg. 3].

We first check whether the first time instant $\vec{t}(1)$ on the time axis is 0. If $\vec{t}(1) = 0$, then the first subtask in the simple path θ_ϕ , i.e., the edge label of the first subtask, is satisfied by the initial robot locations. Thus, we increase the local counters of robots that participate and the global counter by 1 [lines 3-5, Alg. 3]. Otherwise, we solve the corresponding GMRPP as in Appendix B.3. We initialize T by $\vec{t}(c+1) - \vec{t}(c)$ (by default $\vec{t}(0) = 0$), which is the difference between the completion time of the immediately preceding subtask and the current one. We denote by T_e the final T when the GMRPP has a solution [line 8, Alg. 3]. Given a solution to the generalized multi-robot planning problem, Alg. 3 proceeds with the following updates [lines 9-13, Alg. 3].

First, for each robot $[r, j] \in \mathcal{R}$, we append the path segment $\tau'_{r,j}(t)$, for all $t = 1, \dots, T_e$, to its already-executed

Algorithm 3: Executable multi-robot path planning

Input: Workspace E , robot team \mathcal{R} , subtask sequence θ_ϕ , waypoint sequence $\{p_{r,j}\}$, time sequence $\{t_{r,j}\}$, NBA \mathcal{A}_ϕ and $\mathcal{A}_{\text{subtask}}^-$

;

$\tau_{r,j} = s_{r,j}^0, \zeta_{r,j} = 0, \forall [r,j] \in \mathcal{R}, c = 0$; ▷ Initialization

;

for $e = (v_1, v_2) \in \theta_\phi$ **do**

if $\vec{t}(1) = 0$ **then**

$\zeta_{r,j} = \zeta_{r,j} + 1, \forall [r,j] \in \mathcal{R}_{1,2};$

$c = c + 1;$

else

 Formulate the GMRPP ;

 Solve the GMRPP for horizon T as in Appendix B.3 to obtain paths $\tau'_{r,j}, \forall [r,j] \in \mathcal{R};$

$\vec{t}(1) = \vec{t}(c+1) - \vec{t}(c);$ ▷ Update

 Concatenate paths:

$\tau_{r,j} = \tau_{r,j} \cdot \tau'_{r,j}[1 : T_e], \forall [r,j] \in \mathcal{R};$

 Update individual timeline:

$t_{r,j}(\zeta) = t_{r,j}(\zeta) + T_e - (\vec{t}(c+1) - \vec{t}(c)),$

$\forall \zeta \geq \zeta_{r,j}, \forall [r,j] \in \mathcal{R};$

 Upadte time axis:

$\vec{t}(c') = \vec{t}(c') + T_e - (\vec{t}(c+1) - \vec{t}(c)),$

$\forall c' \geq c + 1;$

 Update local counter:

$\zeta_{r,j} = \zeta_{r,j} + 1, \forall [r,j] \in \mathcal{R}_{1,2};$

 Update global counter: $c = c + 1;$

The right-side time instant $\vec{t}(c + 1)$ in line 11 is the one before updates.

path $\tau_{r,j}$ [line 9, Alg. 3]. Note that the final waypoints will be the initial locations of the next instance of GMRPP. Moreover, for each robot $[r, j] \in \mathcal{R}$, we increase the time instants in $t_{r,j}$ with indices larger than or equal to $\zeta_{r,j}$ by $T_e - (\vec{t}(c+1) - \vec{t}(c))$ [line 10, Alg. 3], where $\vec{t}(c+1) - \vec{t}(c)$ is the time span of the current subtask given by the high-level plan whereas T_e is the actual time span given by the low-level executable path. Similarly, we increase the time instants in \vec{t} with indices larger than or equal to $c+1$ by $T_e - (\vec{t}(c+1) - \vec{t}(c))$. In this way, the subsequent subtasks in the high-level plan that have not been executed are shifted into the future by the same amount in order to maintain the correct temporal relation (precedence or simultaneity) between visits to waypoints in $\{p_{r,j}\}$. Next, we increase the local counter by 1 for all robots in $\mathcal{R}_{1,2}$, which reflects local progress towards completing their individual plans [line 12, Alg. 3]. Similarly, we increase the global counter c by 1 [line 13, Alg. 3].

B.3 Solution to the generalized multi-robot path planning problem

Conventional multi-robot path planning problems find feasible or optimal paths for groups of robots starting from a set of initial locations and ending at a set of desired target locations; see, e.g., [Yu and LaValle \(2016\)](#) and the references therein. To find executable paths satisfying the subtasks, we generalize the multi-robot path planning problem in several ways. First, we extend the notion of a single target location to

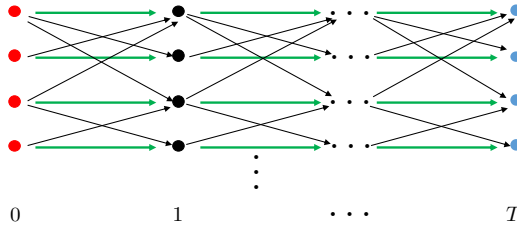


Figure 15. Time-expanded graph over horizon T (modified from Yu and LaValle (2016))

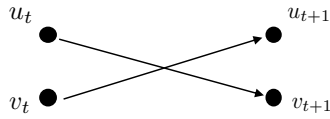


Figure 16. Merge-split gadget for avoiding head-on collision (from Yu and LaValle (2016))

a target region such that reaching any cell in the target region suffices. Second, the path segments that complete the subtask satisfy the complete clauses in the corresponding vertex label and edge label. Third, in the partial execution, only a subset of robots directly involved in the current or future subtasks are allowed to move.

In what follows, we adapt the method proposed in Yu and LaValle (2016) to solve the GMRPP under the full execution with given horizon T . The key idea is to construct a time-expanded graph $\mathcal{G}_T = (\mathcal{V}_T, \mathcal{E}_T)$ of the workspace which contains T copies of the free cells in the workspace E ; see Fig. 15. We organize the vertices and edges of this time-expanded graph \mathcal{G}_T in a matrix structure, so that each row corresponds to a free cell in the workspace E and each column corresponds to a time instant $t \in \{0, \dots, T\}$. Then, a vertex $u_t \in \mathcal{V}_T$ that appears in the t -th column of this matrix structure indicates whether the cell $u \in E$ is occupied by a robot at time instant t . The edges in \mathcal{G}_T capture adjacency relations between neighboring cells in E and consecutive time instants in $\{0, \dots, T\}$. Specifically, for any two adjacent cells u and v in E , an “X”-shape structure, referred to as a *merge-split gadget*, is created to capture the transition from vertex u at time t to vertex v at time $t + 1$; see also Fig. 16. In this way, robots traveling along a given row in the matrix structure corresponding to \mathcal{G}_T effectively remain idle at their current cell, while robots switching between different rows in \mathcal{G}_T transition between adjacent cells in E . We say that a sequence of transitions in \mathcal{G}_T from $t = 0$ to $t = T$ produces a robot path in the workspace E .

Next, we formulate an Integer Linear Programming (ILP) problem to solve the GMRPP. Let $s_{uvrj} \in \{0, 1\}$ be the routing variable such that $s_{u_tv_{t+1}rj} = 1$ if robot $[r, j] \in \mathcal{R}$ traverses the edge $(u_t, v_{t+1}) \in \mathcal{E}_T$. In what follows, we describe the constraints and objective of this ILP.

B.3.1 Routing constraints: The constraint that each edge can be traversed by at most one robot at a given time is given by

$$\sum_{[r,j] \in \mathcal{R}} s_{u_tv_{t+1}rj} \leq 1, \quad \forall (u_t, v_{t+1}) \in \mathcal{E}_T, \quad (38)$$

for all $t = 0, \dots, T - 1$. Furthermore, the flow conservation constraint is written as,

$$\sum_{u_{t-1}:(u_{t-1}, v_t) \in \mathcal{E}_T} s_{u_{t-1}v_trj} = \sum_{w_{t+1}:(v_t, w_{t+1}) \in \mathcal{E}_T} s_{v_tw_{t+1}rj}, \quad (39)$$

for all robots $[r, j] \in \mathcal{R}$ and all $t = 1, \dots, T - 1$. This means that every robot that arrives at a vertex in \mathcal{G}_T has to leave that vertex at the next time step. Next, the constraints at the initial time are encoded as,

$$\sum_{v_1:(u_0, v_1) \in \mathcal{E}_T} s_{u_0v_1rj} = 1, \quad (40a)$$

$$\sum_{w_0:(w_0, v_1) \in \mathcal{E}_T} s_{w_0v_1rj} = 0, \quad \forall w \in E \setminus u, \quad (40b)$$

for all robots $[r, j] \in \mathcal{R}$, where u_0 is the vertex associated with the cell $u = X_I(r, j)$ where robot $[r, j]$ is at the initial time. Constraints (40) state that robot $[r, j]$ has to depart from its initial location. Note that this departure is in the graph \mathcal{G}_T and is associated with time rather than physical location.

B.3.2 Target constraint: The general constraints that robot $[r, j]$ in \mathcal{R}_1 and $\mathcal{R}_{1,2}$ arrives at a cell in the target region $X_G(r, j)$ at certain time instant t can be encoded as

$$\sum_{v:v \in X_G(r, j)} \sum_{u_{t-1}:(u_{t-1}, v_t) \in \mathcal{E}_T} s_{u_{t-1}v_trj} = 1. \quad (41)$$

Specifically, t in constraint (41) takes values ranging from $1, \dots, T - 1$ when encoding the constraint that robot $[r, j] \in \mathcal{R}_1$ stays at the target region $X_G(r, j)$ to maintain the truth of the vertex label of the current subtask. For the constraint that robot $[r, j] \in \mathcal{R}_{1,2}$ arrives at a cell in $X_G(r, j)$ at the time instant T to complete the current subtask, we have $t = T$ in constraint (41).

B.3.3 Running and terminal constraints: The general running and terminal constraints that negative literals $\neg\pi_{i,j}^k$ should be respected at certain time instant t is written as

$$\sum_{[r,j] \in \mathcal{K}_j} \sum_{v \in \ell_k} \sum_{u_{t-1}:(u_{t-1}, v_t) \in \mathcal{E}_T} s_{u_{t-1}v_trj} \leq i - 1. \quad (42)$$

The running constraint that all negative literals $\neg\pi_{i,j}^k \in \text{lits}^-(\gamma_1^-)$ in the vertex label of the current subtask should be respected (excluding time instants 0 and T), can be encoded by assigning to t in constraint (42), values ranging from 1 to $T - 1$. Similarly, we encode the terminal constraint that the negative literal $\neg\pi_{i,j}^k$ in $\text{lits}^-(\gamma_{1,2}^-)$ should be satisfied at the time T by letting t in constraint (42) take the value T .

B.3.4 ILP objective: The ILP objective is to minimize the total travel cost and is defined as

$$\min \sum_{[r,j] \in \mathcal{R}} \sum_{t \in \{0, \dots, T-1\}} \sum_{(u_t, v_{t+1}) \in \mathcal{E}_T} d_{uv} s_{u_tv_{t+1}rj}, \quad (43)$$

where $d_{uv} \in \mathbb{N}$ is the travel cost between cells u and v .

When a solution does not exist for a given horizon T , we increment T and solve the ILP again. The solution provides a collection of executable paths that satisfy the current subtask as well as activate the next subtask at time T .

B.4 Implementations of GMRPP

In this section, we present several implementations of the GMRPP problem. We first address the collision avoidance between robots, then we show how essential robots of subsequent subtasks can simultaneously move with those of the current subtask, and finally show how only necessary robots move.

B.4.1 Collision avoidance: To handle collision avoidance, we first introduce an additional step to pre-process the NBA \mathcal{A}_ϕ (see Section 3.4.2), which removes infeasible clauses due to limited size of regions:

(6) *Violation of region size:* For each clause $\mathcal{C}_p^\gamma \in \text{cls}(\gamma)$, let $\text{lits}^+(k)$ denote literals in $\text{lits}^+(\mathcal{C}_p^\gamma)$ that involve region ℓ_k . We delete the clause \mathcal{C}_p^γ (replacing it with \perp) if the required total number of robots visiting region ℓ_k exceeds the number of free cells it covers, i.e., if there exists $k \in [l]$ such that $\sum_{\pi_{i,j}^k \in \text{lits}^+(k)} i > |\ell_k|$.

Collision avoidance is addressed in the low-level path planning component of our algorithm since the high-level plan generation abstracts away the workspace. In an instance of a GMRPP, we say that the paths of any two distinct robots $[r, j]$ and $[r', j']$ are collision-free if there does not exist a time instant $t \in [T]$ such that $\tau'_{r,j}(t) = \tau'_{r',j'}(t)$ (meet collision, that is, two robots occupy the same cell at the same time) or $\tau'_{r,j}(t) = \tau'_{r',j'}(t-1) \wedge \tau'_{r',j'}(t) = \tau'_{r,j}(t-1)$ (head-on collision, that is, two robots at adjacent cells switch locations with each other). Furthermore, in the case of the partial execution that will be introduced in Appendix B.4.3, we treat those robots that are not allowed to move as obstacles, giving rise to a new workspace $E' = (S', \rightarrow_{E'})$. In the case of full execution, we have $E' = E$. The time-expanded graph in Fig. 15 that captures the connectivity of the workspace is constructed based on the new workspace E' . Finally, we add the following collision avoidance constraints to the ILP for the GMRPP.

Avoiding meet collisions, $\forall v \in E'$, can be captured by the constraint

$$\sum_{[r,j] \in \mathcal{R}} \sum_{u_t:(u_t,v_{t+1}) \in \mathcal{E}_T} s_{u_t v_{t+1} r j} \leq 1, \quad \forall (u_t, v_{t+1}) \in \mathcal{E}_T, \quad (44)$$

for all $t = 0, \dots, T-1$. Moreover, avoiding head-on collisions at every gadget, $\forall u, v \in E'$ with $u \neq v$ can be captured by the constraint

$$\sum_{[r,j] \in \mathcal{R}} (s_{u_t v_{t+1} r j} + s_{v_t u_{t+1} r j}) \leq 1, \quad \forall (u_t, v_{t+1}) \in \mathcal{E}_T, \quad (45)$$

for all $t = 0, \dots, T-1$.

B.4.2 Simultaneous execution: When identifying robots that are involved in one instance of a GMRPP in Appendix B.2.1, we only focused on robots $\mathcal{R}_e = \mathcal{R}_1 \cup \mathcal{R}_{1,2} \cup \mathcal{R}^-$ that are directly involved in the completion of the current subtask (see (1)-(3)). However, the rest of robots that are not involved in the current subtask may concurrently move to begin the execution of subsequent subtasks of the current subtask e . Specifically, these robots can move towards waypoints associated with subsequent subtasks. In

what follows, we find essential robots associated with these subsequent subtasks.

(4) *Essential robots associated with subsequent subtasks:* These robots move simultaneously with the first two types of robots in (1)-(2) towards waypoints associated with subsequent subtasks of the current subtask e . We collect these robots in the set $\mathcal{R}'_{1,2}$ and identify them in the following way. First, we identify the completion time of the current subtask, which is given by $\vec{t}(c+1)$. Next, we iterate over the remaining robots that are not in $\mathcal{R}_1 \cup \mathcal{R}_{1,2}$ since they have been assigned target locations. For every robot $[r, j] \in \mathcal{R} \setminus (\mathcal{R}_1 \cup \mathcal{R}_{1,2})$, the time when it should visit the next waypoint based on its local counter $\zeta_{r,j}$ is given by $t_{r,j}(\zeta_{r,j} + 1)$. Note that $t_{r,j}(\zeta_{r,j} + 1) > \vec{t}(c+1)$ since we proceed along the simple path θ_ϕ and the completion time of subtasks that have not been considered will be larger than that of the current subtask. Finally, we calculate the time difference $\Delta t = t_{r,j}(\zeta_{r,j} + 1) - \vec{t}(c+1)$ and then check whether the robot $[r, j]$ can arrive at the target region $p_{r,j}(\zeta_{r,j} + 1)$ within time Δt starting from its current location by taking the shortest route. If not, robot $[r, j]$ should move simultaneously when completing the current subtask. In this case, the set of robots that are involved in some subtasks becomes $\mathcal{R}_e = \mathcal{R}_1 \cup \mathcal{R}_{1,2} \cup \mathcal{R}'_{1,2} \cup \mathcal{R}^-$.

Next, we determine the target location $X_G(r, j)$ for robot $[r, j] \in \mathcal{R}'_{1,2}$, which is the location from where robot $[r, j]$ can reach the region $p_{r,j}(\zeta(r, j) + 1)$ within time Δt by taking the shortest route in the new workspace S' (obtained by treating robots in the partial execution that do not move as obstacles). To avoid collision, if the selected target location of robot $[r, j]$ has already been assigned to another robot in $\mathcal{R}'_{1,2}$, then we select another free cell on the shortest route to be this robot's target location, which is close to the previously selected occupied cell and has not been assigned. More importantly, if a negative literal $\neg \pi_{i,j}^k$ exists in running or terminal constraints $\gamma_1^- \vee \gamma_{1,2}^-$, the selected free cell for robot $[r, j]$ should not be inside region ℓ_k . In the worst scenario where such a free cell is not available for robot $[r, j] \in \mathcal{R}'_{1,2}$, then we do not assign a specific target location to it, similar to the sequential execution. After determining the target location, the requirement in Definition B.1 of GMRPP on robot $[r, j] \in \mathcal{R}'_{1,2}$ is that it should arrive at the target waypoint at time T , that is, we need to design the path $\tau'_{r,j}$ such that $\tau'_{r,j}(0) = X_I(r, j)$ and $\tau'_{r,j}(T) = X_G(r, j)$. Note that the target $X_G(r, j)$ for $[r, j] \in \mathcal{R}'_{1,2}$ is a single cell, other than a region for robots in $\mathcal{R}_{1,2}$. Similar to robots in $\mathcal{R}_{1,2}$ that complete the current subtask, this requirement can be encoded by setting t equal to T in constraint (41) that handles the target constraint.

B.4.3 Partial execution: In Appendix B.2.1, all robots are involved in the formulation of GMRPP, which leads to a large ILP in Appendix B.3 when the size of robots is large. To reduce the complexity, we introduce the partial execution in which only necessary robots are allowed to move and the remaining are treated as obstacles.

First, we identify robots that need to move, which include essential robots in $\mathcal{R}_1 \cup \mathcal{R}_{1,2}$ and $\mathcal{R}'_{1,2}$ when simultaneous execution is adopted. These robots have target locations. In the full execution, the set \mathcal{R}^- is defined as $\mathcal{R}^- = \{\mathcal{K}_j : \neg \pi_{i,j}^k \in \text{lits}^-(\gamma_1^- \vee \gamma_{1,2}^-)\}$, which contains all robots

whose types are involved in the running and terminal constraints. To shrink the size of \mathcal{R}^- , for every negative literal $\neg\pi_{i,j}^k \in \gamma_1^- \vee \gamma_{1,2}^-$, we identify the number i' of robots of type j that is at region ℓ_k at time instant 0 in each instance of GMRPP. If $i' < i$, we remove robots of type j , i.e., \mathcal{K}_j , from \mathcal{R}^- and update this literal $\neg\pi_{i,j}^k$ to $\neg\pi_{i-i',j}^k$. Note that the case $i' \geq i$ only happens when $\neg\pi_{i,j}^k \in \gamma_{1,2}^-$ since at each instance of GMRPP robot locations at time instant 0 satisfy the starting vertex label, thus also satisfy γ_1^- . In this case, we replace \mathcal{K}_j in \mathcal{R}^- with $i' - i + 1$ robots of type j that are at region ℓ_k and update this literal $\neg\pi_{i,j}^k$ to $\neg\pi_{1,j}^k$. In this way, we reduce the number of robots in \mathcal{R}^- . Then, the robots that need to move constitute the set $\mathcal{R}_e = \mathcal{R}_1 \cup \mathcal{R}_{1,2} \cup \mathcal{R}'_{1,2} \cup \mathcal{R}^-$, and the remaining $\mathcal{R}_0 = \mathcal{R} \setminus \mathcal{R}_e$ are treated as obstacles, giving rise to a new workspace $E' = (S', \rightarrow_{E'})$.

The formulation of ILP to solve the GMRPP remains the same except that no variables are created corresponding to unmoved robots. After obtaining a solution to the GMRPP, we follow similar steps as in lines 9–13 in Alg. 3 to update relevant terms such as paths and timelines. The exception is that in the full execution, we can concatenate paths for each robot in \mathcal{R} [line 9], while in the partial execution, the GMRPP only finds paths for robots in \mathcal{R}_e . For other robots $[r, j] \in \mathcal{R}_0$, we append T_e times the last waypoint of the already-executed $\tau_{r,j}$ to $\tau_{r,j}$ since they remain idle.

Appendix C Proof of Theorem 6.1

To prove Theorem 6.1 that shows the completeness of our proposed method, we first show the completeness of the construction of the prefix part and then the completeness of the whole algorithm. For each part, we analyze the feasibility of the MILP for the time-stamped task allocation plans and the feasibility of the GMRPP for the low-level paths. Before presenting the main results, we first provide some necessary notation.

C.1 Notation

Given a NBA \mathcal{A} , e.g., \mathcal{A}_ϕ , $\mathcal{A}_{\text{relax}}$ and $\mathcal{A}_{\text{subtask}}$, we define by $\mathcal{L}_E(\mathcal{A})$ the set of words in $\mathcal{L}(\mathcal{A})$ that can be realized by robot paths. Recall that we can always map a run in \mathcal{A} to its counterpart in \mathcal{A}_ϕ . If $\mathcal{A} = \mathcal{A}_\phi$, then the counterpart of a run is the run itself. We define by $\mathcal{L}_E^\phi(\mathcal{A})$ the set of words in $\mathcal{L}_E(\mathcal{A})$ such that for any word $w \in \mathcal{L}_E^\phi(\mathcal{A})$ that induces an accepting run in \mathcal{A} , the counterpart of this accepting run in \mathcal{A}_ϕ is a restricted accepting run. In words, if $\mathcal{A} = \mathcal{A}_{\text{subtask}}$, and if a path τ generates a word w in $\mathcal{L}_E^\phi(\mathcal{A}_{\text{subtask}}) \subseteq \mathcal{L}_E(\mathcal{A}_{\text{subtask}})$ and w induces a run ρ in $\mathcal{A}_{\text{subtask}}$ connecting a pair v_0 and v_{accept} , then, we can obtain the corresponding run ρ_ϕ in \mathcal{A}_ϕ that is the counterpart of the run ρ in $\mathcal{A}_{\text{subtask}}$. This motivates us to modify the path τ that satisfies $\mathcal{A}_{\text{subtask}}$ to get another path that can produce this run ρ_ϕ in \mathcal{A}_ϕ . Additionally, let $\tilde{\mathcal{L}}_E^\phi(\mathcal{A}) \subseteq \mathcal{L}_E^\phi(\mathcal{A})$ collect those words in $\mathcal{L}_E^\phi(\mathcal{A})$ that can be generated by paths that satisfy Assumption 3.11.

Next, we consider the prefix and suffix parts separately. Given a pair of initial and accepting vertices, v_0 and v_{accept} , let $\mathcal{L}_E^{\phi, v_0 \rightarrow v_{\text{accept}}}(\mathcal{A})$ be the set that collects finite realizable words that can generate a run in \mathcal{A} connecting v_0 and

v_{accept} , and further the corresponding run in \mathcal{A}_ϕ satisfies the requirements on the prefix part of a restricted accepting run (see conditions (a)–(d) in Definition 3.8). Recall that when building the sub-NBA $\mathcal{A}_{\text{subtask}}^-$ for the suffix part, we rely on the last subtask $(v_{\text{prior}}, v_{\text{accept}})$ in $\mathcal{A}_{\text{subtask}}^-$ for the prefix part to extract the sub-NBA $\mathcal{A}_{\text{subtask}}$ for the suffix part. That is, we remove all outgoing edges from v_{accept} (acting as v_0) from $\mathcal{A}_{\text{relax}}$ if $\gamma_\phi(v_{\text{prior}}, v_{\text{accept}})$ does not imply its edge label in \mathcal{A}_ϕ . Also, we remove all incoming edges to v_{accept} (acting as v_{accept}) from $\mathcal{A}_{\text{relax}}$ if the corresponding edge label in \mathcal{A}_ϕ is not implied by $\gamma_\phi(v_{\text{prior}}, v_{\text{accept}})$; see Appendix A.3.1.1. Also, we rely on final robot locations of the prefix part, denoted by s_{prior} , to interpret the augmented clause $\mathcal{C}_{\text{prior}}^+$. That is, $\mathcal{C}_{\text{prior}}^+$ is satisfied if those robots involved in satisfying $\mathcal{C}_{\text{prior}}^+$ in the prefix part return to regions including their initial locations in s_{prior} ; see Appendix A.3.2. Therefore, we define by $\mathcal{L}_E^{\phi, v_{\text{accept}} \rightarrow v_{\text{accept}}}(\mathcal{A}; s_{\text{prior}}, v_{\text{prior}})$ the set that collects finite realizable words that can generate runs in \mathcal{A} starting from v_{accept} and ending at v_{accept} whose corresponding runs in \mathcal{A}_ϕ are the suffix parts of restricted accepting runs. Furthermore, the path generating a word in this set starts from s_{prior} and the prefix part of this restricted accepting run visits v_{prior} right before v_{accept} .

Finally when the context is clear, we refer to the suffix MILP as the MILP in which robots returning to their initial locations and progressing towards the accepting vertex in the NBA \mathcal{A}_ϕ is made in two steps (see Appendix A.3.2) and the extensions in Appendix A.4 to account for specific needs are not considered, and refer to the GMRPP as the GMRPP in which various implementations in Appendix B.4, collision avoidance, simultaneous execution and partial execution, are not considered. In what follows, we present the main results.

C.2 Existence of feasible paths in the sub-NBA $\mathcal{A}_{\text{subtask}}^-$

The following proposition states that paths exist that can induce accepting runs in the pruned sub-NBA $\mathcal{A}_{\text{subtask}}^-$. This result will be used to show the feasibility of the MILP in Section 5.1 for the time-stamped task allocation plan.

Proposition C.1. (Feasible paths for the sub-NBA $\mathcal{A}_{\text{subtask}}^-$). *Given a workspace satisfying Assumption 3.5 and a valid specification $\phi \in LTL^\chi$, if there exists a path $\tau = \tau^{\text{pre}}[\tau^{\text{suf}}]^\omega$ inducing a restricted accepting run $\rho = \rho^{\text{pre}}[\rho^{\text{suf}}]^\omega = v_0, \dots, v_{\text{prior}}, v_{\text{accept}}[v_{\text{next}}, \dots, v'_{\text{prior}}, v_{\text{accept}}]^\omega$ in \mathcal{A}_ϕ and this path satisfies Assumption 3.11, then there exists another path $\bar{\tau} = \bar{\tau}^{\text{pre}}[\bar{\tau}^{\text{suf}}]^\omega$ such that $\bar{\tau}^{\text{pre}}$ generates a word in $\tilde{\mathcal{L}}_E^{\phi, v_0 \rightarrow v_{\text{accept}}}(\mathcal{A}_{\text{subtask}}^-) \neq \emptyset$. Furthermore, if $v_{\text{accept}} \neq v_{\text{next}}$, then $\bar{\tau}^{\text{suf}}$ generates a word in $\tilde{\mathcal{L}}_E^{\phi, v_{\text{accept}} \rightarrow v_{\text{accept}}}(\mathcal{A}_{\text{subtask}}^-; s_{\text{prior}}, v_{\text{prior}}) \neq \emptyset$, where s_{prior} are the final robot locations of the prefix path τ^{pre} .*

To prove Proposition C.1, we recall the main steps to obtain the sub-NBA $\mathcal{A}_{\text{subtask}}^-$ and characterize the relations between the different NBAs; see Lemmas C.2–C.7. The first lemma shows that the pruning steps in Section 4.1 do not affect the set of restricted accepting runs in \mathcal{A}_ϕ that can be lemma by realizable words.

Lemma C.2. (\mathcal{A}_ϕ and \mathcal{A}_ϕ^-). *The pruning steps in Section 4.1 satisfy $\mathcal{L}_E^\phi(\mathcal{A}_\phi^-) = \mathcal{L}_E^\phi(\mathcal{A}_\phi)$.*

The proof can be found in Appendix C.4.1. Note that any word in $\mathcal{L}_E^\phi(\mathcal{A}_\phi)$ induces a restricted accepting run in \mathcal{A}_ϕ . A direct consequence of Lemma C.2 is that, any path generating a word $w \in \mathcal{L}_E^\phi(\mathcal{A}_\phi^-)$ satisfies ϕ since the word w also belongs to $\mathcal{L}_E^\phi(\mathcal{A}_\phi)$. The following lemma shows that ignoring negative literals expands the set of realizable words accepted by $\mathcal{A}_{\text{relax}}$ compared to that of \mathcal{A}_ϕ^- .

Lemma C.3. (\mathcal{A}_ϕ^- and $\mathcal{A}_{\text{relax}}$). *The relaxation stage that replaces all negative literals with \top in Section 4.1, satisfies $\mathcal{L}_E^\phi(\mathcal{A}_\phi^-) \subseteq \mathcal{L}_E^\phi(\mathcal{A}_{\text{relax}})$.*

The proof can be found in Appendix C.4.2. Lemma C.3 implies that a word in $\mathcal{L}_E^\phi(\mathcal{A}_{\text{relax}})$ may not belong to $\mathcal{L}_E^\phi(\mathcal{A}_\phi^-)$. Hence, a path generating a word in $\mathcal{L}_E^\phi(\mathcal{A}_{\text{relax}})$ may not satisfy the specification ϕ since $\mathcal{A}_{\text{relax}}$ ignores the negative literals. Next, we consider the prefix part. The following two lemmas show that extraction and pruning of the sub-NBA $\mathcal{A}_{\text{subtask}}$ for the prefix part do not empty the subset of words in $\mathcal{L}_E^{\phi, v_0 \rightarrow v_{\text{accept}}}(\mathcal{A}_{\text{subtask}}^-)$ that can be generated by feasible paths satisfying Assumption 3.11. The detailed proofs can be found in Appendices C.4.3- C.4.4.

Lemma C.4. ($\mathcal{A}_{\text{relax}}$ and $\mathcal{A}_{\text{subtask}}$). *The extraction of the sub-NBA $\mathcal{A}_{\text{subtask}}$ in Section 4.2.2 satisfies $\mathcal{L}_E^{\phi, v_0 \rightarrow v_{\text{accept}}}(\mathcal{A}_{\text{relax}}) = \mathcal{L}_E^{\phi, v_0 \rightarrow v_{\text{accept}}}(\mathcal{A}_{\text{subtask}})$.*

Lemma C.5. ($\mathcal{A}_{\text{subtask}}$ and $\mathcal{A}_{\text{subtask}}^-$). *The pruning steps in Section 4.2.3 satisfy $\mathcal{L}_E^{\phi, v_0 \rightarrow v_{\text{accept}}}(\mathcal{A}_{\text{subtask}}^-) \subseteq \mathcal{L}_E^{\phi, v_0 \rightarrow v_{\text{accept}}}(\mathcal{A}_{\text{subtask}})$. Additionally, if there exists a path $\tau = \tau^{\text{pre}}[\tau^{\text{suf}}]^\omega$ inducing a restricted accepting run in \mathcal{A}_ϕ and this path satisfies Assumption 3.11, then there exists a path $\tilde{\tau}^{\text{pre}}$, modified from τ^{pre} , that can generate a word in $\mathcal{L}_E^{\phi, v_0 \rightarrow v_{\text{accept}}}(\mathcal{A}_{\text{subtask}}^-)$, i.e., $\tilde{\mathcal{L}}_E^{\phi, v_0 \rightarrow v_{\text{accept}}}(\mathcal{A}_{\text{subtask}}^-) \neq \emptyset$.*

The following corollary is a direct consequence of the proof of Lemma C.5, which implies that we can construct a sub-NBA $\mathcal{A}_{\text{subtask}}^-$ based on s_{prior} and v_{prior} obtained from the sub-NBA $\mathcal{A}_{\text{subtask}}$ for the prefix part.

Corollary C.6. (s_{prior} and v_{prior}). *The final configuration of the path $\tilde{\tau}^{\text{pre}}$ is s_{prior} , same as the final configuration of the prefix path τ^{pre} , and the induced run visits v_{prior} right before v_{accept} , same as the induced run ρ^{pre} .*

The following proposition draws conclusions similar to Lemma C.4 and C.5 for the suffix part; see Appendix C.4.5 for the proof.

Lemma C.7. ($\mathcal{A}_{\text{subtask}}$ and $\mathcal{A}_{\text{subtask}}^-$). *The extraction and pruning steps in Appendix A.3.1 satisfy $\mathcal{L}_E^{\phi, v_{\text{accept}} \rightarrow v_{\text{accept}}}(\mathcal{A}_{\text{relax}}; s_{\text{prior}}, v_{\text{prior}}) = \mathcal{L}_E^{\phi, v_{\text{accept}} \rightarrow v_{\text{accept}}}(\mathcal{A}_{\text{subtask}}; s_{\text{prior}}, v_{\text{prior}})$. Additionally, if there exists a path $\tau = \tau^{\text{pre}}[\tau^{\text{suf}}]^\omega$ inducing a restricted accepting run in \mathcal{A}_ϕ and this path satisfies Assumption 3.11, then there exists a path $\tilde{\tau}^{\text{suf}}$, modified from τ^{suf} , that can generate a word in $\tilde{\mathcal{L}}_E^{\phi, v_{\text{accept}} \rightarrow v_{\text{accept}}}(\mathcal{A}_{\text{subtask}}^-; s_{\text{prior}}, v_{\text{prior}})$, i.e., $\tilde{\mathcal{L}}_E^{\phi, v_{\text{accept}} \rightarrow v_{\text{accept}}}(\mathcal{A}_{\text{subtask}}^-; s_{\text{prior}}, v_{\text{prior}}) \neq \emptyset$.*

Finally, Proposition C.1 can be established by combining Lemmas C.5 and C.7.

C.3 Completeness

C.3.1 Completeness of the prefix part synthesis: The following proposition states that, with mild assumptions, we can find a path that induces a run in \mathcal{A}_ϕ connecting v_0 and v_{accept} , which ensures the completeness of our method for specifications in LTL^χ that can be satisfied by finite-length paths.

Proposition C.8. (Completeness of the synthesis method for the prefix part). *Assume a workspace that satisfies Assumption 3.5 and a valid specification $\phi \in LTL^\chi$. If there exists a path $\tau = \tau^{\text{pre}}[\tau^{\text{suf}}]^\omega$ that induces a restricted accepting run $\rho = \rho^{\text{pre}}[\rho^{\text{suf}}]^\omega = v_0, \dots, v_{\text{prior}}, v_{\text{accept}}[v_{\text{next}}, \dots, v'_{\text{prior}}, v_{\text{accept}}]^\omega$ in \mathcal{A}_ϕ and this path satisfies Assumption 3.11, then the proposed synthesis method can find a robot path $\tilde{\tau}^{\text{pre}}$ that generates a word \tilde{w}^{pre} that induces a run $\tilde{\rho}^{\text{pre}}$ in \mathcal{A}_ϕ connecting the pair v_0 and v_{accept} .*

We first provide the following three lemmas and then combine with Proposition C.1 to conclude the proof of Proposition C.8. Lemma C.9 states that, if the poset P is inferred from a set of simple paths that includes a simple path associated with a feasible prefix path, then the MILP in Appendix A.2 associated with this poset P is feasible; Lemma C.10 states that a simple path in $\mathcal{A}_{\text{subtask}}^-$ can be extracted from the solution to the MILP and discusses the temporal properties associated with this path, and Lemma C.11 states that the sequence of GMRPP in Section 5.3 associated with the extracted simple path is feasible.

Lemma C.9. (Feasibility of the prefix MILP). *If there exists a path $\tilde{\tau}^{\text{pre}}$ generating a finite word $\tilde{w}^{\text{pre}} \in \tilde{\mathcal{L}}_E^{\phi, v_0 \rightarrow v_{\text{accept}}}(\mathcal{A}_{\text{subtask}}^-)$, and the word \tilde{w}^{pre} induces a simple path $\tilde{\theta}$ in $\mathcal{A}_{\text{subtask}}^-$ that belongs to the set of simple paths that generate the poset P , then the prefix MILP in Appendix A.2 associated with this poset P is feasible.*

The detailed proof can be found in Appendix C.4.6. The key idea is that, the path $\tilde{\tau}^{\text{pre}}$ generating the word \tilde{w}^{pre} can give rise to a high-level plan satisfying constraints (3)-(28) in Appendix A.2.

Lemma C.10. (Properties of the simple path). *If the MILP for the prefix path in Appendix A.2 associated with the poset P produces a solution, then a simple path $\tilde{\theta}$ designed in Appendix B.1 that belongs to the set of simple paths that generate the poset P , can be extracted from the sub-NBA $\mathcal{A}_{\text{subtask}}^-$. Additionally, the following properties hold for subtasks in the simple path $\tilde{\theta}$:*

- (a) *The first subtask in the simple path $\tilde{\theta}$ is activated at time 0;*
- (b) *For any subtask $e \in \tilde{\theta}$, if its starting vertex has a self-loop, then the completion time of the subtask e is no earlier than the activation of its starting vertex label, and at most one time step after the completion of its starting vertex label;*
- (c) *For any two consecutive subtasks $e, e' \in \tilde{\theta}$, the latter subtask e' is activated at most one time step after the completion of the former subtask e .*

The detailed proof can be found in Appendix C.4.7. Property (a) guarantees the initialization of the sequence of subtasks in $\tilde{\theta}$, property (b) ensures that each subtask in $\tilde{\theta}$ is correctly executed, and property (c) prevents gaps when transitioning between consecutive subtasks. Combined these three properties establish that once the first subtask is activated at time 0, each subsequent subtask is completed successfully and inter-subtasks transitions occur seamlessly, until the completion of the last subtask. Note that the extracted simple path $\tilde{\theta}$ may not be identical to the one induced by the word $\bar{w}^{\text{pre}} \in \tilde{\mathcal{L}}_E^{\phi, v_0 \rightarrow v_{\text{accept}}}(\mathcal{A}_{\text{subtask}}^-)$ in Lemma C.9. The following lemma states that low-level paths can be generated from the solution to the prefix MILP in Appendix A.2; the proof can be found in Appendix C.4.8.

Lemma C.11. (Feasibility of the GMRPP in Appendix B.2). *Assume that the workspace satisfies Assumption 3.5. Then, the sequence of the GMRPP in Appendix B.2 that constructs the simple path $\tilde{\theta}$ from the solution to the MILP in Appendix A.2, is feasible. That is, every GMRPP is feasible for a time horizon T .*

Combining Proposition C.1 with Lemmas C.9-C.11, we conclude the proof of Proposition C.8 on the completeness of the proposed synthesis method for the prefix part. Note that Proposition C.8 assumes the existence of a feasible path. By Proposition C.1, $\tilde{\mathcal{L}}_E^{\phi, v_0 \rightarrow v_{\text{accept}}}(\mathcal{A}_{\text{subtask}}^-) \neq \emptyset$, therefore a path $\bar{\tau}^{\text{pre}}$ exists that generates a word $\bar{w}^{\text{pre}} \in \tilde{\mathcal{L}}_E^{\phi, v_0 \rightarrow v_{\text{accept}}}(\mathcal{A}_{\text{subtask}}^-)$. Because in Section 4.2.1 we iterate over all pairs of initial and accepting vertices whose total length is not infinite, we can focus on the NBA $\mathcal{A}_{\text{subtask}}^-$ associated with a pair that produces a feasible path, as required in Proposition C.8. Moreover, since in Section 4.3 we create posets for all subsets of equivalent simple paths connecting the pair v_0 and v_{accept} , by iterating over all these posets we are guaranteed to eventually formulate the MILP over the poset that includes the simple path induced by the path $\bar{\tau}^{\text{pre}}$. According to Lemma C.9, this MILP has a solution. Then, by Lemma C.11, we get that a path $\tilde{\tau}^{\text{pre}}$ can be obtained by concatenating paths from each GMRPP since the final and initial locations of consecutive GMRPPs are identical, which completes the proof.

C.3.2 Completeness of the overall algorithm: Similar to Lemma C.9, we show the feasibility of the suffix MILP in Appendix A.3.2.2; see Appendix C.4.9 for the detailed proof.

Lemma C.12. (Feasibility of the suffix MILP). *Assume a valid specification $\phi \in LTL^0$ and let s_{prior} and v_{prior} denote the final configuration of the path τ^{pre} and the vertex before v_{accept} in the run ρ^{pre} , respectively. If there exists a path $\bar{\tau}^{\text{suf}}$ generating a finite word $\bar{w}^{\text{suf}} \in \tilde{\mathcal{L}}_E^{\phi, v_{\text{accept}} \rightarrow v_{\text{accept}}}(\mathcal{A}_{\text{subtask}}^-; s_{\text{prior}}, v_{\text{prior}})$, and the word \bar{w}^{suf} induces a simple path $\tilde{\theta}^{\text{suf}}$ belonging to the set of simple paths that generate the poset P , then the suffix MILP associated with this poset P , composed of constraints (3)-(26) in Appendix A.2 and constraints (30)-(32) in Appendix A.3.2.2, is feasible.*

Note that the results in Lemmas C.10 and C.11 developed for the prefix part can also be applied to the suffix part. Combined with Lemma C.12, we can obtain an equivalent statement of Proposition C.8 for the suffix part.

Finally, combining Proposition C.8 for the prefix part with Proposition C.1, we can establish completeness of our proposed method; see Appendix C.4.10.

Remark C.13. Note that Lemma C.12 focuses on LTL^0 specifications. The prefix path $\tilde{\tau}^{\text{pre}}$ in Proposition C.8 is obtained by solving the prefix MILP in Appendix A.2, which may allocate a different fleet of robots than $\bar{\tau}^{\text{pre}}$ to satisfy the same induced atomic propositions. Since robots also need to return to initial locations, this may affect the existence of a suffix path and further the satisfaction of the same- $\langle i, j \rangle$ constraint (33) in Appendix A.3.2.2. Therefore, we restrict the specification to the class LTL^0 in the statement.

C.4 Detailed proofs

C.4.1 Proof of Lemma C.2: The basic idea is that the pruning steps in Section 4.1 do not affect any restricted accepting runs. First, removing infeasible transitions and unreachable vertices will not exclude any realizable words. Therefore, the set of realizable words $\mathcal{L}_E(\mathcal{A}_\phi)$ does not change after this operation. Second, according to condition (c) in Definition 3.8, any restricted accepting run does not contain vertices without self-loops except for initial and accepting vertices. Thus, removing such vertices will not affect the set of restricted accepting runs in \mathcal{A}_ϕ . Third, by condition (d), any edge whose label does not strongly imply its end vertex label, except for the case that the end vertex is an accepting vertex, can not appear in any restricted accepting run. Thus removing such edges does not affect the set of restricted accepting runs, either. We conclude that the operations in Section 4.1 do not affect the set of restricted accepting runs in \mathcal{A}_ϕ that can be induced by the realizable words in $\mathcal{L}_E^\phi(\mathcal{A}_\phi)$. Moreover, these restricted accepting runs are also accepting runs in \mathcal{A}_ϕ^- , which implies that $\mathcal{L}_E^\phi(\mathcal{A}_\phi^-) = \mathcal{L}_E^\phi(\mathcal{A}_\phi)$, completing the proof.

C.4.2 Proof of Lemma C.3: The inclusion is straightforward in that, given a clause \mathcal{C} in \mathcal{A}_ϕ^- , the clause \mathcal{C}' in $\mathcal{A}_{\text{relax}}$ obtained by replacing negative literals in \mathcal{C} with \top is a subformula of the original clause \mathcal{C} . In other words, the satisfaction of the original clause \mathcal{C} implies the satisfaction of \mathcal{C}' , which implies that any realizable word w in $\mathcal{L}_E(\mathcal{A}_\phi^-)$ belongs to $\mathcal{L}_E(\mathcal{A}_{\text{relax}})$. Thus, any word $w \in \mathcal{L}_E^\phi(\mathcal{A}_\phi^-) \subseteq \mathcal{L}_E(\mathcal{A}_\phi^-)$ belongs to $\mathcal{L}_E(\mathcal{A}_{\text{relax}})$.

Next, we prove that indeed any word $\tilde{w} \in \mathcal{L}_E^\phi(\mathcal{A}_\phi^-)$ belongs to $\mathcal{L}_E^\phi(\mathcal{A}_{\text{relax}})$ is also in $\mathcal{L}_E(\mathcal{A}_{\text{relax}})$. Because $\tilde{w} \in \mathcal{L}_E^\phi(\mathcal{A}_\phi^-)$, it can induce a run in \mathcal{A}_ϕ^- whose corresponding run in \mathcal{A}_ϕ is a restricted accepting run. Also because \tilde{w} is in $\mathcal{L}_E(\mathcal{A}_{\text{relax}})$ and clauses in $\mathcal{A}_{\text{relax}}$ are the subformulas of the clauses in \mathcal{A}_ϕ^- , \tilde{w} can induce the same run in $\mathcal{A}_{\text{relax}}$ as the run in \mathcal{A}_ϕ^- (same sequence of vertices). Additionally, these two runs correspond to the same restricted accepting run in \mathcal{A}_ϕ^- . Therefore, $\tilde{w} \in \mathcal{L}_E^\phi(\mathcal{A}_{\text{relax}})$, i.e., $\mathcal{L}_E^\phi(\mathcal{A}_\phi^-) \subseteq \mathcal{L}_E^\phi(\mathcal{A}_{\text{relax}})$, completing the proof.

C.4.3 Proof of Lemma C.4: Given the pair of initial and accepting vertices, v_0 and v_{accept} , the corresponding sub-NBA $\mathcal{A}_{\text{subtask}}$ is composed of all vertices and edges in $\mathcal{A}_{\text{relax}}$ that belong to some paths that connect v_0 and v_{accept} with two exceptions. The first exception is that all other initial

and accepting vertices other than v_0 and v_{accept} are removed, and the second exception is that the self-loop of v_0 (if exists) is removed if the initial robot locations do not satisfy its corresponding vertex label in \mathcal{A}_ϕ , and the outgoing edges of the initial vertex are also removed if the initial robot locations do not satisfy their corresponding edge labels in \mathcal{A}_ϕ ; see Section 4.2.2.

To show this result, note first that, according to condition (b) in the Definition 3.8, the prefix part does not include more than one initial vertex and more than one accepting vertex. Since $\mathcal{L}_E^{\phi, v_0 \rightarrow v_{\text{accept}}}(\mathcal{A}_{\text{relax}})$ are related to the initial and accepting vertices v_0 and v_{accept} , removing other initial and accepting vertices does not affect $\mathcal{L}_E^{\phi, v_0 \rightarrow v_{\text{accept}}}(\mathcal{A}_{\text{relax}})$.

Second, any word w that at the beginning satisfies the label of the initial vertex v_0 whose self-loop is removed or labels of outgoing edges that are removed, cannot be generated by feasible paths since initial robot locations violate these labels. Therefore, any such word w does not belong to $\mathcal{L}_E^{\phi, v_0 \rightarrow v_{\text{accept}}}(\mathcal{A}_{\text{relax}})$, meaning that removing the self-loops and outgoing edges does not affect $\mathcal{L}_E^{\phi, v_0 \rightarrow v_{\text{accept}}}(\mathcal{A}_{\text{relax}})$, completing the proof.

C.4.4 Proof of Lemma C.5: The inclusion relation is straightforward since $\mathcal{A}_{\text{subtask}}^-$ is obtained by removing edges from $\mathcal{A}_{\text{subtask}}$ that are decomposable according to the sequential triangle property (see Definition 4.3). In what follows, we focus on the non-emptiness of $\tilde{\mathcal{L}}_E^{\phi, v_0 \rightarrow v_{\text{accept}}}(\mathcal{A}_{\text{subtask}}^-)$. We first show that the given prefix path τ^{pre} can generate a word in $\tilde{\mathcal{L}}_E^{\phi, v_0 \rightarrow v_{\text{accept}}}(\mathcal{A}_{\text{subtask}})$, and then show that based on τ^{pre} another prefix path $\bar{\tau}^{\text{pre}}$ can be synthesized to generate a word in $\tilde{\mathcal{L}}_E^{\phi, v_0 \rightarrow v_{\text{accept}}}(\mathcal{A}_{\text{subtask}}^-)$.

To show that the given prefix path τ^{pre} can generate a word in $\tilde{\mathcal{L}}_E^{\phi, v_0 \rightarrow v_{\text{accept}}}(\mathcal{A}_{\text{subtask}})$, we show that the results in Lemmas C.2-C.4 can be applied to languages $\tilde{\mathcal{L}}(\cdot)$ that satisfy Assumption 3.11. Note that Assumption 3.11 describes how a restricted accepting run is implemented by robots. Specifically, if an accepting word belonging to two languages $\mathcal{L}_E^\phi(\mathcal{A}_1)$ and $\mathcal{L}_E^\phi(\mathcal{A}_2)$ can be generated by robot paths that satisfy Assumption 3.11, then this word should also belong to the languages $\tilde{\mathcal{L}}_E^\phi(\mathcal{A}_1)$ and $\tilde{\mathcal{L}}_E^\phi(\mathcal{A}_2)$. Therefore, the specific implementation of an accepting word is implemented does not affect the relation between languages. We can get that $\tilde{\mathcal{L}}_E^\phi(\mathcal{A}_\phi^-) = \tilde{\mathcal{L}}_E^\phi(\mathcal{A}_\phi)$ by Lemma C.2, $\tilde{\mathcal{L}}_E^\phi(\mathcal{A}_\phi^-) \subseteq \tilde{\mathcal{L}}_E^\phi(\mathcal{A}_{\text{relax}})$ by Lemma C.3, $\tilde{\mathcal{L}}_E^{\phi, v_0 \rightarrow v_{\text{accept}}}(\mathcal{A}_{\text{relax}}) = \tilde{\mathcal{L}}_E^{\phi, v_0 \rightarrow v_{\text{accept}}}(\mathcal{A}_{\text{subtask}})$ by Lemma C.4 and $\tilde{\mathcal{L}}_E^{\phi, v_0 \rightarrow v_{\text{accept}}}(\mathcal{A}_{\text{subtask}}^-) \subseteq \tilde{\mathcal{L}}_E^{\phi, v_0 \rightarrow v_{\text{accept}}}(\mathcal{A}_{\text{subtask}})$ as discussed in the beginning of this proof.

Next, because the accepting word $w = w^{\text{pre}}[w^{\text{suf}}]^\omega$ generated by the path $\tau = \tau^{\text{pre}}[\tau^{\text{suf}}]^\omega$ induces a restricted accepting run and this path satisfies Assumption 3.11, i.e., $w \in \tilde{\mathcal{L}}_E^\phi(\mathcal{A}_\phi)$, we have that $w \in \tilde{\mathcal{L}}_E^\phi(\mathcal{A}_\phi^-)$ and further $w^{\text{pre}} \in \tilde{\mathcal{L}}_E^{\phi, v_0 \rightarrow v_{\text{accept}}}(\mathcal{A}_{\text{relax}})$. Therefore, $w^{\text{pre}} \in \tilde{\mathcal{L}}_E^{\phi, v_0 \rightarrow v_{\text{accept}}}(\mathcal{A}_{\text{subtask}})$, that is, τ^{pre} generates a word in $\tilde{\mathcal{L}}_E^{\phi, v_0 \rightarrow v_{\text{accept}}}(\mathcal{A}_{\text{subtask}})$. In what follows, we synthesize another prefix path $\bar{\tau}^{\text{pre}}$ based on τ^{pre} .

First, consider 3 different vertices v_1, v_2, v_3 in $\mathcal{A}_{\text{subtask}}$ that satisfy the ST property. Assume $\mathcal{A}_{\text{subtask}}$ is currently at the vertex v_1 . We show that, given robot configuration s in a path that completes the subtask (v_1, v_3) , i.e., a path that drives the transition to vertex v_3 , we can simply repeat

this robot configuration one more time so that the sub-NBA $\mathcal{A}_{\text{subtask}}^-$ reaches v_3 by traversing edges (v_1, v_2) and (v_2, v_3) . Specifically, according to Definition 4.3 of ST property, since the robot configuration s satisfies the edge label $\gamma(v_1, v_3)$ and $\gamma(v_1, v_3) = \gamma(v_1, v_2) \wedge \gamma(v_2, v_3)$, it also satisfies the edge label $\gamma(v_1, v_2)$. Thus, s can drive the transition to vertex v_2 from v_1 . At the next time step, if robots remain idle, the edge label $\gamma(v_2, v_3)$ can be satisfied since the robot configuration s satisfies $\gamma(v_1, v_3)$ and $\gamma(v_1, v_3)$ implies $\gamma(v_2, v_3)$. Therefore, by simply repeating this robot configuration, the sub-NBA $\mathcal{A}_{\text{subtask}}^-$ traverses edges (v_1, v_2) and (v_2, v_3) to reach v_3 , without satisfying the vertex label $\gamma(v_2)$.

Based on this observation, we continue showing the non-emptiness of $\tilde{\mathcal{L}}_E^{\phi, v_0 \rightarrow v_{\text{accept}}}(\mathcal{A}_{\text{subtask}}^-)$. With a slight abuse of notation, let ρ^{pre} denote the run in $\mathcal{A}_{\text{subtask}}$ induced by the word w^{pre} . We assume the run ρ^{pre} traverses an edge (v_1, v_3) in $\mathcal{A}_{\text{subtask}}$ corresponding to a composite subtask, which will be removed according to ST property. Otherwise, the run ρ^{pre} will persist in $\mathcal{A}_{\text{subtask}}^-$. When the run ρ^{pre} traverses a composite edge, we locate the robot configuration s in τ^{pre} that enables this composite subtask, let the robots remain idle for one time step as discussed above, and then continue along the path τ^{pre} . Let $\bar{\tau}^{\text{pre}}$ denote the new path, which also satisfies conditions (a)-(b) in Definition 3.10 since the robots remain idle for one time step. Furthermore, the path $\bar{\tau}^{\text{pre}}$ generates a word \bar{w}^{pre} that induces a run $\bar{\rho}^{\text{pre}}$ in $\mathcal{A}_{\text{subtask}}^-$ traversing the two elementary edges (v_1, v_2) and (v_2, v_3) .

Next, we prove that since ρ^{pre} is a prefix part that satisfies the conditions (a)-(d) in Definition 3.8, so does the run $\bar{\rho}_\phi^{\text{pre}}$ that corresponds to the run $\bar{\rho}^{\text{pre}}$. Observe that $\bar{\rho}^{\text{pre}}$ differs from ρ^{pre} only in that ρ^{pre} traverses edge (v_1, v_3) while $\bar{\rho}^{\text{pre}}$ traverses edges (v_1, v_2) and (v_2, v_3) consecutively. Obviously, the run $\bar{\rho}_\phi^{\text{pre}}$ satisfies conditions (a)-(c) in Definition 3.8. Furthermore, $\gamma_\phi(v_1, v_2) \Rightarrow_s \gamma_\phi(v_2)$ and $\gamma_\phi(v_2, v_3) \Rightarrow_s \gamma_\phi(v_3)$; otherwise, they would be pruned in Section 4.1. Thus, the run $\bar{\rho}_\phi^{\text{pre}}$ satisfies condition (d), that is, the word \bar{w}^{pre} generated by $\bar{\tau}^{\text{pre}}$ belongs to $\tilde{\mathcal{L}}_E^{\phi, v_0 \rightarrow v_{\text{accept}}}(\mathcal{A}_{\text{subtask}}^-)$, completing the proof.

C.4.5 Proof of Lemma C.7: This proof is similar to the proofs of Lemmas C.4 and C.5. Recall from Appendix A.3.1 that to obtain the sub-NBA $\mathcal{A}_{\text{subtask}}$, we remove all other accepting vertices from $\mathcal{A}_{\text{relax}}$, all initial vertices without self-loops, all outgoing edges from v_{accept} if the corresponding label is not implied by the label $\gamma_\phi(v_{\text{prior}}, v_{\text{accept}})$, which is the edge label in the NBA \mathcal{A}_ϕ that corresponds to the last completed subtask in the prefix part, and all incoming edges to v_{accept} if the corresponding label is not implied by the label $\gamma_\phi(v_{\text{prior}}, v_{\text{accept}})$. According to conditions (b) and (f) in Definition 3.8, the suffix part does not traverse these removed vertices and edges. Therefore, removing them does not affect $\mathcal{L}_E^{\phi, v_{\text{accept}} \rightarrow v_{\text{accept}}}(\mathcal{A}_{\text{relax}}; s_{\text{prior}}, v_{\text{prior}})$, i.e.,

$$\mathcal{L}_E^{\phi, v_{\text{accept}} \rightarrow v_{\text{accept}}}(\mathcal{A}_{\text{relax}}; s_{\text{prior}}, v_{\text{prior}}) = \mathcal{L}_E^{\phi, v_{\text{accept}} \rightarrow v_{\text{accept}}}(\mathcal{A}_{\text{subtask}}; s_{\text{prior}}, v_{\text{prior}}).$$

To prove that $\tilde{\mathcal{L}}_E^{\phi, v_{\text{accept}} \rightarrow v_{\text{accept}}}(\mathcal{A}_{\text{subtask}}^-; s_{\text{prior}}, v_{\text{prior}}) \neq \emptyset$, we follow similar steps as those in the proof of Lemma C.5. First, the suffix path τ^{suf} can generate a word in $\tilde{\mathcal{L}}_E^{\phi, v_{\text{accept}} \rightarrow v_{\text{accept}}}(\mathcal{A}_{\text{subtask}}; s_{\text{prior}}, v_{\text{prior}})$, same as τ^{pre} can generate a word in $\tilde{\mathcal{L}}_E^{\phi, v_0 \rightarrow v_{\text{accept}}}(\mathcal{A}_{\text{subtask}})$. Second, the path $\bar{\tau}^{\text{suf}}$ can

be obtained from τ^{suf} by repeating the robot configuration that completes a composite subtask one more time, so that the resulting run traverses two elementary edges successively. This drives the transition to the same vertex as that reached by traversing a composite edge. Since v_{accept} does not have a self-loop, when $v_3 = v_{\text{accept}}$, we do not remove the composite edge (v_1, v_3) from $\mathcal{A}_{\text{subtask}}^-$ for the suffix part (see Definition 4.3). Thus, we can reuse the robot configuration that enables the edge (v_1, v_{accept}) , which satisfies condition (c) in Definition 3.10 that robots return to s_{prior} , completing the proof.

C.4.6 Proof of Lemma C.9: Consider a path $\bar{\tau}^{\text{pre}}$ that generates a finite word $\bar{w}^{\text{pre}} \in \tilde{\mathcal{L}}_E^{\phi, v_0 \rightarrow v_{\text{accept}}}(\mathcal{A}_{\text{subtask}}^-)$ inducing a simple path $\bar{\theta}^{\text{pre}}$ in $\mathcal{A}_{\text{subtask}}^-$. Then, for two consecutive subtasks in the simple path $\bar{\theta}^{\text{pre}}$, it is possible that their edge labels are satisfied by two consecutive symbols in the word \bar{w}^{pre} . In this case, the starting vertex label of the second subtask is not satisfied by the path $\bar{\tau}^{\text{pre}}$. We first show that $\bar{\tau}^{\text{pre}}$ can be used to construct a new path such that this new path can also induce the simple path $\bar{\theta}^{\text{pre}}$ in $\mathcal{A}_{\text{subtask}}^-$, and the starting vertex label, if exists, of each subtask in the simple path $\bar{\theta}^{\text{pre}}$ is satisfied by the new path at least once. This is because constraint (9) states that any vertex or edge label of any subtask in a simple path must be satisfied. Since the new path is similar to the original path $\bar{\tau}^{\text{pre}}$, with a slight abuse of notation, we still use $\bar{\tau}^{\text{pre}}$ to denote the new path. Given the new path $\bar{\tau}^{\text{pre}}$, our goal is to show that $\bar{\tau}^{\text{pre}}$ can generate a time-stamped task allocation plan that can also be generated by a solution to the prefix MILP in Appendix A.2. To this end, we first obtain an *essential word* w^* based on the word \bar{w}^{pre} generated by the path $\bar{\tau}^{\text{pre}}$, such that the path $\bar{\tau}^{\text{pre}}$ can also generate the essential word and the essential word w^* is the tightest word that can induce the same run $\bar{\rho}^{\text{pre}}$ as \bar{w}^{pre} does; see Appendix C.4.6.1. Then, we show that the essential word w^* can produce a graph that is a subgraph of the routing graph \mathcal{G} built in Appendix A.1; see Appendix C.4.6.2. Finally, we show that this subgraph can be viewed as a graphical solution to the MILP; see Appendix C.4.6.3.

The construction of new path is straightforward. According to condition (d) in Definition 3.8, for any subtask e in the simple path $\bar{\theta}^{\text{pre}}$ that is not the first one to be completed, its starting vertex label is strongly implied by the edge label of the subtask e' immediately preceding e . Therefore, when the edge label of subtask e' is enabled, robots can remain idle for one time step to satisfy the starting vertex label of subtask e . Also, the satisfied clause in the edge label of e' implies the satisfied clause in the starting vertex label of subtask e . On the other hand, if subtask e is the first subtask in the simple path $\bar{\theta}^{\text{pre}}$, and also the vertex v_0 has a self-loop, then the initial robot locations satisfy the label of v_0 . Similarly robots can remain idle to make the label of v_0 true at least once. We still use $\bar{\tau}^{\text{pre}}$ to denote the new path as the only change is the idleness of robots. The new path $\bar{\tau}^{\text{pre}}$ still generates a word belonging to $\tilde{\mathcal{L}}_E^{\phi, v_0 \rightarrow v_{\text{accept}}}(\mathcal{A}_{\text{subtask}}^-)$ and induces the same simple path $\bar{\theta}^{\text{pre}}$ as the original path. Note that $\bar{\theta}^{\text{pre}}$ is a linear extension of the poset P based on which, the prefix MILP in Appendix A.2 is formulated. No two subtasks are completed at the same time in the path $\bar{\tau}^{\text{pre}}$.

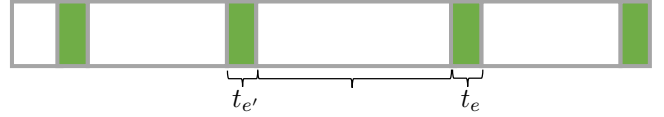


Figure 17. The divided essential word w^* .

C.4.6.1 Construction of the essential word: Given the path $\bar{\tau}^{\text{pre}}$ that induces the simple path $\bar{\theta}^{\text{pre}}$, let $\bar{w}^{\text{pre}} = \sigma_0 \sigma_1 \sigma_2 \dots \sigma_k$ denote the generated finite word in $\tilde{\mathcal{L}}_E^{\phi, v_0 \rightarrow v_{\text{accept}}}(\mathcal{A}_{\text{subtask}}^-)$, and $\bar{\rho}^{\text{pre}} = v_0 v_1 v_2 \dots v_{\text{accept}}$ denote the induced run in $\mathcal{A}_{\text{subtask}}^-$. Next we obtain an *essential word*, denoted by $w^* = \sigma_0^* \sigma_1^* \sigma_2^* \dots \sigma_k^*$, such that $\sigma_i^* \subseteq \sigma_i$ is the tightest subset of atomic propositions that enables a clause of label $\gamma(v_i, v_{i+1})$, where v_i and v_{i+1} are consecutive vertices in the run $\bar{\rho}^{\text{pre}}$, so that removing any atomic proposition from σ_i^* violates this clause. We identify the satisfied clause in the label $\gamma(v_i, v_{i+1})$ and add all positive literals in this clause to σ_i^* . If two sets of atomic propositions σ_i and σ_j correspond to the same vertex label, then $\sigma_i^* = \sigma_j^*$ since by condition (a) in Definition 3.10, it is always the same clause that is satisfied in a vertex label. Furthermore, if σ_i corresponds to an edge label and σ_{i+1} corresponds to the immediate following vertex label, then $\sigma_{i+1}^* \subseteq \sigma_i^*$ since by condition (b), the satisfied clauses in the edge labels implies the satisfied clauses in the immediately following vertex labels. By default, $\sigma_i^* = \{\top\}$ if $\gamma(v_i, v_{i+1}) = \top$. In this way, we have that $w^* \in \tilde{\mathcal{L}}_E^{\phi, v_0 \rightarrow v_{\text{accept}}}(\mathcal{A}_{\text{subtask}}^-)$ since it induces the same run $\bar{\rho}^{\text{pre}}$ as \bar{w}^{pre} does, and that the path $\bar{\tau}^{\text{pre}}$ generating the word \bar{w}^{pre} can generate the word w^* .

C.4.6.2 Construction of a subgraph of the routing graph \mathcal{G} : In this part, we construct a routing graph \mathcal{G}_{w^*} based on the essential word w^* which is a subgraph of the routing graph \mathcal{G} built in Appendix A.1. Given the essential word w^* , we can divide it into parts by locating the components where edges in the induced run $\bar{\rho}^{\text{pre}}$ in $\mathcal{A}_{\text{subtask}}^-$ are enabled. Fig. 17 demonstrates such a partition where green columns represent single time instants when edges are enabled, i.e., subtasks are completed, e.g., time instants $t_{e'}$ and t_e where e' is the subtask that is completed immediately preceding e , and the white areas between any two green columns represent the time intervals, e.g., $[t_{e'} + 1, t_e - 1]$, when the vertex labels are satisfied. Note that $t_e - 1 \geq t_{e'} + 1$ since we adjusted the path $\bar{\tau}^{\text{pre}}$ so that each starting vertex label is satisfied at least one. In this way, the time interval $[t_{e'} + 1, t_e - 1]$ and the time instant t_e make up the time span of the subtask e in the simple path $\bar{\theta}^{\text{pre}}$. Thus, given the path $\bar{\tau}^{\text{pre}}$, we can obtain an array of time spans of subtasks in $\bar{\theta}^{\text{pre}}$ such that consecutive time spans are disjoint with others and subtasks are completed sequentially. In what follows, we build a graph \mathcal{G}_{w^*} based on the essential word w^* . We begin with the vertex set.

(1) Construction of the vertex set:

(1a) Location vertices associated with initial robot locations: First, we create the vertex set $\mathcal{V}_{\text{init}}$ that corresponds to initial robot locations, as in Appendix A.1.1.1 for \mathcal{G} . We assign visit time $t_{vr}^- = t_{vr}^+ = 0$ to each vertex $v \in \mathcal{V}_{\text{init}}$, where robot r is the specific robot that is associated with v . In what follows, we also create vertices associated

with clauses in edge or vertex labels that are satisfied by the path $\bar{\tau}^{\text{pre}}$.

(1b) *Literal vertices associated with edge labels:* Consider a time instant t_e when the edge $e = (v_1, v_2)$ in $\bar{\theta}^{\text{pre}}$ is enabled. The set $\sigma_{t_e}^*$ of atomic propositions contains all literals appearing in the single clause satisfied in the edge label $\gamma(v_1, v_2)$. If $\gamma(v_1, v_2) = \top$, then $\sigma_{t_e}^* = \{\top\}$ and we do not create any vertices, as in Appendix A.1.1.2. Otherwise, for each atomic proposition $\pi_{i,j}^{k,\chi}$ in $\sigma_{t_e}^*$, we know that there are i robots of type j at region ℓ_k in the t_e -th configuration of the path $\bar{\tau}^{\text{pre}}$, and we also know which these i robots are. Similar to the construction of the routing graph \mathcal{G} in Appendix A.1.1.2, we construct i vertices pointing to region ℓ_k . Recall that we associated all robots of type j with each of these i vertices in \mathcal{G} . However, for \mathcal{G}_{w^*} , we know which specific i robots of type j visit region ℓ_k at time t_e by checking the path $\bar{\tau}^{\text{pre}}$. We create a one-to-one correspondence between these i robots with these i vertices. In this way, each vertex is visited by one specific robot. These robots are referred to as the essential robots in Appendix B.1. Furthermore, the time a specific robot r visits its assigned vertex v is t_e , which is denoted by $t_{vr}^- = t_{vr}^+ = t_e$. Continuing this way, we create vertices for other atomic propositions in $\sigma_{t_e}^*$, which only correspond to a single clause satisfied in $\gamma(v_1, v_2)$. Recall that when building the vertex set of \mathcal{G} in Appendix A.1.1.2, we build such vertices for each clause in the given edge label. Therefore, the set of vertices in \mathcal{G}_{w^*} corresponding to the edge label satisfied at t_e is a subset of the vertex set in \mathcal{G} for the same edge label.

(1c) *Literal vertices associated with vertex labels:* Following the same logic, we build the vertex set for the satisfied clause in the starting vertex label of e . We proceed depending on whether e is the first completed subtask. If e is not the first completed subtask in the simple path $\bar{\theta}^{\text{pre}}$, according to Definition 3.10, the clauses satisfied in this vertex label remain the same, that is, σ_t^* 's remain the same for all $t = t_{e'} + 1, \dots, t_e - 1$ where e' is the subtask immediately preceding e . Also, it is the same fleet of robots that satisfy this clause. Likewise, we can associate each vertex with one single robot, and the visit time interval is set as $[t_{e'} + 1, t_e - 1]$. That is, the robot r remains at its assigned vertex v within this time interval, denoted by $t_{vr}^- = t_{e'} + 1$ and $t_{vr}^+ = t_e - 1$. This vertex set also exists in \mathcal{G} since vertices are created for any starting vertex label in Appendix A.1.1.3. Otherwise, if e is the first completed subtask in the path $\bar{\tau}^{\text{pre}}$ and its starting vertex has a self-loop, then, we create vertices for the satisfied clause as usual and associate them with time interval $[0, t_e - 1]$. That is, $t_{vr}^- = 0$ and $t_{vr}^+ = t_e - 1$. Recall also that, the routing graph \mathcal{G} contains vertices for all clauses in all starting vertex labels. Furthermore, we do not create vertices for \top or \perp labels, similar to the case in Appendix A.1.1.3. Therefore, we can conclude that the vertex set of \mathcal{G}_{w^*} is a subset of that of \mathcal{G} .

(2) *Construction of the edge set:* Next, we prove that the edge set in \mathcal{G}_{w^*} is also a subset of the edge set in \mathcal{G} . Consider the edge label that is satisfied at the time instant t_e . For a vertex v among those associated with this edge label, we already know the robot r that visits v . Our goal is to determine the unique vertex in \mathcal{G}_{w^*} from which robot r comes. Let $\bar{\tau}_{r,j}$ denote the path of robot r of type j . Going backward from the $(t_e - 1)$ -th waypoint in $\bar{\tau}_{r,j}$,

(included), we identify the most recent time instant $t \leq t_e - 1$ when robot r takes part in the satisfaction of a literal $\pi_{i,j}^{k,\chi}$ that appears in the set σ_t^* of atomic propositions, that is, participate in a certain subtask.

(2a) *Time instant t does not exist:* In this case, subtask e is the first subtask that robot r participates in, and we can create an edge starting from the vertex u that is associated with the initial location of robot r and ending at vertex v . We assign the travel time $T_{uv} = t_e$ to the edge (u, v) , which is obtained by $T_{uv} = t_{vr}^- - t_{ur}^+ = t_e - 0$. In Appendix A.1.2.1, the edge (u, v) is also created in \mathcal{G} .

(2b) *Time instant t exists:* In this case, let e' denote the subtask that the literal $\pi_{i,j}^{k,\chi}$ corresponds to. If $e \neq e'$, e' occurs before e in the given path $\bar{\tau}^{\text{pre}}$ since the time spans of subtasks are disjoint and $t < t_e$. Thus, $e' \in X_{<_P}^e \cup X_{\parallel P}^e$. We identify the vertex u in \mathcal{G}_{w^*} that is associated with this literal $\pi_{i,j}^{k,\chi}$ and is visited by robot r , then create an edge starting from u and ending at v . Furthermore, we assign the weight $t_{vr}^- - t_{ur}^+$ to this edge (where $t_{vr}^- = t_e$), which is the travel time of robot r between these two consecutive subtasks. We emphasize that the edge (u, v) also exists in \mathcal{G} since vertices u and v are associated with the same robot type, and u is associated with a prior subtask e' of e . In Appendix A.1.2.2 that discusses leaving vertices from prior subtasks, the edge (u, v) exists in \mathcal{G} .

(2c) $e' = e$: In this case, the vertex u that robot r visits is associated with the starting vertex label of the same subtask e . We create the edge (u, v) and assign the travel time $T_{uv} = t_{vr}^- - t_{ur}^+$. This edge is also created in \mathcal{G} in Appendix A.1.2.3. Therefore, all edges in \mathcal{G}_{w^*} with end vertices associated with edge labels also exist in \mathcal{G} .

Following the same logic, we create edges associated with the starting vertex label of subtask e . Given a vertex v in \mathcal{G}_{w^*} that is associated with the vertex label $\gamma(v_1)$ of subtask e , we find the associated specific robot r of type j .

(2d) *Subtask e is the first completed subtask in the path $\bar{\tau}^{\text{pre}}$:* If the starting vertex v_0 of subtask e has a self-loop, then the initial locations should satisfy the starting vertex label of e . We locate the vertex u associated with the initial location of robot r of type j , create an edge starting from vertex u and ending at v , and assign the travel time $T_{uv} = 0$. This edge also exists in cases (1) or (2) in Appendix A.1.2.3.

(2e) *Subtask e is not the first completed subtask:* We move backwards from the $t_{e'}\text{-th}$ waypoint (the subtask e' immediately precedes e) in the path $\bar{\tau}_{r,j}$ to find the most recent time instant t that this robot has participated in another subtask preceding e . Condition (b) in Definition 3.10 states that all the robots satisfying the starting vertex label of a given subtask belong to the robots that satisfy the edge label of the subtask immediately preceding the given subtask, which implies that t should be identical to $t_{e'}$ since the path $\bar{\tau}^{\text{pre}}$ satisfies condition (b). We locate the vertex u associated with the edge label of subtask e' that robot r visits, create an edge between u and v , and assign the travel time $T_{uv} = t_{vr}^- - t_{ur}^+$ to the edge. This edge is also created in case (2) in Appendix A.1.2.3. Thus, the edge set of \mathcal{G}_{w^*} is a subset of the edge set of \mathcal{G} . Finally, we conclude that the graph \mathcal{G}_{w^*} constructed from the essential word w^* is a subgraph of the routing graph \mathcal{G} used to formulate the prefix MILP in Appendix A.2.

The graph \mathcal{G}_{w^*} has the property that there are no cycles and any two paths in \mathcal{G}_{w^*} , starting from vertices pointing to initial robot locations and ending at vertices without outgoing edges, do not share the same vertex since each path is associated with a specific robot. Therefore, every vertex except for the starting and end vertices in one path has indegree 1 (number of incoming edges) and outdegree 1 (number of outgoing edges). Moreover, vertices in \mathcal{G}_{w^*} are assigned the tightest visit time intervals for the specific robot. Consequently, starting from the vertex corresponding to the initial location of robot r of type j , we can extract a high-level plan $p_{r,j}$ for this robot by traversing along edges, which is a concise description of the low-level path $\bar{\tau}_{r,j}$. Observe that, given a feasible solution to the prefix MILP in Appendix A.2, we can build a subgraph of \mathcal{G} by removing any vertices and edges that are not visited by any robots and assigning robots and visit times to the remaining vertices. In this sense, such a subgraph of \mathcal{G} can be viewed as the graphical depiction of the solution to the MILP. In what follows, we show that the graph \mathcal{G}_{w^*} is such a graph. That is, it gives rise to a feasible solution that satisfies constraints (3)-(28) in Appendix A.2.

C.4.6.3 Satisfaction of the prefix MILP constraints in Appendix A.2:

(1) *Routing constraints:* Any vertex in \mathcal{G}_{w^*} is visited by a single robot of certain type, thus, constraint (3) that each vertex is visited by at most one robot of certain type is satisfied as follows. Given a vertex $v \in \mathcal{G}_{w^*}$, its associated robot r and unique vertex u that is connected to v , we set $x_{uvr} = 1$ and $x_{uvr'} = 0$ for other robots r' of the same type as r . In what follows, we omit the detailed assignment when it is clear to recognize. Furthermore, each vertex not in $\mathcal{V}_{\text{init}}$ is either a sink vertex (indegree is 1, outdegree is 0) or a vertex with indegree equal to its outdegree. Therefore, the flow constraint (4) is satisfied. For each vertex in $\mathcal{V}_{\text{init}}$ of \mathcal{G}_{w^*} , its outdegree is either 0 or 1, thus, constraint (5a) is satisfied. Each vertex in $\mathcal{V}_{\text{init}}$ is associated with a unique robot, which satisfies constraint (5b).

(2) *Scheduling constraints:* Since the visit time of each vertex is non-negative and the visit time associated with the vertices in $\mathcal{V}_{\text{init}}$ is set to $t_{vr}^- = t_{vr}^+ = 0$ (see case (1a) in Appendix C.4.6.2), constraints (6) and (7) are trivially satisfied. When creating edges in \mathcal{G}_{w^*} , we denote the travel time T_{uv} between connected vertices u and v in \mathcal{G}_{w^*} by $t_{vr}^- - t_{ur}^+$, which is the actual time robot r needs to travel between regions associated with u and v . Obviously, T_{uv} is no less than the shortest travel time T_{uv}^* between these two regions, i.e., $T_{uv}^* \leq T_{uv}$. When $u \in \mathcal{V}_{\text{init}}$ or $u <_P v$ or $(u, v) \in X_P$ and when robot r travels along the edge (u, v) , i.e., $x_{uvr} = 1$, constraint (8b) holds since $t_{ur}^+ + T_{uv}^* \leq t_{ur}^+ + T_{uv} = t_{vr}^-$. Next, we show that, when $u \parallel_P v$, constraint (8a) can be satisfied if all robots remain idle for one time step within the time interval $[t_{ur}^+, t_{vr}^-]$. More importantly, the elongated path can still generate a word belonging to $\tilde{\mathcal{L}}_E^{\phi, v_0 \rightarrow v_{\text{accept}}}(\mathcal{A}_{\text{subtask}}^-)$. This analysis proceeds depending on the types of NBA vertices that vertices u and v are associated with.

(2a) *Starting vertex u in \mathcal{G}_{w^*} is associated with a vertex label in $\mathcal{A}_{\text{subtask}}^-$:* Recall that we assign $t_e - 1$ to t_{ur}^+ when constructing the vertex set which is the time instant right before the subtask is completed (see case (1c)

in Appendix C.4.6.2). Thus, at the time instant t_{ur}^+ , the run $\bar{\rho}^{\text{pre}}$ has not left the NBA vertex in $\mathcal{A}_{\text{subtask}}^-$ that vertex u is associated with. We can repeat one more time the locations of all robots in the path $\bar{\tau}^{\text{pre}}$ at the time instant t_{ur}^+ so that the run visits the same NBA vertex one more time. In this way, the travel time assigned to the edge (u, v) becomes $T_{uv} + 1$, where T_{uv} is the time robot r takes in the path $\bar{\tau}^{\text{pre}}$ and 1 is the extra time it takes when all robots remain idle for one time step. Therefore, constraint (8a) is satisfied.

(2b) *End vertex v is associated with a vertex label in $\mathcal{A}_{\text{subtask}}^-$:* Recall that we assign $t_{e'} + 1$ to t_{vr}^- when constructing the vertex set which is the time instant right after a subtask is completed (see case (1c) in Appendix C.4.6.2). The vertex label is satisfied at t_{vr}^- since the label of each vertex in the simple path $\bar{\theta}^{\text{pre}}$ is satisfied at least once according to the construction of the path $\bar{\tau}^{\text{pre}}$ at the beginning of Appendix C.4.6. Thus, we can repeat one more time the locations of all robots in the path $\bar{\tau}^{\text{pre}}$ at the time instant t_{vr}^- so that the run visits the same NBA vertex one more time. Same as before, the travel time assigned to the edge (u, v) becomes $T_{uv} + 1$.

(2c) *Both u and v in \mathcal{G}_{w^*} are associated with an edge label in $\mathcal{A}_{\text{subtask}}^-$:* These two vertices must correspond to two different subtasks. Furthermore, there must be an NBA vertex with a self-loop between these two subtasks in the simple path $\bar{\theta}^{\text{pre}}$. This is because according to condition (c) in Definition 3.8, only initial and accepting vertices are allowed not to have self-loops but these vertices cannot be between two edges in the path $\bar{\theta}^{\text{pre}}$ if they do not have self-loops. In this case, robots can remain idle for one more time when this vertex label is true. Same as before, the travel time assigned to the edge (u, v) becomes $T_{uv} + 1$.

Therefore, constraint (8a) is satisfied in these three cases. We emphasize that the path $\bar{\tau}^{\text{pre}}$ after modification still produces the prefix part of a restricted accepting run since the only result of idleness is that a vertex in the run $\bar{\rho}^{\text{pre}}$ is visited for one more time step. Thus, requiring that all robots remain idle for a period of time does not affect the satisfaction of other constraints. In what follows, we still focus on the path $\bar{\tau}^{\text{pre}}$ since if it satisfies the others constraints, so does the modified path.

(3) *Logical constraints:* Each set σ_i^* of atomic propositions in the essential word w^* collects all literals inside one clause, and all σ_i^* 's that are associated with the same vertex label collect literals of the same clause. Therefore, constraint (9) that one and only one clause is true is satisfied. Although the path $\bar{\tau}^{\text{pre}}$ can simultaneously satisfy more than one clauses in a label, we construct the essential word w^* by selecting only one clause, and build the graph \mathcal{G}_{w^*} based on w^* . In this sense, we can state that only one clause is true on the graph \mathcal{G}_{w^*} . Moreover, because every vertex in \mathcal{G}_{w^*} associated with the same clause is visited by one robot, constraint (10) is satisfied. When constructing the vertex set of \mathcal{G}_{w^*} associated with edge labels (see case (1b) in Appendix C.4.6.2), we associate each vertex v corresponding to the same edge label with time $t_{vr}^- = t_{vr}^+ = t_e$. Therefore, the simultaneous visit constraint (11) is satisfied.

(4) *Temporal constraints:*

(4a) *Temporal constraints on one subtask:* As discussed before, each vertex v in \mathcal{G}_{w^*} associated with the same edge label is assigned time $t_{vr}^- = t_{vr}^+ = t_e$,

and only one clause is true. Therefore, constraint (12) specifying the completion time is satisfied. In case (1c) in Appendix C.4.6.2, we associate each vertex v corresponding to the same vertex label (neither \perp nor \top) with the same arriving time $t_{vr}^- = t_{e'} + 1$ and the same leaving time $t_{vr}^+ = t_e - 1$, where t_e is the completion time of the subtask that the vertex label corresponds to and $t_{e'}$ is the completion time of the subtask immediately preceding e . Since subtasks in the simple path $\bar{\theta}^{\text{pre}}$ are sequentially completed, $t_{vr}^- = t_{e'} + 1 \leq t_e$, thus the left side of constraint (13) is satisfied. The right side is satisfied trivially since $t_e = t_e - 1 + 1 = t_{vr}^+ + 1$. Next, if the initial vertex does not have a self-loop, and if the outgoing edge in the simple path $\bar{\theta}^{\text{pre}}$ is labeled with \top , there is no vertex in \mathcal{G}_{w^*} that corresponds to this edge. In this case, we can define the completion time of this edge label as 0, as stated by (14). Otherwise, if the outgoing edge label is not \top , the initial robot locations satisfy this edge label, that is, the set σ_0^* of atomic propositions include literals that appear in the satisfied clause in the edge label. Therefore, vertices are created in \mathcal{G}_{w^*} for these literals and the assigned visit time corresponds to the index of σ_0^* , i.e., 0. Thus, in this case (14) also holds.

(4b) *Temporal constraints on the completion of two sequential subtasks:* Since the simple path $\bar{\theta}^{\text{pre}}$ in $\mathcal{A}_{\text{subtask}}^-$, induced by the path $\bar{\tau}^{\text{pre}}$, is a linear extension of the poset P , we have that the temporal order of subtasks in $\bar{\theta}^{\text{pre}}$ respects the partial order in the poset P . Thus, given a subtask e in the simple path $\bar{\theta}^{\text{pre}}$, any subtask $e' \in \bar{\theta}^{\text{pre}}$ with $e' \prec_P e$ is completed before e in the path $\bar{\tau}^{\text{pre}}$. Therefore, $t_{e'} + 1 \leq t_e$, which satisfies constraint (15).

(4c) *Temporal constraints on the completion of the current subtask and the activation of subsequent subtasks:* For each subtask e except for the last one in the simple path $\bar{\theta}^{\text{pre}}$, the subtask e' immediately following it belongs to the set $X_{\succ_P}^e \cup X_{\parallel_P}^e$. If $e' \in X_{\succ_P}^e \neq \emptyset$ as in case (1) in Appendix A.2.4, since the only subtask in the simple path $\bar{\theta}^{\text{pre}}$ that immediately follows e is subtask e' , constraint (16) holds. The completion time of subtasks e' immediately following e in the simple path is larger than the completion time of e by at least 1. Therefore, constraint (17) is satisfied. Furthermore, we associate each vertex v associated with the edge label of subtask e' with the arrival time $t_{vr}^- = t_e + 1$, which satisfies constraint (18). Since the simple path $\bar{\theta}^{\text{pre}}$ is a linear extension of the poset P , no subtasks are completed at the same time, which satisfies constraint (19). If $X_{\succ_P}^e = \emptyset$ as in case (2) in Appendix A.2.4, then $e' \in X_{\parallel_P}^e$. Because subtask e' follows e , i.e., $b_{ee'} = 0$, and subtask e is not the last completed one, constraints (20a)-(20c) are satisfied by setting $b_{ee'} = 1$. If e is the last subtask in the simple path, $b_{ee'} = 0$ and $b_e^{e'} = 1$ in constraints (20a)-(20c).

On the other hand, any subtask e in the simple path $\bar{\theta}^{\text{pre}}$ except for the first one, immediately follows a subtask e' , which should be in $X_{\succ_P}^e \cup X_{\parallel_P}^e$. If $e' \in X_{\succ_P}^e \neq \emptyset$, since the only subtask in the simple path $\bar{\theta}^{\text{pre}}$ that immediately precedes e is subtask e' , constraint (21) holds. Otherwise, if $X_{\succ_P}^e = \emptyset$, then $e \in X_{\parallel_P}^e$. As subtask e' precedes e , i.e., $b_e^{e'} = 1$, and subtask e is not the first completed one, constraints (22a)-(22c) are satisfied by setting $b_{e'e} = 1$. If e

is the first subtask in the simple path, $b_{e'e} = 0$ and $b_e^{e'} = 0$ in constraints (22a)-(22c).

(4d) *Temporal constraints on the activation of the first subtask:* Consider the first completed subtask e in the path $\bar{\tau}^{\text{pre}}$. If its starting vertex has a self-loop, and also the vertex label is not \top , then this vertex label is satisfied at least once by the construction of the path $\bar{\tau}^{\text{pre}}$, and there are vertices in \mathcal{G}_{w^*} associated with the satisfied clause in this vertex label. Since the assigned time t_{vr}^- to these vertices is 0 (see case (1c) in Appendix C.4.6.2), constraint (23) is satisfied. For the first subtask e , since there is no subtask before it, the robots visiting vertices associated with the starting vertex label of e come from vertices in $\mathcal{V}_{\text{init}}$. Thus, constraint (25a) is satisfied for subtask e . For subtasks in P_{\max} other than e , the vertices associated with their vertex labels are connected to vertices associated with the edge labels of subtasks that are completed immediately before them (see case (2e) in Appendix C.4.6.2). Therefore, constraint (25b) is satisfied.

(5) *Same- $\langle i, j \rangle$ constraints:* Any two vertex subsets in \mathcal{G}_{w^*} that are associated with two literals that share the same nonzero connector are visited by the same fleet of robots since the essential word w^* belongs to $\mathcal{L}_E^{v_0 \rightarrow v_{\text{accept}}}(\mathcal{A}_{\text{subtask}}^-)$. We enumerate these two vertex subsets such that there is a one-to-one correspondence between vertices in these two subsets and the matched pair of vertices are visited by the same robot. In this way, constraint (26) is satisfied.

(6) *Constraints on the transition between the prefix and suffix parts:* Since we iterate over all subtasks that can be the last to be completed and also iterate over all clauses in the edge label of the selected last subtask, we can formulate a prefix MILP in Appendix A.2 in which the selected last subtask and the clause are the same as that induced by the feasible path $\bar{\tau}^{\text{pre}}$. Therefore, constraints (27) and (28) are satisfied, which completes the proof.

C.4.7 Proof of Lemma C.10: To prove that a simple path $\bar{\theta}$ can be extracted from the sub-NBA $\mathcal{A}_{\text{subtask}}^-$, we show that the solution to the MILP in Appendix A.2 gives rise to a simple path in the set of simple paths Θ from which the poset P is inferred. Then, since the graph-search version of the depth-first search on finite graphs is complete and since the backtracking search is a form of a depth-first-search (Russell and Norvig 2002), such a simple path can be found in $\mathcal{A}_{\text{subtask}}^-$. In the prefix MILP in Appendix A.2, we define a variable for each subtask in X_P which indicates its completion time (see Appendix A.2.4) and require that the completion times of two subtasks are different (see constraint (19)). Thus, we can sort the subtasks in X_P in an ascending order with respect to their completion time. The sorted subtasks respect the partial order in P since precedence relations among subtasks are captured by constraint (15), which means that the sequence of sorted subtasks is a linear extension of the poset P . Furthermore, the set of simple paths Θ is equivalent to the set of linear extensions of the poset P , which is ensured in Section 4.3. Therefore, the sequence of sorted subtasks corresponds to a simple path in Θ , which is in $\mathcal{A}_{\text{subtask}}^-$.

In what follows, we prove the three properties of this simple path $\bar{\theta}$ as stated in Lemma C.10: First, if the initial vertex v_0 of the initial subtask in the simple path $\bar{\theta}$ does not have a self-loop, according to constraint (14), it must

be completed at time 0. Thus, the activation time is also 0. Otherwise, if v_0 has a self-loop and also the vertex label in $\mathcal{A}_{\text{subtask}}^-$ is \top , then it can be activated at anytime, including 0; else if v_0 has a self-loop for which the label is not \top , according to constraint (23), the activation of the vertex label is 0. Therefore, property (a) in Lemma C.10 holds.

Second, for any subtask e in the simple path $\tilde{\theta}$, if its starting vertex label has a self-loop and the vertex label is \top , property (b) in Lemma C.10 holds trivially. Otherwise, if the vertex label is not \top , constraint (13) ensures that property (b) in Lemma C.10 holds.

Finally, for any two consecutive subtasks e and e' in the simple path $\tilde{\theta}$, we prove that it is exactly $e' \in S_3^e = X_{\prec_P}^e \cup X_{\parallel_P}^e$ that makes $b_{ee'} = 1$ in constraint (16). If so, according to constraint (18), subtask e' is activated at most one time step after the completion of e . Therefore, property (c) in Lemma C.10 holds. To see this, we use induction.

Consider e_0 and e_1 to be the first two subtasks in the simple path $\tilde{\theta}$. Because e_1 is completed immediately after e_0 , we have that $e_1 \in X_{\succ_P}^{e_0} \cup X_{\parallel_P}^{e_0}$. Thus, $e_0 \in X_{\prec_P}^{e_1} \cup X_{\parallel_P}^{e_1}$. Since subtask e_1 is not the first one in $\tilde{\theta}$, it must immediately follow a subtask. By constraints (21)-(22), there must exist a subtask $e \in X_{\prec_P}^{e_1} \cup X_{\parallel_P}^{e_1}$ such that $b_{ee_1} = 1$. Assume that $e \neq e_0$. By constraint (17), subtask e must be completed before e_1 , but it is only subtask e_0 that occurs before e_1 in the simple path $\tilde{\theta}$, a contradiction. Therefore, $e = e_0$, i.e., it is exactly subtask e_1 that makes $b_{e_0e_1} = 1$. Next, assume that for any two consecutive subtasks e_{i-1} and e_i in the simple path $\tilde{\theta}$, it holds that $b_{e_{i-1}e_i} = 1$. Given the next two subtasks e_i and e_{i+1} , assume that e_{i+1} immediately follows subtask e' but $e' \neq e_i$. By constraint (17), e' is completed before e_{i+1} . However, e' cannot be any subtask in e_0, \dots, e_{i-1} , since this will contradict constraint (16) that the immediately following subtask of any subtask in e_0, \dots, e_{i-1} is unique. Therefore, $e' = e_i$, completing the proof.

C.4.8 Proof of Lemma C.11: Given a subtask $e = (v_1, v_2)$ in the simple path $\tilde{\theta}$, the goal of the GMRPP in Appendix B.2 is to design paths for the robots to reach locations that satisfy the complete clause $\gamma_{1,2}^+ \wedge \gamma_{1,2}^-$ in the edge label $\gamma(v_1, v_2)$ so as to complete the current subtask and activate the next subtask, while respecting the complete clause $\gamma_1^+ \wedge \gamma_1^-$ in the starting vertex label $\gamma(v_1)$ en route. Starting from the first subtask in the simple path $\tilde{\theta}$, we proceed along the simple path to prove that each GMRPP instance with initial locations generated by the previous instance is feasible.

Consider the first subtask (v_1, v_2) with $v_1 = v_0$. We first discuss the case where the initial vertex v_0 has a self-loop in the sub-NBA $\mathcal{A}_{\text{subtask}}^-$, which implies that the initial robot locations satisfy the label $\gamma_\phi(v_0)$ in the NBA \mathcal{A}_ϕ , otherwise we remove its self-loop (see Sections 4.2.1 and 4.2.2). We continue based on whether the sets of essential robots \mathcal{R}_1 and $\mathcal{R}_{1,2}$ are disjoint.

C.4.8.1 $\mathcal{R}_1 \cap \mathcal{R}_{1,2} = \emptyset$: According to property (b) in Lemma C.10, the complete clause $\gamma_1^+ \wedge \gamma_1^-$ can only become false when $\gamma_{1,2}^+ \wedge \gamma_{1,2}^-$ becomes true. At the initial time 0, according to property (a) in Lemma C.10, the robot locations satisfy $\gamma_1^+ \wedge \gamma_1^-$, including those robots in $\mathcal{R}_{1,2}$. Thus, all robots can move around safely within their respective regions

without violating γ_1^- . By Assumption 3.5, there is a label-free path between any two regions, and between any label-free cells and any regions. Thus, the robots in $\mathcal{R}_{1,2}$ can move to label-free cells without passing through other regions, and, therefore, they can travel along label-free paths to reach label-free cells that are adjacent to their target regions. This process does not violate the negative clause γ_1^- . Also, γ_1^+ is satisfied due to $\mathcal{R}_1 \cap \mathcal{R}_{1,2} = \emptyset$. At this point, the essential clause $\gamma_{1,2}^+$ can be satisfied in one time step. If, at this time, there are robots in $\mathcal{R}^- \setminus \mathcal{R}_{1,2}$ that violate $\gamma_{1,2}^-$ (robots in $\mathcal{R}_{1,2}$ stay at label-free cells now), then without passing through other regions, these robots move to locations within their respective regions from where they can reach the label-free cells in one time step. This process also respects the complete clause $\gamma_1^+ \wedge \gamma_1^-$. Finally, at the same time, the robots in $\mathcal{R}_{1,2}$ move to their target regions and the robots in $\mathcal{R}^- \setminus \mathcal{R}_{1,2}$ that violate $\gamma_{1,2}^-$ move from their regions to label-free cells. As a result, the complete label $\gamma_{1,2}^+ \wedge \gamma_{1,2}^-$ is satisfied. Note that robots moving to target regions to satisfy $\gamma_{1,2}^+$ do not violate the negative clause $\gamma_{1,2}^-$ since infeasible clauses are removed during the pre-processing step (4) in Section 3.4.2.

C.4.8.2 $\mathcal{R}_1 \cap \mathcal{R}_{1,2} \neq \emptyset$: In this case, for a robot $r \in \mathcal{R}_1 \cap \mathcal{R}_{1,2}$, the shortest travel time between its source region and target region is less than or equal to 1 since by constraint (13) in Appendix A.2, the completion time of a subtask is at most one time step after the completion time of its starting vertex label. This implies that its source region and target region are identical or adjacent. Same as in Appendix C.4.8.1 where $\mathcal{R}_1 \cap \mathcal{R}_{1,2} = \emptyset$, the robots in $\mathcal{R}_{1,2} \setminus \mathcal{R}_1$ move to label-free cells from where they can reach their target regions in one time step, while the robots in $\mathcal{R}_{1,2} \cap \mathcal{R}_1$ move to locations within their respective source regions from where they can reach the target regions and leave the source regions in one time step. Without pass through other regions, the complete clause $\gamma_1^+ \wedge \gamma_1^-$ remains satisfied. Next, similar to Appendix C.4.8.1 where $\mathcal{R}_1 \cap \mathcal{R}_{1,2} = \emptyset$, the robots in $\mathcal{R}^- \setminus \mathcal{R}_{1,2}$ move to locations within their respective regions from where they can reach the label-free cells in one time step. In this way, $\gamma_{1,2}^+ \wedge \gamma_{1,2}^-$ can be satisfied at the next time step.

We have shown the feasibility of GMRPP when the initial vertex v_0 in $\mathcal{A}_{\text{subtask}}^-$ has a self-loop. In the case where v_0 does not have a self-loop in $\mathcal{A}_{\text{subtask}}^-$, the initial robot locations satisfy the complete clause $\gamma_{1,2}^+ \wedge \gamma_{1,2}^-$ in the edge label; otherwise, the edge is removed (see Sections 4.2.1 and 4.2.2). We do not formulate the GMRPP in this case; see line 2 in Algorithm 3.

Whether or not v_0 has a self-loop, the complete clause $\gamma_{1,2}^+ \wedge \gamma_{1,2}^-$ is satisfied at last. By condition (d) in Definition 3.8 and condition (b) in Definition 3.10, the complete clause in the end vertex label $\gamma_\phi(v_2)$ can be satisfied automatically, which activates the next subtask, as per property (c) in Lemma C.10 states that the next subtask is activated at most one time step after the current one. We can apply the same logic in Appendices C.4.8.1 where $\mathcal{R}_1 \cap \mathcal{R}_{1,2} = \emptyset$ and C.4.8.2 where $\mathcal{R}_1 \cap \mathcal{R}_{1,2} \neq \emptyset$ to the remaining subtasks in the simple path $\tilde{\theta}$ since each subtask being activated by the previous subtask is similar to the first

subtask being activated by initial robot locations, completing the proof.

C.4.9 Proof of Lemma C.12: The MILP in Appendix A.3.2.2 for the suffix part shares most constraints with that for the prefix part, so we can follow the same procedure as in Appendix C.4.6.

First, we construct an essential word w^* based on the given path $\bar{\tau}^{\text{suf}}$, as in Appendix C.4.6.1. Note that the essential word is constructed with respect to the sub-NBA $\mathcal{A}_{\text{subtask}}^-$ in Fig. 12 where we add a clause $\mathcal{C}_{\text{prior}}^+$ to each edge label of subtasks that can be the last to be completed. By condition (c) in Definition 3.10, all robots return to s_{prior} at last while driving the transition back to v_{accept} . This implies that those robots involved in the clause $\mathcal{C}_{\text{prior}}^+$ of $\gamma(v_{\text{prior}}, v_{\text{accept}})$ return to regions corresponding to their initial locations. By Assumption 3.5, any region spans consecutive cells. Therefore, the last waypoint in $\bar{\tau}^{\text{suf}}$ must satisfy the clause $\mathcal{C}_{\text{prior}}^+$, and further the last set of atomic propositions in w^* is $\mathcal{C}_{\text{prior}}^+$. Following steps similar to Appendix C.4.6.2, we can construct a graph \mathcal{G}_{w^*} that is also a subgraph of the routing graph \mathcal{G} .

Next, since the MILP in Appendix A.3.2.2 for the suffix part includes constraints (3)-(26) in Appendix A.2 for prefix MILP, our analysis for these constraints is the same as that in Appendix C.4.6.3. Thus, we focus on constraints (30)-(33) from Appendix A.3.2.2. First, no two subtasks are satisfied at the same time in the given path $\bar{\tau}^{\text{suf}}$. Thus, constraints (30) and (31) are satisfied. Each vertex in \mathcal{G}_{w^*} associated with clause $\mathcal{C}_{\text{prior}}^+$ of the last subtask is visited by a specific robot. Therefore, constraint (32) is satisfied.

C.4.10 Proof of Theorem 6.1: We emphasize that we discuss the class LTL^0 of formulas in this proof. Because $LTL^0 \subset LTL^\chi$, Proposition C.8 and Lemma C.12 apply also to the class LTL^0 . Proposition C.8 ensures that we can find a feasible prefix part $\tilde{\tau}^{\text{pre}}$ that induces a run $\tilde{\rho}^{\text{pre}}$ connecting v_0 and v_{accept} . Therefore, our goal is to prove that a corresponding suffix part $\tilde{\tau}^{\text{suf}}$ exists.

We divide the proof into two cases depending on whether the suffix part ρ^{suf} of the run induced by the assumed path $\tau = \tau^{\text{pre}}[\tau^{\text{suf}}]^w$ in Theorem 6.1 is a single vertex or not. When ρ^{suf} only consists of the accepting vertex v_{accept} , we next show that condition (e) in Definition 3.8 can be satisfied. If $\gamma_\phi(v_{\text{accept}}) = \top$, this condition is satisfied automatically. Otherwise, if $\gamma_\phi(v_{\text{accept}}) \neq \top$, because in condition (c) in Definition 4.3 we do not remove any composite edges leading to v_{accept} and in constraints (27) and (28) in Appendix A.2 we iterate over subtasks that can be the last to be completed, eventually we can formulate a prefix MILP where the edge label of the last subtask implies the label of vertex v_{accept} . Therefore, condition (e) in Appendix A.2 is met, which means that the final locations of the prefix path $\tilde{\tau}^{\text{pre}}$ satisfy the vertex label $\gamma_\phi(v_{\text{accept}})$. Combined with Proposition C.8, we can find a path that induces a run in \mathcal{A}_ϕ connecting v_0 and v_{accept} and ensures that the NBA \mathcal{A}_ϕ remains at v_{accept} forever, satisfying the specification ϕ .

Next, we discuss the case where the suffix part ρ^{suf} includes more than one vertices. Recall that s_{prior} and v_{prior} are the last waypoint in the prefix path τ^{pre} and the last vertex before v_{accept} in the induced run ρ^{pre} . We denote by \tilde{s}_{prior} and \tilde{v}_{prior} the last waypoint in the found prefix path $\tilde{\tau}^{\text{pre}}$ and

the last vertex before $\tilde{v}_{\text{accept}}$ in its induced run, respectively. By Proposition C.1, there exists a suffix path $\bar{\tau}^{\text{suf}}$ generating a word in $\tilde{\mathcal{L}}_E^{\phi, v_{\text{accept}} \rightarrow v_{\text{accept}}}(\mathcal{A}_{\text{subtask}}^-; s_{\text{prior}}, v_{\text{prior}})$. However, this word may not belong to $\tilde{\mathcal{L}}_E^{\phi, v_{\text{accept}} \rightarrow v_{\text{accept}}}(\mathcal{A}_{\text{subtask}}^-; \tilde{s}_{\text{prior}}, \tilde{v}_{\text{prior}})$, since the pair s_{prior} and v_{prior} may not be same as the pair \tilde{s}_{prior} and \tilde{v}_{prior} . In what follows we show that a feasible suffix path $\bar{\tau}^{\text{suf}}$, modified from $\bar{\tau}^{\text{suf}}$, exists that generates a finite word $\bar{w}^{\text{suf}} \in \mathcal{L}_E^{\phi, v_{\text{accept}} \rightarrow v_{\text{accept}}}(\mathcal{A}_{\text{subtask}}^-; \tilde{s}_{\text{prior}}, \tilde{v}_{\text{prior}})$ and satisfies conditions (a) and (b) in Definition 3.10. Then, we rely on Lemma C.12 to prove the final result. Note that the word \bar{w}^{suf} belongs to language $\mathcal{L}_E^{\phi, v_{\text{accept}} \rightarrow v_{\text{accept}}}$ instead of $\tilde{\mathcal{L}}_E^{\phi, v_{\text{accept}} \rightarrow v_{\text{accept}}}$ since the path $\bar{\tau}^{\text{suf}}$ does not satisfy condition (c) in Definition 3.10.

First, we show that eventually we have $\tilde{v}_{\text{prior}} = v_{\text{prior}}$ and \tilde{s}_{prior} and s_{prior} satisfy the same clause $\mathcal{C}_{\text{prior}}$. As we iterate over subtasks that can be the last to be completed in the prefix part (see constraint (27) in Appendix A.2.6), we can eventually formulate a prefix MILP whose solution gives rise to a run with $\tilde{v}_{\text{prior}} = v_{\text{prior}}$. Furthermore, as we iterate over clauses in the selected last subtask (see constraint (28)), we can obtain the final configuration \tilde{s}_{prior} such that \tilde{s}_{prior} and s_{prior} satisfy the same clause $\mathcal{C}_{\text{prior}}$ in the edge label $\gamma_\phi(v_{\text{prior}}, v_{\text{accept}})$. Note however that it is possible that different robots in \tilde{s}_{prior} and s_{prior} satisfy the positive subformula $\mathcal{C}_{\text{prior}}^+$. Based on \tilde{s}_{prior} and v_{prior} , we can obtain a sub-NBA $\mathcal{A}_{\text{subtask}}^-$ for the suffix part (see Appendix A.3.1), which differs from the sub-NBA obtained based on s_{prior} and v_{prior} only in the interpretation of the clause $\mathcal{C}_{\text{prior}}^+$, that is, on those robots that return to their respective regions; these regions are identical for \tilde{s}_{prior} and s_{prior} since they satisfy the same clause $\mathcal{C}_{\text{prior}}^+$. In other words, these two sub-NBAs are graphically equivalent. We denote by $\mathcal{A}_{\text{subtask}}^-(\tilde{s}_{\text{prior}}, v_{\text{prior}})$ the sub-NBA based on \tilde{s}_{prior} and v_{prior} .

Next, based on the fact that $\bar{\tau}^{\text{suf}}$ generates a word $\bar{w}^{\text{suf}} \in \mathcal{L}_E^{\phi, v_{\text{accept}} \rightarrow v_{\text{accept}}}(\mathcal{A}_{\text{subtask}}^-; s_{\text{prior}}, v_{\text{prior}})$, we construct another feasible path $\bar{\tau}^{\text{suf}}$, modified from $\bar{\tau}^{\text{suf}}$, that generates a word $\bar{w}^{\text{suf}} \in \mathcal{L}_E^{\phi, v_{\text{accept}} \rightarrow v_{\text{accept}}}(\mathcal{A}_{\text{subtask}}^-; \tilde{s}_{\text{prior}}, v_{\text{prior}})$. The path $\bar{\tau}^{\text{suf}}$ begins with the final locations \tilde{s}_{prior} of the found prefix part $\tilde{\tau}^{\text{pre}}$ in Proposition C.8. By condition (f) in Definition 3.8, $\gamma_\phi(v_{\text{prior}}, v_{\text{accept}}) \implies \gamma_\phi(v_{\text{accept}}, v_{\text{next}})$, therefore, \tilde{s}_{prior} and s_{prior} satisfy the same clause in label $\gamma_\phi(v_{\text{accept}}, v_{\text{next}})$ since they satisfy the same clause $\mathcal{C}_{\text{prior}}$ in $\gamma_\phi(v_{\text{prior}}, v_{\text{accept}})$. Moreover, by conditions (d) and (f) in Definition 3.8, \tilde{s}_{prior} and s_{prior} satisfy the same clauses in the edge label $\gamma_\phi(v_{\text{accept}}, v_{\text{next}})$ and vertex label $\gamma_\phi(v_{\text{next}})$, respectively. Therefore, \tilde{s}_{prior} and s_{prior} satisfy the same clause in $\gamma(v_{\text{next}})$ in the sub-NBA $\mathcal{A}_{\text{subtask}}^-(\tilde{s}_{\text{prior}}, v_{\text{prior}})$. Note that, at the time when the sub-NBA $\mathcal{A}_{\text{subtask}}^-(\tilde{s}_{\text{prior}}, v_{\text{prior}})$ remains at the vertex v_{next} , robots can start from \tilde{s}_{prior} and reach a configuration \bar{s}_{prior} that is almost identical to s_{prior} except for the specific robots at the specific cells. In other words, if we consider robots in the same type to be indistinguishable, \bar{s}_{prior} is identical to s_{prior} . To show this, we construct a one-to-one correspondence between robots in \tilde{s}_{prior} and robots in s_{prior} .

Specifically, for a literal $\pi_{i,j}^k$ in the satisfied clause of $\gamma(v_{\text{next}})$ in $\mathcal{A}_{\text{subtask}}^-$, we identify i robots of type j in configuration \tilde{s}_{prior} that satisfy this literal and another i

robots of type j in s_{prior} . Then we construct a random one-to-one correspondence between these two sets of robots, i.e., i pairs of robots, such that every robot from the i robots associated with \tilde{s}_{prior} starts from its location in \tilde{s}_{prior} , travels inside region ℓ_k and reaches the location in s_{prior} where its paired robot is. This maintains the satisfaction of $\gamma(v_{\text{next}})$. This point-to-point navigation is feasible since those i robots associated with \tilde{s}_{prior} and their corresponding robots associated with s_{prior} are all in region ℓ_k and, according to Assumption 3.5 every region spans consecutive cells. Enumerating other robots of type j in \tilde{s}_{prior} that do not participate in the satisfaction of $\gamma(v_{\text{next}})$, we can construct another one-to-one correspondence between them and those of type j in s_{prior} that do not participate in the satisfaction of $\gamma(v_{\text{next}})$. Such robots in \tilde{s}_{prior} , by Assumption 3.5, can leave their regions corresponding to their locations in \tilde{s}_{prior} to go to label-free cells without passing through other regions, then travel along label-free paths to the regions where their paired robots are located in s_{prior} and finally reach the specific cells inside these regions. Robots traveling inside regions do not violate the label $\gamma(v_{\text{next}})$ since \tilde{s}_{prior} and s_{prior} satisfy $\gamma(v_{\text{next}})$. In this way, robots reach a configuration \bar{s}_{prior} while the NBA $\mathcal{A}_{\text{subtask}}^-(\tilde{s}_{\text{prior}}, v_{\text{prior}})$ remains at the vertex v_{next} .

When robots reach the configuration \bar{s}_{prior} from \tilde{s}_{prior} , conditions (a) and (b) in Definition 3.10 are not violated since these robots in \tilde{s}_{prior} that participate in the satisfaction of a clause in $\gamma(v_{\text{next}})$ do not leave their respective regions. We append this path segment from \tilde{s}_{prior} to \bar{s}_{prior} to the current $\bar{\tau}^{\text{suf}}$. Note that \bar{s}_{prior} and s_{prior} are identical if robots that belong to the same type are indistinguishable. After reaching the configuration \bar{s}_{prior} , every robot travels along the suffix path in $\bar{\tau}^{\text{suf}}$ (both beginning with and ending at s_{prior}) that its paired robot does. Appending this path to the current $\bar{\tau}^{\text{suf}}$ concludes the construction of $\bar{\tau}^{\text{suf}}$. At last, the transition in the sub-NBA $\mathcal{A}_{\text{subtask}}^-(\tilde{s}_{\text{prior}}, v_{\text{prior}})$ is driven back to v_{accept} . Note that the last configuration in $\bar{\tau}^{\text{suf}}$ is not identical to \tilde{s}_{prior} , that is, robot trajectories are not closed yet. Thus, condition (c) in Definition 3.10 is not met. However, in the last configuration of $\bar{\tau}^{\text{suf}}$ those robots participating in the satisfaction of $\mathcal{C}_{\text{prior}}^+$ return to their respective regions since $\bar{\tau}^{\text{suf}}$ at last returns to s_{prior} , and s_{prior} and \tilde{s}_{prior} satisfy the same positive subformula $\mathcal{C}_{\text{prior}}^+$. Therefore, we can construct a path $\bar{\tau}^{\text{suf}}$ that satisfies conditions (a) and (b) in Definition 3.10 and generates a word $\bar{w}^{\text{suf}} \in \mathcal{L}_E^{\phi, v_{\text{accept}} \rightarrow v_{\text{accept}}}(\mathcal{A}_{\text{subtask}}^-, \tilde{s}_{\text{prior}}, v_{\text{prior}})$. More importantly, those robots participating in the satisfaction of $\mathcal{C}_{\text{prior}}^+$ return to regions corresponding to their initial locations.

Subsequently, from Lemma C.12 we conclude that we can obtain a low-level path and we denote it by $\tilde{\tau}^{\text{suf},1}$. We note that Lemma C.12 assumes that a path exists satisfying condition (c) in Definition 3.10 which requires robots to return to their initial locations, while in $\bar{\tau}^{\text{suf}}$ only those robots participating in satisfying $\mathcal{C}_{\text{prior}}^+$ return to their respective regions. Even so, it suffices to establish the feasibility of the MILP (excluding constraint (33)) in Appendix A.3.2.2 for the suffix part since in the MILP, the clause needed to be satisfied in the last completed subtask is $\mathcal{C}_{\text{prior}}^+$ (see Fig. 12), i.e., robots are not required to return to their initial locations. After obtaining the path $\tilde{\tau}^{\text{suf},1}$, the run in \mathcal{A}_ϕ induced by $\tilde{\tau}^{\text{suf},1}$ is a cycle around the accepting vertex v_{accept} .

Finally, we prove that closing the trajectories in Appendix A.3.2.3 is feasible. The last configuration in the low-level path $\tilde{\tau}^{\text{suf},1}$ satisfies the clause $\mathcal{C}_{\text{prior}}$, and so do the initial locations \tilde{s}_{prior} . Also, the robots in the last configuration of $\tilde{\tau}^{\text{suf},1}$ participating in the satisfaction of $\mathcal{C}_{\text{prior}}^+$ are identical to those in \tilde{s}_{prior} . Therefore, they can return to their initial locations in \tilde{s}_{prior} inside the same regions, while maintaining the truth of $\mathcal{C}_{\text{prior}}^+$. The rest of the robots can return to their initial locations by leaving their regions in the last configuration to go to label-free cells, then traveling along the label-free paths to the regions where their initial locations in \tilde{s}_{prior} are located, and finally returning to initial locations inside these regions. This respects the negative subformula $\mathcal{C}_{\text{prior}}^-$ since both the last configuration in $\tilde{\tau}^{\text{suf},1}$ and \tilde{s}_{prior} satisfy $\mathcal{C}_{\text{prior}}$. We denote by $\tilde{\tau}^{\text{suf},2}$ the path segment from the last configuration of $\tilde{\tau}^{\text{suf},1}$ to \tilde{s}_{prior} , which satisfies the clause $\mathcal{C}_{\text{prior}}$, and further satisfies the label $\gamma_\phi(v_{\text{prior}}, v_{\text{next}})$ and $\gamma_\phi(v_{\text{next}})$ according to conditions (d) and (f) in Definition 3.8. Therefore, the NBA \mathcal{A}_ϕ can remain at vertex v_{next} while robots execute the path segment $\tilde{\tau}^{\text{suf},2}$. In a nutshell, we leverage the vertex v_{next} to reach \bar{s}_{prior} from \tilde{s}_{prior} in order to reuse the suffix path $\bar{\tau}^{\text{suf}}$, and similarly we leverage the vertex v_{next} to deviate from the path $\bar{\tau}^{\text{suf}}$ in order to return to \tilde{s}_{prior} . Finally, we can obtain the suffix path by concatenating $\tilde{\tau}^{\text{suf},1}$ with $\tilde{\tau}^{\text{suf},2}$, i.e., $\tilde{\tau}^{\text{suf}} = \tilde{\tau}^{\text{suf},1}\tilde{\tau}^{\text{suf},2}$, which gives rises to a path $\tilde{\tau} = \tilde{\tau}^{\text{pre}}[\tilde{\tau}^{\text{suf}}]^\omega$ that satisfies the specification ϕ , completing the proof.